



Fifth Generation Communication Automotive Research and innovation

# **Deliverable D3.2**

## **Report on Channel Modelling and Positioning for 5G V2X**

Version: v1.0

2018-11-30

*This project has received funding from the European Union's Horizon 2020 research and innovation programme under grant agreement No 761510. Any 5GCAR results reflects only the authors' view and the Commission is thereby not responsible for any use that may be made of the information it contains.*



<http://www.5g-ppp.eu>

# Deliverable D3.2

## Report on Channel Modelling and Positioning for 5G V2X

<b>Grant Agreement Number:</b>	761510
<b>Project Name:</b>	Fifth Generation Communication Automotive Research and innovation
<b>Project Acronym:</b>	5GCAR
<b>Document Number:</b>	5GCAR/D3.2
<b>Document Title:</b>	Report on Channel Modelling and Positioning for 5G V2X
<b>Version:</b>	v1.0
<b>Delivery Date:</b>	2018-11-30
<b>Editors:</b>	Stephan Saur (Nokia), Mate Boban (Huawei)
<b>Authors:</b>	Nil Garcia, Henk Wymeersch, Fuxi Wen (Chalmers), Hieu Do (Ericsson), Mate Boban, Anastasios Kakkavas, Qi Wang (Huawei), Giuseppe Destino, Toktam Mahmoodi (KCL), Silvio Mandelli, Stephan Saur, Stefan Wesemann (Nokia), Dinh-Thuy Phan-Huy (Orange), Efstathios Katranaras (Sequans), Taimoor Abbas (Volvo Cars)
<b>Keywords:</b>	5GCAR, 5G, New Radio, V2X, channel modelling, channel measurements, positioning
<b>Status:</b>	Final
<b>Dissemination level:</b>	Public

# Abstract

5GCAR has identified the most important use cases for future V2X communications together with their key performance indicators and respective requirements. One outcome of this study is that accurate positioning is important for all these use cases, however with different level of accuracy. In this deliverable we summarize existing solutions for positioning of road users and justify that they are not sufficient to achieve the required performance always and everywhere. Therefore, we propose a set of solutions for different scenarios (urban and highway) and different frequency bands (below and above 6 GHz). Furthermore, we link these new technical concepts with the ongoing standardization of 3GPP New Radio Rel-16.

An important prerequisite for this work is the availability of appropriate channel models. For that reason, we place in front a discussion of existing channel models for V2X, including the sidelink between two road users, their gaps, as well as our 5GCAR contributions beyond the state of the art. This is complemented with results from related channel measurement campaigns.



## Executive summary

In this deliverable we present results obtained in 5GCAR for two important topics related to V2X: channel modelling and positioning. Section 2 deals with channel modelling. First, the state-of-the-art channel models for V2X communications are described, including their most relevant components: LOS blockage analysis, path loss and shadow fading modelling, and fast fading modelling. Based on the existing work, Section 2 describes the gap in terms of the key missing components required for complete solution for V2X channel modelling. Based on the gap and beyond prior art, Section 2 describes:

- New V2V measurements and characterization of channels above 6 GHz
- Multi-link shadowing model based on measurements below 6 GHz
- Channel measurements for massive MIMO adaptive beamforming.

In terms of positioning, Section 3 firstly summarizes existing solutions for positioning and their limitations, including both non-radio and radio-based techniques. As part of the 5GCAR contributions, Section 3 describes the following technology components that are essential for a positioning solution needed to enable 5G V2X use cases:

- Trajectory prediction with channel bias compensation and tracking
- Beam-based V2X positioning
- Multi-array V2V relative positioning
- Tracking of a vehicle's position and orientation with a single base station in the downlink
- Harnessing data communication for low latency positioning
- Enhanced assistance messaging scheme for GPS and OTDOA positioning.

For both channel modelling and positioning, this deliverable analyzes the compliance of 5GCAR solutions with existing standards and provides an overview of ongoing standardization with focus on 3GPP New Radio Rel-16.

In a nutshell we claim:

- Very good alignment between 5GCAR activities and ongoing 3GPP NR standardization for both channel modelling and positioning. In particular our channel modelling activities led to agreements in 3GPP meetings and results achieved in 5GCAR are reflected in 3GPP V2X channel models.
- While positioning in LTE is based on time measurements only, most 5GCAR approaches integrate enhanced time measurements with angle measurements. This becomes possible through smaller antenna array sizes in the frequency range above 6 GHz. In this deliverable we show that the desired accuracy below one meter is in principle achievable. By rule of thumb this corresponds to an improvement of one order of magnitude with respect to the reference cases LTE and GPS.



# Contents

1	Introduction .....	9
1.1	Objective of the Document .....	9
1.2	Structure of the Document .....	9
2	Channel Modelling .....	10
2.1	V2X Environments and Link Types .....	10
2.2	State of the Art Channel Models for V2X.....	11
2.2.1	Channel Modelling Framework and Gap Analysis .....	11
2.2.2	Path Loss Models .....	17
2.2.3	Shadow Fading Models .....	20
2.2.4	Fast-Fading Parameters .....	22
2.2.5	Summary .....	22
2.3	Contributions in 5GCAR Beyond State of the Art .....	24
2.3.1	V2V Measurements in cmWave and mmWave .....	24
2.3.2	mmWave V2V (Sidelink) Channel Modelling .....	29
2.3.3	Multi-Link Shadowing Extensions.....	32
2.4	New Channel Measurements for Predictor Antenna for M-MIMO Adaptive Beamforming.....	35
2.5	Status of Standardization and Contributions of 5GCAR .....	40
3	Positioning .....	45
3.1	Review of Existing Solutions .....	45
3.1.1	Positioning with GNSS.....	45
3.1.2	Positioning in IEEE 802.11p Vehicular Ad-Hoc Networks (VANET) .....	47
3.1.3	Positioning with Cellular Radio Access Technologies .....	48
3.2	5GCAR Technology Components .....	49
3.2.1	Trajectory Prediction with Channel Bias Compensation and Tracking.....	51
3.2.2	Beam-Based V2X Positioning .....	55
3.2.3	Tracking of a Vehicle’s Position and Orientation with Single Base Station in the Downlink .....	57
3.2.4	Harnessing Data Communication for Low-Latency Positioning .....	60
3.2.5	Enhanced Assistance Messaging Scheme for GNSS and OTDOA Positioning....	63
3.2.6	Multi-Array V2V Relative Positioning: Performance Bounds.....	69



---

3.3	Status of Standardization .....	73
4	Conclusions .....	77
5	References .....	79
A	Simulation Assumptions.....	85
A.1	System-Level Simulation Assumptions .....	85
A.1.1	Deployment Scenarios for Base Stations .....	85
A.1.2	Deployment Scenarios for Road Sign Units .....	86
A.1.3	Deployment Scenarios for UEs .....	87
A.1.4	User Deployment and Mobility .....	88
A.1.5	Data Traffic Models.....	89
A.1.6	In-Band Emission Model .....	90
A.1.7	Performance Metrics.....	90
A.2	Link-level Simulation Assumptions.....	91



# List of Abbreviations and Acronyms

<b>3GPP</b>	Third Generation Partnership Project
<b>5G-PPP</b>	5G Private Public Partnership
<b>ABG</b>	Alpha Beta Gamma
<b>AGC</b>	Automatic Gain Control
<b>AI</b>	Artificial Intelligence
<b>AOA</b>	Angle of Arrival
<b>AOD</b>	Angle of Departure
<b>AS</b>	Angular Spread
<b>ASA</b>	Spread of AOA
<b>ASD</b>	Spread of AOD
<b>B2P</b>	Base Station-to-Pedestrian (-UE)
<b>B2R</b>	Base Station-to-Roadside Unit
<b>B2V</b>	Base Station-to-Vehicle
<b>BLADE</b>	Blind Learning Algorithm for the channel bias Distribution Estimation
<b>BS</b>	Base Station
<b>CA</b>	Carrier Aggregation
<b>CDF</b>	Cumulative Density Function
<b>CP</b>	Control Plane / Cyclic Prefix
<b>CRB</b>	Cramér-Rao Bound
<b>CTRV</b>	Constant Turn Rate and Velocity
<b>CV</b>	Constant Velocity
<b>D2D</b>	Device-to-Device
<b>DGNSS</b>	Differential Global Navigation Satellite System
<b>DL</b>	Downlink
<b>DMRS</b>	Demodulation Reference Signal
<b>DS</b>	Delay Spread
<b>DSRC</b>	Dedicated Short Range Communication
<b>efeMTC</b>	even further enhanced Machine Type Communications
<b>eMBB</b>	extreme Mobile Broadband
<b>EVM</b>	Error Vector Magnitude
<b>eVTX</b>	enhanced Vehicle-to-Everything

<b>FF</b>	Fast Fading
<b>FR</b>	Frequency Range
<b>FTM</b>	Fine-Time Measurement
<b>GBS</b>	Geometry Based Stochastic
<b>GDOP</b>	Geometric Dilution of Precision
<b>GNSS</b>	Global Navigation Satellite System
<b>GPS</b>	Global Positioning Signal
<b>IMU</b>	Inertial Measurement Unit
<b>ISD</b>	Inter Site Distance
<b>ITS</b>	Intelligent Transportation Systems
<b>ITU</b>	International Telecommunication Union
<b>KPI</b>	Key Performance Indicator
<b>LOS</b>	Line of Sight
<b>LPP</b>	LTE Positioning Protocol
<b>LR</b>	Linear Regression
<b>LS</b>	Location Server
<b>LTE-A</b>	LTE Advanced
<b>MAP</b>	Maximum-A-Posteriori
<b>MEC</b>	Mobile Edge Computing
<b>MIMO</b>	Multiple Input Multiple Output
<b>M-MIMO</b>	Massive MIMO
<b>mMTC</b>	Massive Machine Type Communications
<b>MRT</b>	Maximum Ratio Transmission
<b>MSE</b>	Mean Squared Error
<b>NAS</b>	Non-Access Stratum
<b>NB-IOT</b>	Narrow-Band Internet of Things
<b>NLOS</b>	Non-Line of Sight
<b>NLOS<sub>b</sub></b>	NLOS due to buildings
<b>NLOS<sub>v</sub></b>	NLOS due to vehicles
<b>NMSE</b>	Normalized Mean Squared Error
<b>NR</b>	New Radio
<b>OEB</b>	Orientation Error Bound
<b>OFDM</b>	Orthogonal Frequency Division Multiplexing



<b>OLOS</b>	Obstructed Line of Sight
<b>OMA</b>	Open Mobile Alliance
<b>OSM</b>	Open Street Map
<b>OTDOA</b>	(Downlink) Observed Time Difference of Arrival
<b>P2B</b>	Pedestrian (-UE)-to-Base Station
<b>P2P</b>	Pedestrian-to-Pedestrian
<b>PDF</b>	Probability Density Function
<b>PDP</b>	Power Delay Profile
<b>PEB</b>	Position Error Bound
<b>PF</b>	Particle Filter
<b>PL</b>	Path Loss
<b>PRR</b>	Packet Reception Ratio
<b>PRS</b>	Positioning Reference Signal
<b>R2R</b>	Roadside Unit-to-Roadside Unit
<b>RAN</b>	Radio Access Network
<b>RAT</b>	Radio Access Technology
<b>RMa</b>	Rural Macro
<b>RSS</b>	Received Signal Strength
<b>RSTD</b>	Received Signal Time Difference
<b>RSU</b>	Roadside Unit
<b>RTK</b>	Real-Time Kinematic
<b>RX</b>	Receive
<b>SF</b>	Shadow Fading
<b>SI</b>	Study Item
<b>SIB</b>	System Information Block
<b>SISO</b>	Single Input Single Output
<b>SL</b>	Sidelink
<b>SNR</b>	Signal-to-Noise Ratio
<b>SOTA</b>	State of the Art
<b>SRS</b>	Sounding Reference Signal
<b>SUMO</b>	Simulation of Urban Mobility

<b>SUPL</b>	Secure User Plane Location
<b>SUV</b>	Sport Utility Vehicle
<b>TDD</b>	Time Division Duplex
<b>TDOA</b>	Time Difference of Arrival
<b>TOA</b>	Time of Arrival
<b>TRP</b>	Transmit Receive Point
<b>TX</b>	Transmit
<b>UE</b>	User Equipment
<b>UKF</b>	Unscented Kalman Filter
<b>UL</b>	Uplink
<b>ULA</b>	Uniform Linear Array
<b>UMa</b>	Urban Macro
<b>UMi</b>	Urban Micro
<b>UP</b>	User Plane
<b>UTDOA</b>	Uplink (Observed) Time Difference of Arrival
<b>V2B</b>	Vehicle-to-Base Station
<b>V2I</b>	Vehicle-to-Infrastructure
<b>V2P</b>	Vehicle-to-Pedestrian
<b>V2R</b>	Vehicle-to-Roadside Unit
<b>V2V</b>	Vehicle-to-Vehicle
<b>V2X</b>	Vehicle-to-Everything
<b>VA</b>	Virtual Anchor
<b>VANET</b>	Vehicular Ad Hoc Network
<b>V-UE</b>	Vehicular User Equipment
<b>VRU</b>	Vulnerable Road User
<b>WI</b>	Work Item
<b>ZOA</b>	Zenith of Arrival
<b>ZOD</b>	Zenith of Departure
<b>ZSA</b>	Spread of ZOA
<b>ZSD</b>	Spread of ZOD





# 1 Introduction

## 1.1 Objective of the Document

This deliverable summarizes 5GCAR activities concerning channel modelling and positioning. It is inspired from the public deliverable of 5GCAR about scenarios, use cases, requirements and Key Performance Indicators (KPIs) [5GC17-D21]. All identified use cases in 5GCAR need accurate, ubiquitous and real-time positioning, a requirement that cannot be fulfilled with existing technologies which are mainly based on cameras, radar, Global Navigation and Satellite Systems (GNSS), such as the Global Positioning System (GPS), as well as vehicle sensors. It is envisaged to complement these existing systems to fill gaps, e.g. in tunnels, and to enhance the overall reliability. This deliverable also reflects recent results and agreements from V2X radio design [5GC18-D31] and V2X system level architecture [5GC18-D41] aiming at an overall 5G-based V2X solution with accurate positioning as one of the fundamental features.

The availability of appropriate channel models for V2X communications are an imperative prerequisite for the air interface design activities in 5GCAR. Existing models do not yet consider the full range of V2X-specific scenarios, such as the direct communication between two moving vehicles in a dense urban environment, or the characteristics of V2X-specific network elements like Roadside Units (RSUs). In particular, there are still significant gaps in the frequency range above 6 GHz. We aim to derive extended channel models based on the measurement campaigns presented in this deliverable.

In addition, we link the research activities in 5GCAR with the ongoing standardization in 3GPP.

## 1.2 Structure of the Document

This deliverable is organized as follows: Section 2 is dedicated to channel modelling and channel measurements. After an introduction of the scenarios and link types we consider in 5GCAR, we give an overview of existing channel models and a gap analysis. Important aspects are Line-of-Sight (LOS) probability and path loss, shadowing and fast fading. Next, we present the activities in 5GCAR beyond prior art. Important components are measurement campaigns in different frequency bands, scenarios, link types and antenna configurations. Based on that, extended channel model parameters for different frequencies are discussed. We conclude this first part of the deliverable with a status update of the ongoing standardization in 3GPP.

The topic of Section 3 is positioning. First, we briefly summarize the capabilities of common positioning methods used for Vehicle-to-Everything (V2X) Communications today. Afterwards, we introduce the ongoing research activities in 5GCAR concerning positioning and present the current status of the performance evaluation. Again, we consider different frequency bands and scenarios. Finally, we summarize recent agreements in the related 3GPP Rel-16 Study Item.

## 2 Channel Modelling

This section covers the relevant state of the art channel models for V2X communication, along with describing the work done beyond state of the art in the 5GCAR project. First, the section describes environments relevant for V2X communication, together with link types subsumed under the term “V2X”. Next, we describe state of the art channel models, including their most relevant components: LOS blockage analysis, path loss and shadow fading modelling, and fast fading modelling. The contributions beyond state of art pertain to: i) new Vehicle-to-Vehicle (V2V) measurements and characterization of channels above 6 GHz; ii) multi-link shadowing model based on measurements below 6 GHz; and iii) channel measurements for massive MIMO adaptive beamforming. Finally, the section concludes by analyzing the compliance of 5GCAR channels with existing standards and providing possible recommendations from 5GCAR to standardization bodies.

### 2.1 V2X Environments and Link Types

Radio propagation is influenced by the type of objects found in the environment where the communication occurs. In case of V2X communications, the most important objects that influence the propagation are buildings, vehicles (both static and mobile), and different types of vegetation (e.g., trees, shrubbery, etc.). Relevant scenarios for V2X channel modelling, link types, vehicle types, and main propagation states are described in Figure 2.1 below. Environments can be divided qualitatively into highway, rural, and (sub)urban, with a word of caution: the division between environments is not an exact one, and the differences in certain cases might be hard to define. For example, rural and highway scenario differ in the number of lanes (typically larger in case of highways) and surroundings (typically more foliage in rural, guard rails more often existent in highways), but the two environments can also share a lot of characteristics. Furthermore, the impact of foliage cannot be neglected in any of the environments, as shown in measurements studies [ABV+16; BBT14].

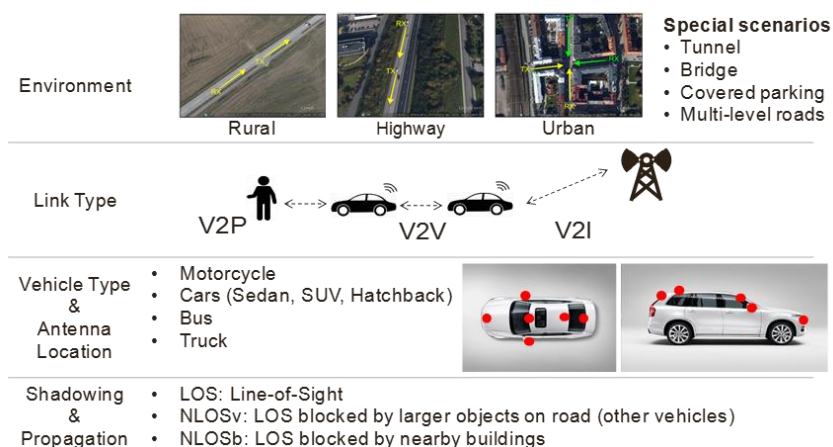


**Figure 2.1: Environments, link types, and specific considerations for V2X channel modelling.**



## 2.2 State of the Art Channel Models for V2X

The goal of this section is to define the most relevant state of art models available for use in the simulations across the 5GCAR project. Below we list the relevant channel modelling components.

### 2.2.1 Channel Modelling Framework and Gap Analysis

The technical report 3GPP TR 38.901: “Study on channel model for frequencies from 0.5 to 100 GHz” [3GPP17-38901] defines a Geometry-Based Stochastic (GBS) framework for channel modelling from 0.5 GHz to 100 GHz. It Specifies parameters for LOS probability, Path Loss (PL), Shadow Fading (SF), and Fast Fading (FF) and covers several scenarios: Urban Macro (UMa), Urban Micro (UMi), Indoor Office, and Rural Macro (RMa). The report is focused on BS-to-UE communication and does not explicitly address V2X channels. Specifically, the following components important for V2X are not covered:

- No dual mobility (V2V)
- No V2X-specific scenarios (RSU-Vehicle, V2V)
- No V2X antenna considerations
- No V2X-specific parameterization (especially for V2V)
- No PL, SF, FF for V2V
- No LOS probability and blockage evolution for V2V and V2P channels.

Components above are crucial for realistic modelling of vehicular channels. To enhance the 3GPP framework, this deliverable attempts at filling as many gaps as possible by using state of art literature on V2X channels and by also providing new channel parameterization based on recent measurements. In sections 2.2.2 to 2.2.4 we elaborate on specific components of V2X channel model, predominantly focusing on V2V case, since [3GPP17-38901] covers the Vehicle-to-Infrastructure (V2I) channels comprehensively (particularly the vehicle-to-base station case). More specifically, we describe the parameters to be included in [3GPP17-38901], as depicted in Figure 2.2 ranging from selecting the correct scenario (block 1) to LOS propagation condition (block 2), path loss (block 3), etc. In summary, we propose to use the framework in [3GPP17-38901] for all channel generations, whereas for specific components of the process, to use the parameters and models listed in sections 2.2.2 to 2.2.4.

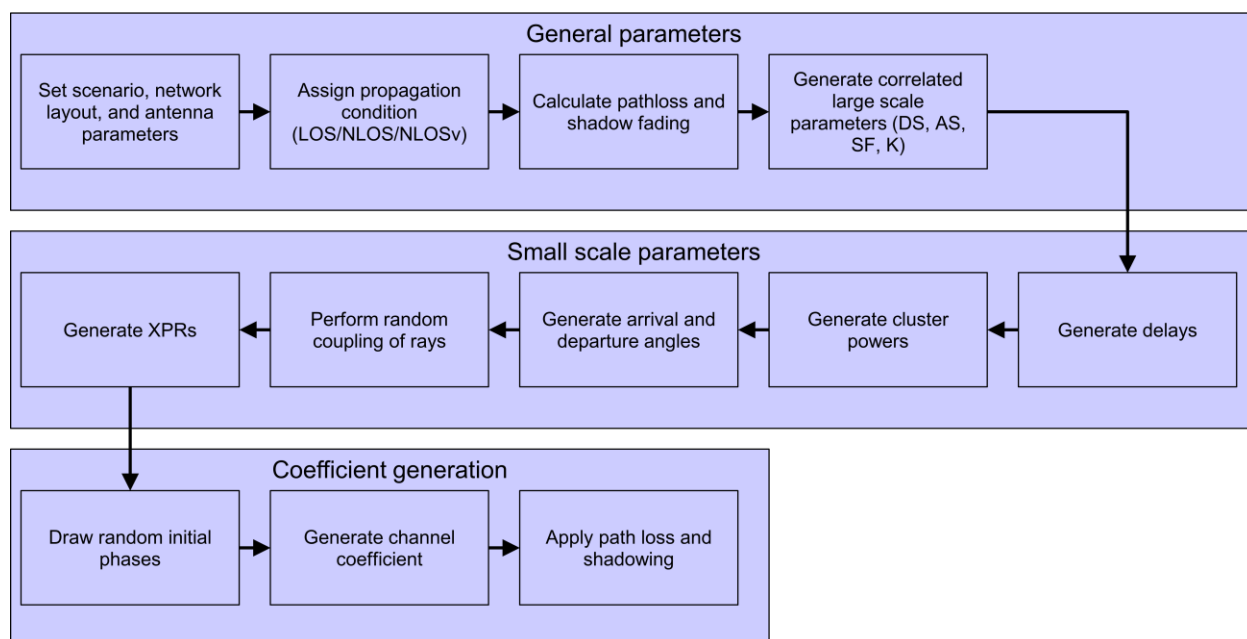


Figure 2.2: Channel Coefficient Generation Process based on [3GPP17-38901].

Table 2.1: Summary of the availability of V2X channel modelling aspects.

V2X channel model components & their availability in SOTA		Model exists / effect accounted for in state of art	
		<6GHz	>6GHz
Propagation Mechanism	• LOS blockage	+ V2X	+ V2X
	• Path loss	+ V2X	+ V2I; -V2V/P
	• Shadow fading	+ V2X	+ V2I; -V2V/P
	• Small-scale fading	+ V2X	+ V2I; -V2V/P
	• Correlated fading effects for single and multi-links	+ V2I/V; N/A V2P	+ V2I; -V2V/P
Modeling approach	• Non-geometry based (e.g., TDL)	+ V2I/V; - V2P	+ V2I/V; - V2P
	• Geometry based deterministic	+ V2X	+ V2I; - V2V/P
	• Geometry based stochastic	+ V2I/V; - V2P	+ V2I; - V2V/P
Model properties	Must have	Good to have	
	<ul style="list-style-type: none"> <li>• Spatial-temporal dependencies (esp. for V2V)</li> <li>• Non-stationarity (esp. for V2V)</li> <li>• Applicability</li> </ul>	<ul style="list-style-type: none"> <li>• Extensibility</li> <li>• Double-directional, antenna configuration dependency</li> <li>• Scalability and complexity</li> </ul>	

Legend: “+”: the model exists in the literature; “-“:the model does not exist in the literature

Table 2.1 provides a summary of the availability in the existing literature of models for specific propagation effect, along with desirable properties of the models. While it is difficult to provide a comprehensive summary, we attempt to identify which components of V2X channel modelling are available in well-defined, feasible channel models available in the literature.

### Assigning propagation condition for V2V channels – LOS blockage and evolution model

In relation to defining LOS/NLOS conditions in the different scenarios, there exists a need to model the transitions between different LOS states as described in [BGX16]. Realistic LOS blockage realization is required in order to assign the appropriate path loss, shadowing, small-scale, and large-scale parameters over time and space. LOS blockage modelling is particularly important for V2X communication, because of:

- High mobility, possibly on both sides of the link (e.g., in the case of V2V communication), resulting in more dynamic LOS blockage
- Have low antenna heights, resulting in more frequent LOS blockage
- V2X communication will be used for applications related to safety, either directly (e.g., emergency braking, intersection collision avoidance application, etc.) or indirectly (e.g., platooning, lane-change maneuvers, etc.). LOS blockage is critical for safety related applications because the reliability of the communication link suffers from sudden fluctuations of the received signal.

The work described in [BGX16] designs a time and space consistent model for LOS blockage of V2V channels. It models the evolution of states using Markov chain as shown in Figure 2.3. The three-state discrete-time Markov chain was used, comprised of the following states: i) Line-of-Sight (LOS), ii) Non-Line-of-Sight (NLOS) due to static objects, e.g., buildings, trees, etc. (NLOSb) and iii) non-LOS due to mobile objects (vehicles) (NLOSv). If the LOS is blocked by both a static object and a vehicle at the same time, we assume the static object (e.g., building) is the dominant one and categorize the channel as NLOSb. Results presented in [BGX16] showed significant difference compared to standard cellular models for LOS blockage, thus emphasizing the need for bespoke modelling of blockage for V2V links.

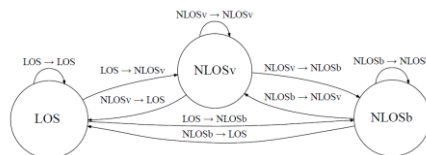


Figure 2.3: Markov chain for modelling the time evolution of V2V links [BGX16].

### LOS probability and transition probability curves

Based on the extensive ray-tracing simulations in real cities (combined Rome, New York, Munich, Tokyo, and London) with real road layout and realistic vehicle mobility simulation explained in [BGX16], Figure 2.4, Figure 2.5, Figure 2.6, and Figure 2.7 (all from [BGX16]), which show the extracted LOS probability and transition probability curves for the Markov model shown in Figure 2.3 depending on the distance between transmitting and receiving vehicle.

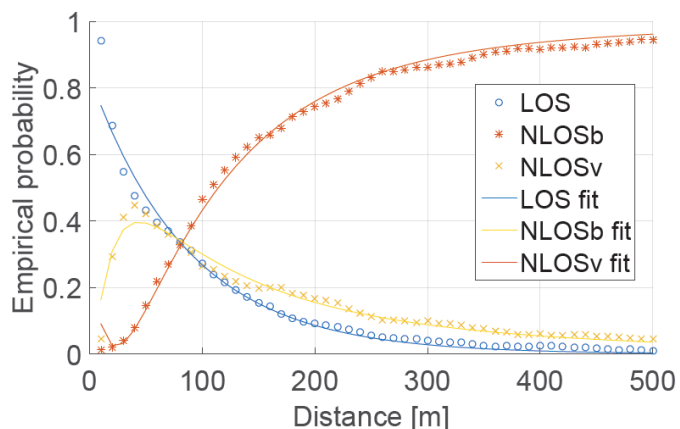


Figure 2.4: LOS probabilities in urban environment, medium density.

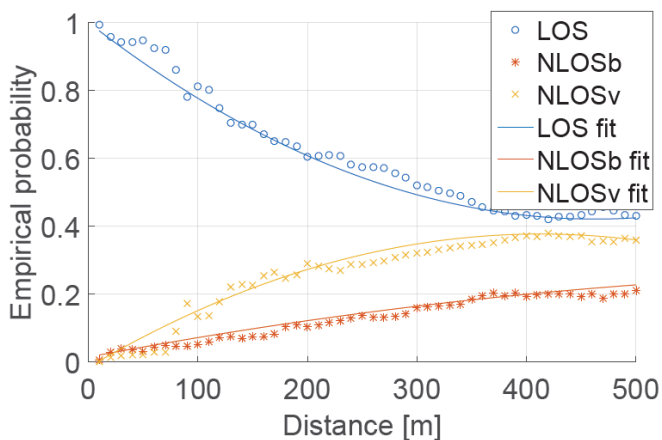
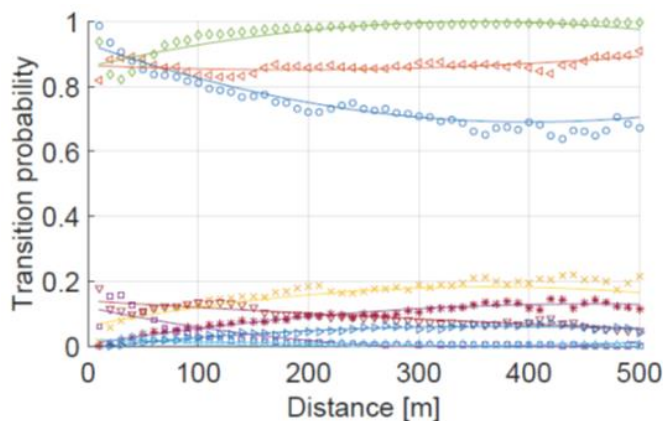
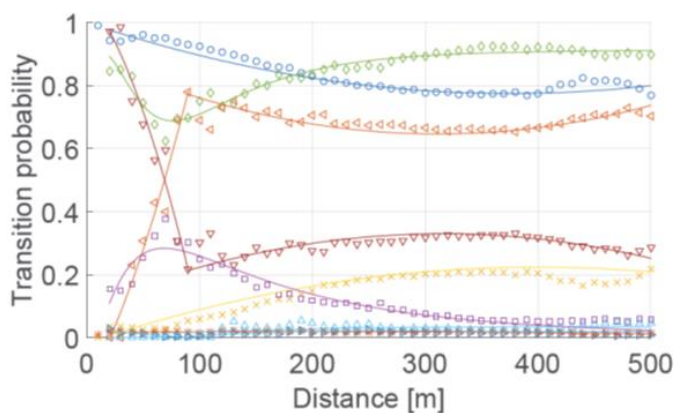


Figure 2.5: LOS probabilities on highway, medium density.



○ LOS->LOS \* LOS->NLOSb × LOS->NLOSv □ NLOSb->LOS ◇ NLOSb->NLOSb △ NLOSb->NLOSv ▽ NLOSv->LOS ▷ NLOSv->NLOSb ◁ NLOSv->NLOSv

Figure 2.6: Transition probabilities in urban environment, medium density.



○ LOS->LOS \* LOS->NLOSb × LOS->NLOSv □ NLOSb->LOS ◇ NLOSb->NLOSb △ NLOSb->NLOSv ▽ NLOSv->LOS ▹ NLOSv->NLOSb ◀ NLOSv->NLOSv

**Figure 2.7: Transition probabilities on A6 highway, medium density.**

As key take-away from these results, we derived a tractable model for the generation of time-evolved V2V links through curve fitting for LOS (Figure 2.4, Figure 2.5) and transition (Figure 2.6, Figure 2.7) probabilities. This resulted in two sets of equations, one from LOS probabilities curves (Table 2.2, from [BGX16]) and the second set for transition probabilities (Table III in [BGX16]).

**Table 2.2: LOS probability equations for highway and urban environment, medium density.**

LOS PROBABILITY FOR HIGHWAY AND URBAN ENVIRONMENT

**Highway: LOS probability  $y$  vs. distance  $d$**

$$y = \min(1, \max(0, ad^2 + bd + c))$$

Straight, highway-only part			
	a	b	c

LOS	$2.1013e^{-6}$	-0.002	1.0193
NLOSv	$P(NLOSv) = 1 - P(LOS)$		

Including on-ramp traffic			
	a	b	c

LOS	$2.7e^{-6}$	-0.0025	1
NLOSb	$-3.7e^{-7}$	0.00061	0.015
NLOSv	$P(NLOSv) = 1 - (P(LOS) + P(NLOSb))$		

**Urban: LOS probability  $y$  vs. distance  $d$**

$$d \geq 0 : y = \min(1, \max(0, f(d)))$$

LOS	$0.8372e^{-0.0114d}$
NLOSv	$\frac{1}{0.0312d} e^{\frac{-(\ln(d)-5.0063)^2}{2.4544}}$
NLOSb	$P(NLOSb) = 1 - (P(LOS) + P(NLOSv))$



Since LOS, NLOS, and NLOSv states were shown to have distinct path loss, shadowing, large-scale, and small-scale parameters [BBT14], when transitioning between states, it is necessary to avoid hard transitions in the adjacent channel realizations resulting from different path loss and fast fading parameters. To circumvent such hard transitions between all three states, the optional “soft LOS” state from [3GPP17-38901] can be considered to determine the PL and the channel impulse responses containing characteristics of the preceding and following state.

### **Path loss comparison of V2V LOS probability model with 3GPP/ITU Urban Micro (UMi) LOS probability model**

Since there are no comprehensive V2V link LOS blockage and transition probability models available in the literature, we compare the proposed model with the well-established 3GPP/ITU Urban Micro (UMi) LOS probability model, which is currently used by 3GPP for LOS probability of V2X and D2D links [3GPP17-38901]:

$$P(\text{LOS}) = \min\left(\frac{d_1}{d}, 1\right) \times \left(1 - e^{-\frac{d}{d_2}}\right) + e^{-\frac{d}{d_2}}$$

where  $d$  is distance between Tx and Rx,  $d_1$  is a parameter set to 18 meters, and  $d_2$  to 36 meters. For illustration purposes, we use the states generated by the two models to calculate the path loss for a Tx-Rx pair that moves apart at 1 m/s starting from 1 to 500 meters. We use the parameters for urban medium density. For LOS and NLOSb path loss parameters, we use the values based on measurements reported in [BBT14]. For NLOSv, we use the multiple knife-edge attenuation model described in [BBT14]. For clarity, we show path loss only (i.e., without additional log-normal distributed shadow fading). Figure 2.8 shows the path loss results for the proposed model and 3GPP UMi LOS probability model [3GPP17-38901]. Since UMi model does not model dependency on the previous LOS state, the number of transitions between the states is considerably higher than in the proposed model, particularly when the probability of LOS is close to 50% (i.e., between 50 and 100 meters). This is clearly an unrealistic behavior, since two vehicles will not move between LOS and NLOS states so rapidly. While Figure 2.8 shows a single realization of state changes and resulting path loss, we ran simulations for a large number ( $10^5$ ) of V2V pairs with distances between 0 and 500 m. UMi model resulted in an average state change every 5 seconds, while the proposed model averaged one state change every 17 seconds.



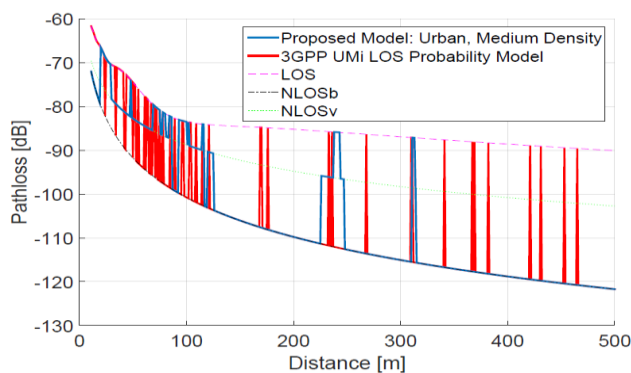


**Figure 2.8: Comparison of path loss generated by proposed model and 3GPP UMi LOS probability model for a single V2V link with Tx and Rx moving apart from 0 to 500 m with relative speed of 1 m/s [BGX16].**

For reference, path loss for LOS, NLOSv, and NLOSb states is plotted Figure 2.8 also indicates why models based on correlation distance for spatial consistency (e.g., model in Section 7.6.3 in [3GPP17-38901]) are not sufficient for modelling time- and space- evolved V2V links. Shadowing decorrelation distance in urban and highway environment for V2V links is on the order of tens of meters (e.g., [ASK+15] reports decorrelation distances of 5 m in urban and 30 m in highway environment) and is assumed to be independent of the Tx-Rx distance. However, Figure 2.8 shows that a single decorrelation distance value cannot capture the changing behavior as Tx-Rx distance changes: at low distances, the LOS decorrelation distance is high and decreases with increasing Tx-Rx distance, whereas NLOSb decorrelation distance increases with increasing Tx-Rx distance. By using distance-dependent transition probabilities, the proposed model is capable of capturing this behavior.

## 2.2.2 Path Loss Models

### Path loss for V2V LOS links

#### Free space path loss

The free space path loss model is the resulting loss in signal strength when the electromagnetic wave traverses from TX to RX through free space, without any obstacles nearby that could cause reflections or diffractions. The free space path loss FSPL is given by the equation

$$FSPL = 20 \log_{10}(d) + 20 \log_{10}(f) + 20 \log_{10} \left( \frac{4\pi}{c} \right) - G_{Tx} - G_{Rx}$$

where  $d$  is the distance between the transmitter and receiver in meter,  $f$  is the carrier frequency in Hz,  $G_{Tx}$  and  $G_{Rx}$  are the dimensionless gains of the transmitting and receiving antenna, respectively. Free space is a theoretical model which by itself does not model well the path loss for V2X channels since, at the very least, there are perturbations of the free space signal by the reflections coming from the road on which the vehicles travel.

### Two-ray ground reflection model

The free space propagation model assumes the existence of only the LOS ray. However, due to the inherent structure of the environment where V2V communication occurs – over the face of road surface – in case of LOS communication the propagation characteristics are most often influenced by at least two dominant rays: LOS ray and ground-reflected ray. Two-ray ground reflection model with appropriately adjusted reflection coefficient was shown as a very good path loss model for LOS V2V channels [KCP11; BVT13]. In this scenario, the LOS path interferes with the ground reflected path. The two rays arrive at the receiver with a different phase and a different power. The different phase leads to constructive and destructive interference depending on the distance,  $d$ , between the receiver and the transmitter, as shown in Figure 2.9. When increasing the distance between the transmitter and the receiver, the alternating pattern of constructive and destructive interference stops at break point  $d_b$ . From this distance onwards, the length difference between the two rays is smaller than half the wavelength and the small Angle of Arrival (AOA) on the ground causes a phase shift of  $180^\circ$  for the reflected wave, leading to destructive interference.

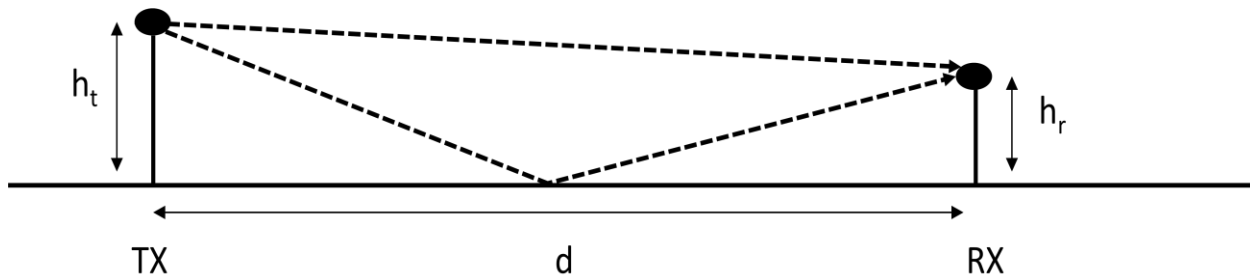


**Figure 2.9: The two-ray ground reflection model.**

For these two rays and referring to Figure 2.9 the resulting E-field is equal to:

$$E_{TOT} = E_{LOS} + E_{Ground} = \frac{E_0 d_0}{d_{LOS}} \cos \left[ \omega_c \left( t - \frac{d_{LOS}}{c} \right) \right] + R_{Ground} \frac{E_0 d_0}{d_{ground}} \cos \left[ \omega_c \left( t - \frac{d_{ground}}{c} \right) \right], \quad (1)$$

where  $E_{Ground}$  is the E-field of the ground-reflected ray,  $R_{Ground}$  is the ground reflection coefficient, and  $d_{ground}$  is the propagation distance of the ground-reflected ray, where  $h_t$  and  $h_r$  is the height of the transmitting and receiving antenna, respectively, and  $d_{LOS}$  is the ground distance between the antennas ( $d$  in Figure 2.9). Note that using the exact height of the antennas ( $h_t$  and  $h_r$ ) is important, since a small difference in terms of either  $h_t$  or  $h_r$  results in significantly different interference relationship between the LOS and ground-reflected ray. When the originating medium is free space, the reflection coefficient  $R$  is calculated as follows for vertical and horizontal polarization respectively:

$$R_{||} = \frac{-\epsilon_r \sin \theta_i + \sqrt{\epsilon_r - \cos^2 \theta_i}}{\epsilon_r \sin \theta_i + \sqrt{\epsilon_r - \cos^2 \theta_i}} \quad (2)$$

and

$$R_{\perp} = \frac{\sin \theta_i + \sqrt{\epsilon_r - \cos^2 \theta_i}}{\sin \theta_i + \sqrt{\epsilon_r - \cos^2 \theta_i}} \quad (3)$$

where  $\theta_i$  is the incident angle, and  $\epsilon_r$  is the relative permittivity of the material. From E-fields in eq.1, the ensuing received power  $P_r$  (in Watts) is calculated as follows (assuming unit antenna gain at the receiver):

$$P_r = \frac{|E_{TOT}|^2 \lambda^2}{4\pi\eta} \quad (4)$$

where  $\lambda$  is the wavelength and  $\eta$  is the intrinsic impedance ( $\eta = 120 \pi\Omega$  in free space). Appropriate reflection coefficient needs to be used to match the measurements. To that end in [BVT13] curve fitting of the above model to measurement data yielded  $\epsilon_r$  value of 1.003 as the best fit (note that remaining parameters in the calculation of reflection coefficient are dependent on geometry only).

### Path loss for V2V channels obstructed by vehicles: Vehicles-as-obstacles

When vehicles are causing the blockage to the LOS link, they induce additional attenuation. Model for vehicles-as – obstacles is described in [BVF+11], where vehicles are modelled using the (multiple) knife-edge diffraction. The model uses free space path loss model as the baseline, with additional attenuation due to each of the vehicles blocking the LOS link. Attenuation (in dB) due to a single knife-edge obstacle  $A_{sk}$  is obtained using the following equation:

$$A_{sk} = \begin{cases} 6.9 + 20 \log_{10} \left[ \sqrt{(v - 0.1)^2 + 1} + v - 0.1 \right]; & \text{for } v > -0.7 \\ 0; & \text{otherwise,} \end{cases} \quad (5)$$

where  $v = 21/2H/r_f$ ,  $H$  is the difference between the height of the obstacle and the height of the straight line that connects TX and RX, and  $r_f$  is the Fresnel ellipsoid radius (as shown in Figure 2.10).

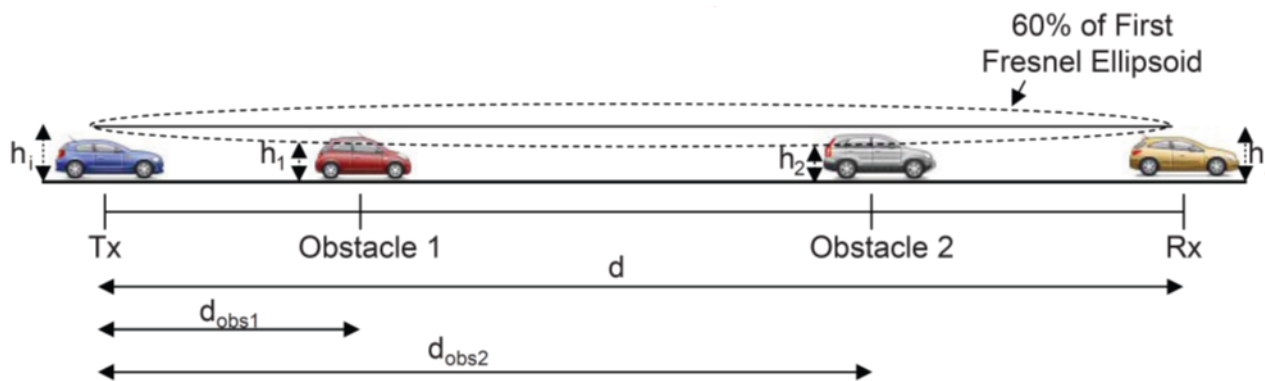


**Figure 2.10: Vehicles-as-obstacles path loss model (figure adapted from [BVF+11]).**

To calculate the attenuation due to multiple vehicles, the model employs the ITU-R multiple-knife diffraction method [ITU13]. Vehicles-as-obstacles model was validated experimentally and was shown to model well the path loss of V2V channels obstructed by other vehicles [BBT14].

## Path loss for V2V channels obstructed by buildings and other objects: Log-distance path loss model

Log-distance path loss is an extension of the free space path loss, where the path loss exponent does not necessarily equal two (as is the case in free space propagation) but is a function of the environment surrounding TX and RX.

Log-distance path loss model is formally expressed as:

$$PL(d) = PL(d_0) + 10\gamma\log(d/d_0) + X_\sigma$$

where PL is the total path loss measured in decibel (dB),  $PL(d_0)$  is the path loss at the reference distance  $d_0$ ,  $d$  is the distance between TX and RX,  $\gamma$  is the path loss exponent and  $X_\sigma$  describes the random shadowing effects.

Finally, the received power  $P_r$  is calculated as

$$P_r = P_t + G_t + G_r - PL(d)$$

where  $P_t$  is the transmit power and  $G_t$  and  $G_r$  are antenna gains in dBi. Log-distance path loss with appropriate path loss exponent and shadowing deviation was experimentally shown to model well the path loss for V2V links in non-LOS cases [BBT14]. For V2V links at 5.9GHz, the following values can be used [BBT14]:

- $d_0 = 1$  meter
- $PL(d_0) = 47.8649$  dB
- $\gamma = 2.5$  (slight obstruction by building)
- $\gamma = 3$  (strong obstruction by building).

### 2.2.3 Shadow Fading Models

#### Single-link shadow fading for V2V and V2I channels

In log-distance path loss equation, the value of standard deviation  $\sigma$  of the shadow fading variable  $X_\sigma(0, \sigma)$ , can be adjusted so that it better describes a specific environment and the link type. For V2V links, [BBT14] contains a detailed measurement-based analysis of  $\sigma$  for both highway and urban environments for the 6 GHz band. Furthermore, the code implementing both the path loss and shadow fading model is available at <http://vehicle2x.net/>. The values of  $\sigma$  are shown in Table 2.3.

**Table 2.3: Shadow-fading parameter  $\sigma$  for V2V communication (6 GHz band).**

Environment Link type	Highway	Urban
LOS	3.3 dB	5.2 dB
NLOSv	3.8 dB	5.3 dB
NLOSb	4.1 dB	6.8 dB

Due to the differences in terms of antenna height, scatterer density, and relative speed, V2I links exhibit different propagation characteristics compared to V2V links. Of particular importance is a subset of V2I links where the infrastructure end of a link is a roadside unit (RSU), since these links are distinguished compared to well-studied cellular V2I links. Aygun et al. [ABV+16] used measurement data collected in urban environment of Bologna to evaluate the shadow fading for four propagation conditions of RSUs V2I links: LOS, NLOS due to vehicles, NLOS due to foliage, and NLOS due to buildings (i.e., the non-LOS due to static objects -- NLOSb link type -- further divided to blockage due to buildings and blockage due to foliage). Assuming log-normal shadow fading process, the authors extract the resulting mean, minimum, and maximum of  $\sigma$ , the standard deviation of the shadow fading process. The summarized results are shown in Table 2.4, with following remarks: a) for highway environment, NLOSb state is not applicable; b) for the lack of measurements in highway, LOS and NLOSv results for urban environment are reused for highway as well.

**Table 2.4: Shadow-fading parameter  $\sigma$  for Vehicle-to-Roadside Unit (V2R) communication (6GHz band).**

Environment Link type		Highway	Urban
LOS		2.2dB	2.2dB
NLOSv		2.6dB	2.6dB
NLOSb	Buildings Foliage	N/A	3.3dB 2.4dB

### Multi-link shadow fading for V2V channels

Abbas et al. performed V2V measurements and showed that a single vehicle can incur more than 10 dB attenuation, in line with previous results. Based on the measurements, the authors designed a GBS propagation model for highway environments that incorporates vehicular obstructions and determines the time duration that the link spends in LOS and NLOS states. By extracting the probability distributions of each state from measurements, it uses a probabilistic model based on Markov chains to transition between different LOS conditions. The model demonstrates the importance of differentiating a LOS link from a NLOS link as well as energy contributed from LOS and NLOS rays. However, this model was developed for a single link communication and one important factor in VANET simulations, which is often neglected, is to include the cross-correlation of the different communication links. This is important for the wireless communication systems using multi-hop techniques to overcome the issue with shadowed vehicles in V2V systems. Two models are presented [Nil17] of the cross-correlation for a convoy scenario on a highway; one when using a joint path loss model for all communication links between all vehicles, including LOS and Non-LOS due to vehicles (NLOSv) cases (17), and another one when using a specific path loss model for each communication link, as well LOS and NLOSv separately (18). The auto- and cross- correlations do not affect the



average value of the received power if the data ensemble is big enough. However, the correlations will cause the system to experience longer large-scale fading dip durations compared to the uncorrelated case. This is especially important for VANET safety applications, where the consecutive packet error rate is a critical factor. The findings in [Nil17] regarding path loss models, autocorrelation behavior and the cross-correlation of the large-scale fading processes stress the benefits of GBM for VANET simulators. It is important that the geometry-based models distinguish between LOS and NLOS communication and apply different path loss models for the two cases. Otherwise the VANET simulator needs to consider the cross-correlation between different communication links i.e., implementing (17), to achieve results close to reality. On the other hand, when using a geometry-based model as an input to the VANET simulator, the cross correlation can actually be neglected and the implementation of (18) is not necessary. This is a very useful and practical result, since it makes it much easier to implement VANET simulators for multi-link scenarios. The computational complexity could easily become an issue if the cross-correlation between many links has to be considered.

#### **2.2.4 Fast-Fading Parameters**

For <6 GHz, we propose to use the parameters described in [AI07]. For >6GHz, we propose to use the shadow and fast fading parameters presented in Section 2.2.3 and in more detail in [3GPP18-1802721].

#### **2.2.5 Summary**

Table 2.5 below summarizes which models to use for each of the V2X channel modelling components as part of the channel modelling framework described in [3GPP17-38901]. By and large, for V2I channels the components in [3GPP17-38901] itself are suitable for use. On the other hand, LOS blockage, path loss, shadow fading, and fast fading in [3GPP17-38901] are not suitable for V2V channels; therefore, alternative parameterization for those components is proposed based on the existing literature. For any parameters not mentioned in Table 2.5, for initial evaluations, the existing parameters in [3GPP17-38901] can be used, with the note that some of the parameters (e.g., elevation angles) need to be revisited.



**Table 2.5: Summary of the channel modelling components to include into the framework in [3GPP17-38901].**

V2V						
	Urban			Highway		
<=6 GHz	LOS	NLOSv	NLOSb	LOS	NLOSv	NLOSb
LOS_blockage	[BGX16]			[BGX16]		
PL	[BBT14]	[BBT14]	[BBT14]	[BBT14]	[BBT14]	[BBT14]
SF	[BBT14; ASK+15]	[BBT14; ASK+15]	[BBT14; ASK+15]	[BBT14; ASK+15]	[BBT14; ASK+15]	[BBT14; ASK+15]
FF	[AI07]	[AI07]	[AI07]	[AI07]	[AI07]	[AI07]
>6 GHz						
LOS_blockage	[BGX16]			[BGX16]		
PL	[3GPP18-1802720]			[3GPP18-1802720]		
SF	[3GPP18-1802720]			[3GPP18-1802720]		
FF	[3GPP18-1802721]			[3GPP18-1802721]		
V2I (Vehicle-to-Base station: V2B)						
	Urban			Highway		
V2B <=6 & > 6GHz V2R > 6GHz	LOS	NLOS		LOS	NLOS	
LOS_blockage	[3GPP17-38901]					
PL						
SF						
FF						
V2I (V2R)						
	Urban			Highway		
V2R <= 6GHz	LOS	NLOSv	NLOSb	LOS	NLOSv	NLOSb
LOS_blockage	[3GPP17-38901]			[3GPP17-38901]		
PL	[BBT14]			[BBT14]		
SF	[ABV+16]			[ABV+16]		
FF	[3GPP17-38901]			[3GPP17-38901]		

---

## 2.3 Contributions in 5GCAR Beyond State of the Art

### 2.3.1 V2V Measurements in cmWave and mmWave

#### Measurement Set-up and Scenarios

Six channel measurement campaigns (indicated as C1-C5, C7) related to vehicle blockage and one (indicated as C6) related to building blockage have been carried out by the Electronic Measurements and Signal Processing group of the Technische Universität Ilmenau, Germany (TUIL) in the campus of the TUIL, at carrier frequencies of 6.75, 30 and 60 GHz. A dual-polarized ultra-wideband multi-channel sounder was used, which offers after back to back calibration a null-to-null bandwidth of 5.1 GHz. The spatial characterization of the environment has been done by automatically rotating dual-polarized horn antennas with 30° HPBW in 30° steps, covering the whole azimuth range at transmitter (Tx) and receiver (Rx). On the other hand, a single elevation of 0° was measured at both sides. The scenario was a “T” intersection in an urban environment with parked cars, multi-story buildings, and lampposts as shown in Figure 2.11.

In C1-C3, two parked cars were present during the measurements to increase the scattering effects. A third car, denominated blocking vehicle (labeled as obstructing car in Figure 2.11), was located in 15 different positions (Position 1-15 as indicated in Figure 2.11.) emulating an overtaking situation. Further, a Position 0 has been defined to indicate the case without the presence of the third car (the blocking vehicle). All the measurements were performed in a static scenario as possible by restricting the access of the streets. The Tx and Rx antennas were 44 m apart, emulating two cars communicating to each other. The antennas were located at two possible heights, emulating two possible antenna locations at cars: 1) Rooftop level antennas (1.55 m for the 30 GHz and 60 GHz bands, and 1.66 m for the 6.75 GHz band); 2) Bumper level antennas (0.75 m for the 30 GHz and 60 GHz bands, and 0.86 m for the 6.75 GHz band). Further, two types of blockers were used: 1) Small blocker (A Volkswagen Sharan - normal car); 2) Big blocker (a MB Sprinter - a delivery van). The following configurations have been used in C1-C3: C1 – Rooftop antennas and small blocker; C2 - Rooftop antennas and big blocker; C3 – Bumper antennas and small blocker.



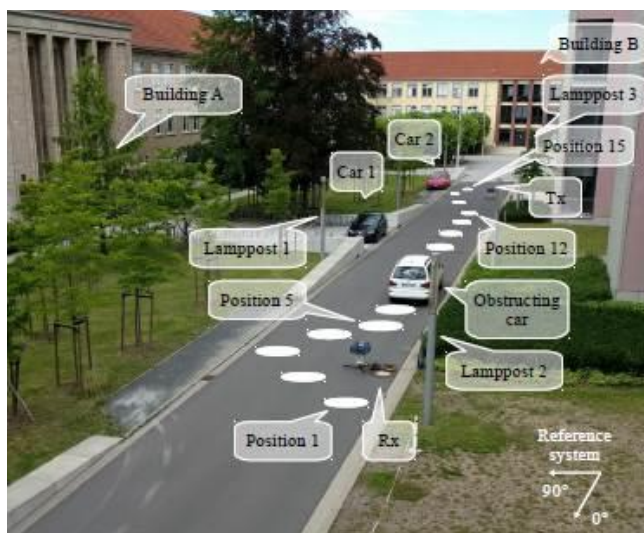


**Figure 2.11. Measurement scenario and set up of C1-C3 in the campus of TU Ilmenau.**

The campaigns C4, C5, C6, and C7 use only rooftop antennas. Figure 2.12 shows the scenario of C4, where the Tx was located in a fixed position and the Rx was moved away from 19 meter to 44 meter in 5 meter steps. A big blocking vehicle is located between Tx and Rx, with a fixed distance of 9.4 meter to the Tx. Two passenger cars are parked around the Tx. C7 is an extended version of C4, where the Rx was moved from 17 meter to 57 meter in 5 meter steps.

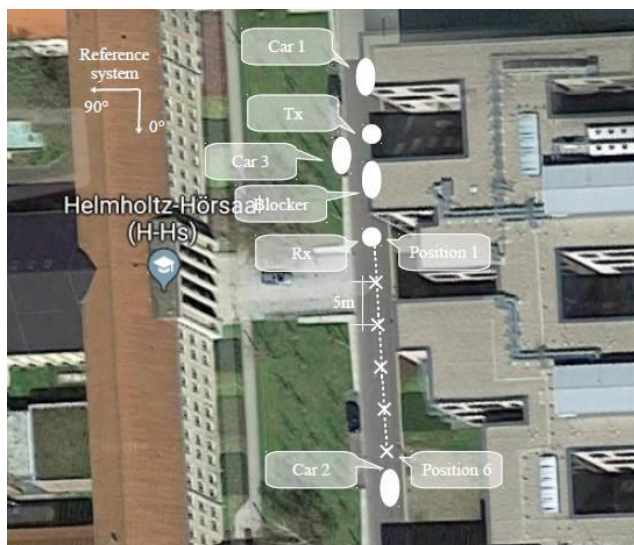


**Figure 2.12. Measurement scenario and set up of C4 in the campus of TU Ilmenau.**

Figure 2.13 shows the scenario of C5, where the Tx and Rx were located at fixed positions, with a Tx-Rx distance of 76.9 meters. Three different measurements were performed: A direct LOS, one blocking vehicle (big), two blocking vehicles (big and small). The distances of the first and second blocking vehicles to the Tx are 10.5 meters and 14.9 meters, respectively. There were also parked cars in the surrounding area.

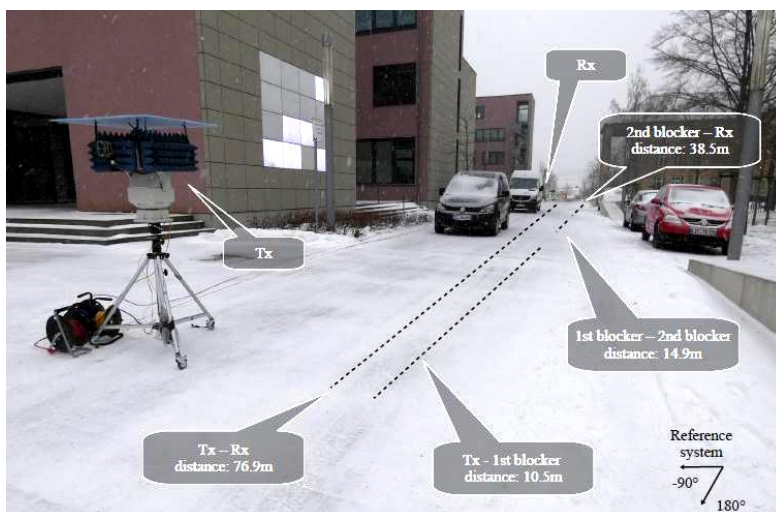


**Figure 2.13. Measurement scenario and set up of C5 in the campus of TU Ilmenau.**

Figure 2.14 shows the scenario of C6, where the Tx and Rx were located around the corner of a building. The Tx was fixed, while the Rx had different locations with 10 meter distance between neighboring ones. Position 1 represents LOS, position 2 represents a NLOS (obstructed LOS) by foliage, and position 3-5 NLOS by building. There were also two cars parked around the corner.



**Figure 2.14. Measurement scenario and set up of C6 in the campus of TU Ilmenau.**

## Measurement results

### Power Delay Profile (PDP)

The synthetic omni-directional PDP of each band for the Position 1 (as indicated in Figure 2.11) and Position 5 are plotted in Figure 2.15. All the plots normalized to the LOS component of the case where no vehicles are present. The dynamic range threshold of 25 dB is also displayed in dashed lines, which is used to identify the visible multipath components for a communication receiver and to calculate the delay spread. From Figure 2.15, we can clearly see strong multipath propagation. The actual scatterers in the environment (e.g. building A etc.) are identified and indicated in Figure 2.15.

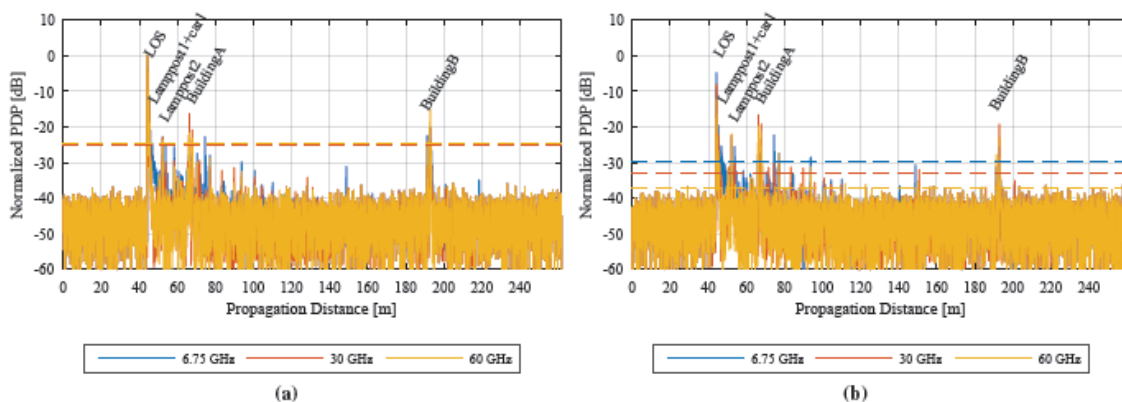


Figure 2.15. Synthetic Omni-directional PDP for (a) Position 1, and (b) Position 5 in C1.

The effect of the blockage on LOS and scatterers in the PDP can be observed in Figure 2.16. In Figure 2.16 (a), where the blocking vehicle is on the left-hand side of the Rx (Position 4), it can be observed that the reflection from the building A is attenuated, while the parked car 2 is still visible. In Figure 2.16 (b), where the blocking vehicle is in front of the Rx, i.e. blocking the LOS (Position 5), it can be observed that the building A component appears again, while the components of LOS, parked car 1, parked car 2, and lamppost 3 are attenuated.

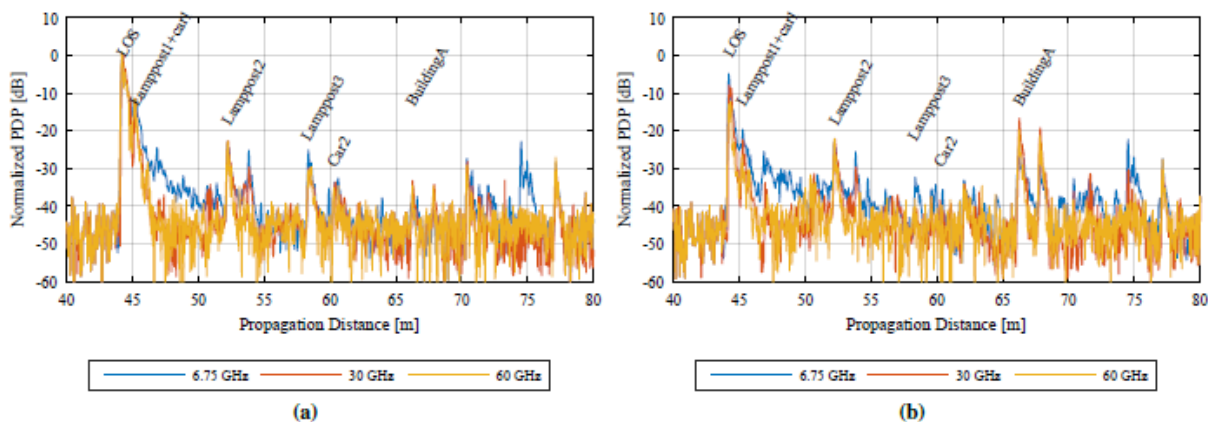


Figure 2.16. Detailed synthetic Omni-directional PDP for (a) Position 4, and (b) Position 5 in C1.

### Selected angular spread results

The marginal PAP of the positions 0 and 5 in C2 are shown in Figure 2.17 and Figure 2.18, respectively. While position 0 represents the LOS scenario, position 5 represents the scenario with vehicle blockage. Figure 2.19 (a) and (b) show the azimuth spread at the Rx and Tx of each position, respectively. As can be seen from Figure 2.17, Figure 2.18 and Figure 2.19, vehicle blockage causes increase in azimuth spread. Further, the closer the blockage vehicle is to the Tx or Rx, the more increase the azimuth spread at the Tx or Rx will have, respectively.

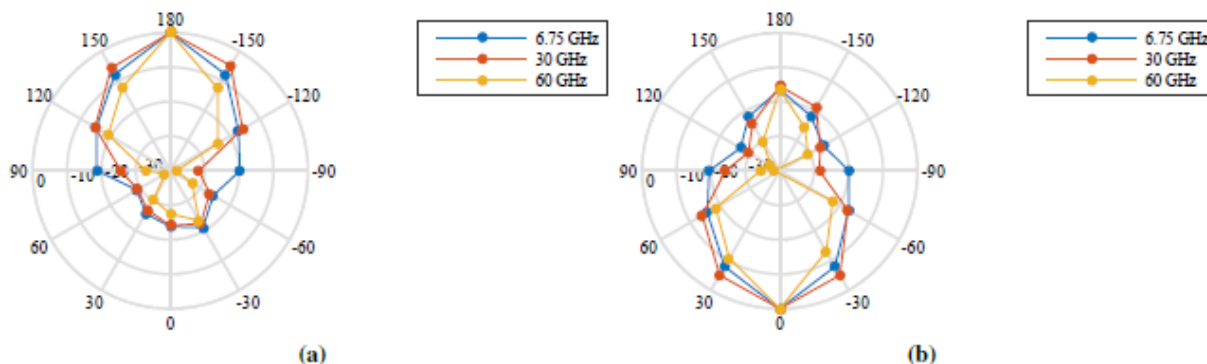


Figure 2.17. Marginal power azimuth profile at (a) Rx and (b) Tx for the Position 0 in C2.

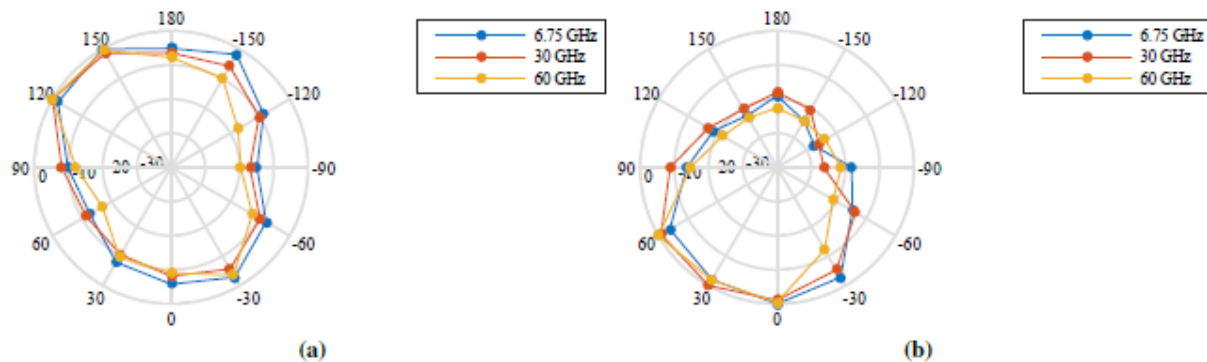


Figure 2.18. Marginal power azimuth profile at (a) Rx and (b) Tx for the Position 5 in C2.

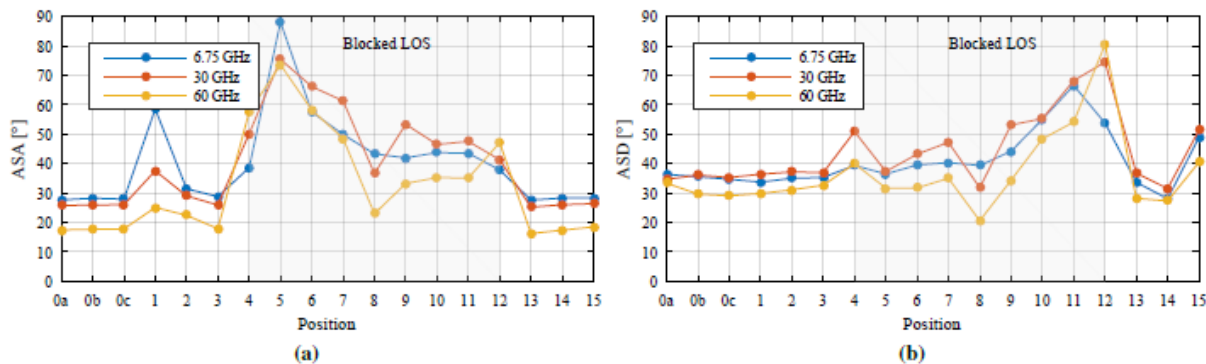


Figure 2.19. Azimuth spread at the (a) Rx and (b) Tx for the different positions and bands in C2.

### 2.3.2 mmWave V2V (Sidelink) Channel Modelling

#### Directional Channel Characterization

The above measurements can be used for directional channel characterization of mmWave V2V channels. Different scatterers were identified using the large resolution in the time domain and the different scans in the angular domain. The interpolated and normalized per position power bi-azimuthal profiles are shown for Position 0 (LOS) and Position 5 (NLOSv) in Figure 2.17 and Figure 2.18, respectively. In the Position 0 (Figure 2.17), the strongest scatterers are the LOS, building A, and a back reflection in the T intersection in building B. In the Position 5 (Figure 2.18), the LOS is completely blocked. The above results of directional characterizations show that NLOSv V2V propagation significantly increases the angular spread of MPCs at 60 GHz.

#### Path loss

The Alpha-Beta-Gamma (ABG) path loss (PL) model is applied in [3GPP18-1802720] for V2V channels in various urban and highway scenarios under LOS, and under building and vehicle blockage cases. Note that the ABG path loss model is currently used in the 3GPP 3D model [3GPP17-38901]. For the reason of aligning the V2V path loss modelling to [3GPP17-38901], we propose to use the path loss equations in [3GPP18-1802720].

The ABG PL model is given as:

$$PL^{ABG}(f, d)[dB] = 10\alpha \log_{10}(d) + \beta + 10\gamma \log_{10}(f) + X_{\sigma}^{ABG}$$

where  $\alpha$  captures how the PL increase as the transmit-receive in distance (in meters) increases,  $\beta$  is the floating offset value in dB,  $\gamma$  captures the PL variation over the frequency  $f$  in GHz, and  $X_{\sigma}^{ABG}$  is the SF term in dB. Formula above allows the fitting of the ABG path loss model for different environments. We note that that the models in [3GPP18-1802720] are multi-frequency models, with the parameters in the model extracted from measurements above-6GHz band (specifically, 6.75, 30, 60, and 73 GHz).



Table 2.6 presents the ABG model parameters at different scenarios for V2V links in LOS and NLOSb case, whereas Table 2.7 presents the vehicle blockage effect model for V2V (i.e., NLOSv case). Further details are available in [3GPP18-1802720]. Note that values  $\alpha < 2$  (free space) results from the curve fitting.

**Table 2.6: ABG model parameters for different scenarios at LOS and NLOSb.**

Scenarios		ABG Model Parameters
Urban grid	LOS	$\alpha = 1.67, \beta = 38.77, \gamma = 1.82, SF = 2.04\text{dB}$
	NLOSb	$\alpha = 2.38, \beta = 36.85, \gamma = 1.89, SF = 3.05\text{dB}$
Highway	LOS	$\alpha = 1.58, \beta = 37.9, \gamma = 2, SF = 3.13\text{dB}$
	NLOSb	$\alpha = 2.73, \beta = 25.98, \gamma = 2, SF = 3.47\text{dB}$

**Table 2.7: Path loss model for different scenarios at NLOSv.**

Scenarios		Separate for normal and large size vehicle		Combined for normal and large size vehicle
		Normal size (passenger car/ van)	Large size (truck/big van)	passenger car/ SUV/truck/big van
Urban grid	NLOSv	Mu = 5.86 Sigma = 3.08dB	Mu = 10.43dB Sigma = 4.48dB	Mu = 8.95 Sigma = 4.61
Highway	NLOSv	Mu = 4.77dB Sigma = 4.26dB	Mu = 15.39dB Sigma = 5.02dB	Mu = 10.08 Sigma = 7.06

### Shadow and fast fading parameter analysis

The dynamics of the blocked scatterers have significant impact on mmWave V2V channels. The mean and variance of the parameters have been calculated considering positions 0 to 3 and 13 to 15 as LOS, and positions 4 to 12 as NLOSv. The synthetic omnidirectional characteristic of the channel has been utilized to calculate the DS, shadow fading, and Rice K-factor. This is computed by averaging the PDPs from the different directional scans. Angular Spread (AS) has been calculated using the marginal power angular profiles. The values are summarized in Table 2.8 (based on [3GPP18-1802721]), showing that the DS and AS increase under blockage. On the other hand, due to the obstruction of the LOS component, the K-factor is reduced from approx. 10 dB to -5 dB. The mean vehicle blocking loss (mean additional attenuation due to



vehicle blockage in Position 4 to 12 compared to Position 0) is about 12 dB. For each of the states, Table 2.8 contains the parameters values extracted from the measurements explained in Section 2.3.1. and [3GPP18-1802721]. While the NLOS<sub>b</sub> state in urban environment is due to building blockage, in highway environment it is due to blocking by foliage. In Table 2.8, in the case of values in square brackets, parameters are taken from UMi model in [3GPP17-38901] (Table 7.5-6). In case when new measurement results do not contain a certain parameter for NLOS<sub>v</sub>, we reuse the value for NLOS state from UMi model in [3GPP17-38901] (Table 7.5-6) for both urban and highway scenario. Note again that UMi model parameters are used for a lack of better solution. To that end, some of the parameters (e.g., elevation angles) might need to be further investigated and updated, when appropriate measurements become available. Further details are available in [3GPP18-1802721].

**Table 2.8: Fast fading parameters for V2V sidelink.**

Scenarios		Urban			Highway	
		LOS	NLOS	NLOS <sub>v</sub>	LOS	NLOS <sub>v</sub>
Delay Spread (DS) lgDS=log <sub>10</sub> (DS/1s)	$\mu_{lgDS}$	-0.2 log <sub>10</sub> (1+fc) - 7.5	-0.3 log <sub>10</sub> (1+fc) - 7	-0.4 log <sub>10</sub> (1+fc) - 7	-8.3	-8.3
	$\sigma_{lgDS}$	0.1	0.28	0.1	0.2	0.3
AOD Spread (ASD) lgASD=log <sub>10</sub> (ASD/1°)	$\mu_{lgASD}$	-0.1 log <sub>10</sub> (1+fc) + 1.6	-0.08 log <sub>10</sub> (1+fc) + 1.81	-0.1 log <sub>10</sub> (1+fc) + 1.7	1.4	1.5
	$\sigma_{lgASD}$	0.1	0.05 log <sub>10</sub> (1+fc) + 0.3	0.1	0.1	0.1
AOA Spread (ASA) lgASA=log <sub>10</sub> (ASA/1°)	$\mu_{lgASA}$	-0.1 log <sub>10</sub> (1+fc) + 1.6	-0.08 log <sub>10</sub> (1+fc) + 1.81	-0.1 log <sub>10</sub> (1+fc) + 1.7	1.4	1.5
	$\sigma_{lgASA}$	0.1	0.05 log <sub>10</sub> (1+fc) + 0.3	0.1	0.1	0.1
ZOA Spread (ZSA) lgZSA=log <sub>10</sub> (ZSA/1°)	$\mu_{lgZSA}$	-0.1 log <sub>10</sub> (1+fc) + 0.73	-0.04 log <sub>10</sub> (1+fc) + 0.92	-0.04 log <sub>10</sub> (1+fc) + 0.92	-0.1 log <sub>10</sub> (1+fc) + 0.73	-0.04 log <sub>10</sub> (1+fc) + 0.92
	$\sigma_{lgZSA}$	-0.04 log <sub>10</sub> (1+fc) + 0.34	-0.07 log <sub>10</sub> (1+fc) + 0.41	-0.07 log <sub>10</sub> (1+fc) + 0.41	-0.04 log <sub>10</sub> (1+fc) + 0.34	-0.07 log <sub>10</sub> (1+fc) + 0.41
ZOD Spread (ZSD) lgZSD=log <sub>10</sub> (ZSD/1°)	$\mu_{lgZSD}$	-0.1 log <sub>10</sub> (1+fc) + 0.73	-0.04 log <sub>10</sub> (1+fc) + 0.92	-0.04 log <sub>10</sub> (1+fc) + 0.92	-0.1 log <sub>10</sub> (1+fc) + 0.73	-0.04 log <sub>10</sub> (1+fc) + 0.92
	$\sigma_{lgZSD}$	-0.04 log <sub>10</sub> (1+fc) + 0.34	-0.07 log <sub>10</sub> (1+fc) + 0.41	-0.07 log <sub>10</sub> (1+fc) + 0.41	-0.04 log <sub>10</sub> (1+fc) + 0.34	-0.07 log <sub>10</sub> (1+fc) + 0.41
K-factor (K) [dB]	$\mu_K$	3.48	N/A	0	9	0
	$\sigma_K$	2	N/A	4.5	3.5	4.5
Cross-Correlations	ASD vs DS	0.5	0	0.5	0.5	0.5
	ASA vs DS	0.8	0.4	0.8	0.8	0.8
	ASA vs SF	-0.4	-0.4	-0.4	-0.4	-0.4
	ASD vs SF	-0.5	0	-0.5	-0.5	-0.5
	DS vs SF	-0.4	-0.7	-0.4	-0.4	-0.4
	ASD vs ASA	0.4	0	0.4	0.4	0.4
	ASD vs K	-0.2	N/A	-0.2	-0.2	-0.2
	ASA vs K	-0.3	N/A	-0.3	-0.3	-0.3



	<i>DS vs K</i>	-0.7	N/A	-0.7	-0.7	-0.7
	<i>SF vs K</i>	0.5	N/A	0.5	0.5	0.5
Cross-Correlations	<i>ZSD vs SF</i>	0	0	0	0	0
	<i>ZSA vs SF</i>	0	0	0	0	0
	<i>ZSD vs K</i>	0	N/A	0	0	0
	<i>ZSA vs K</i>	0	N/A	0	0	0
	<i>ZSD vs DS</i>	0	-0.5	0	0	0
	<i>ZSA vs DS</i>	0.2	0	0.2	0.2	0.2
	<i>ZSD vs ASD</i>	0.5	0.5	0.5	0.5	0.5
	<i>ZSA vs ASD</i>	0.3	0.5	0.3	0.3	0.3
	<i>ZSD vs ASA</i>	0	0	0	0	0
	<i>ZSA vs ASA</i>	0	0.2	0	0	0
	<i>ZSD vs ZSA</i>	0	0	0	0	0
	Delay scaling parameter $r_t$		3	2.1	2.1	3
XPR [dB]	$\mu_{XPR}$	9	8.0	8.0	9	8.0
	$\sigma_{XPR}$	3	3	3	3	3
Number of clusters $N$		12	19	19	12	19
Number of rays per cluster $M$		20	20	20	20	20
Cluster $DS$ ( $C_{DS}$ ) in [ns]		5	11	11	5	11
Cluster $ASD$ ( $C_{ASD}$ ) in [deg]		3	10	10	3	10
Cluster $ASA$ ( $C_{ASA}$ ) in [deg]		17	22	22	17	22
Cluster $ZSA$ ( $C_{ZSA}$ ) in [deg]		7	7	7	7	7
Per cluster shadowing std $\zeta$ [dB]		4	4	4	4	4
Correlation distance in the horizontal plane [m]	<i>DS</i>	7	10	10	7	10
	<i>ASD</i>	8	10	10	8	10
	<i>ASA</i>	8	9	9	8	9
	<i>SF</i>	10	13	13	10	13
	<i>K</i>	15	N/A	N/A	15	N/A
	<i>ZSA</i>	12	10	10	12	10
	<i>ZSD</i>	12	10	10	12	10
$f_c$ is carrier frequency in GHz. Procedure for generating both ZOA and ZOD is the same and based on the ZOA procedure in 3GPP TR38.901.						

### 2.3.3 Multi-Link Shadowing Extensions

For realistic performance evaluation of V2V communication systems, it is crucial that the channel models used for system simulations are realistic and cover all important aspects of the NLOS case in urban intersections. In [NGA+18] path loss and fading parameters for vehicles of different kinds and sizes are provided, addressing multilink shadowing effects in urban intersections. As well, auto-correlation properties of a single link and cross-correlation properties of the large scale fading between different links are analyzed in [NGA+18]. A NLOS channel gain model which consider that a communication link can be obstructed by other vehicles (NLOSv) and which is reciprocal is described as



$$G(d_t, d_r)|_{\text{dB}} = \underbrace{10\log_{10}(m^2)}_{\text{Offset}} + \Psi_\sigma + 10\log_{10} \left( \underbrace{\left( g_1 \frac{\lambda}{4\pi(d_t + d_r)} \right)^2}_{\text{Single interactions}} + \underbrace{\left( g_2^N \frac{\lambda}{4\pi(d_t + d_r)} \right)^2}_{\text{Multiple interactions}} \right)$$

where

$$N = \max\left\{2\sqrt{\frac{d_t d_r}{w_t w_r}} - 1, 0\right\}$$

and where the width of the streets at which the transmitting and receiving vehicles are located are denoted by  $w_t$ ,  $w_r$ , and  $d_t$ ,  $d_r$  are the distances to the intersection center. The term  $\Psi_\sigma$  represent the large-scale fading and is modeled as a non-zero mean Gaussian process (which is not the common case) for each communication link and iteration (repetitive measurement runs in the same intersection). The mean of  $\Psi_\sigma$  has a Gaussian distribution that represents the differences in the particular traffic situation and gain of the involved antennas for the particular communication link during that specific iteration. Estimated parameters of  $g_1$ ,  $g_2$ ,  $m$ , and  $\sigma$  for two different intersections, Yngve (T-crossing with buildings in two corners) and Xerxes (X-crossing with buildings in four corners) are presented in Table 2.9 and a schematic description of the channel gain model is shown in the Figure 2.20.

**Table 2.9: Estimated parameters of the NLOS model.**

Link type	Yngve				Xerxes			
	$g_1$ [dB]	$g_2$ [dB]	$m$ [dB]	$\sigma$ [dB]	$g_1$ [dB]	$g_2$ [dB]	$m$ [dB]	$\sigma$ [dB]
Truck-to-truck	-6.12	-1.05	-3.31	4.92	-58.02	-1.96	4.55	4.34
Truck-to-car	-9.63	-2.00	1.03	7.38	-14.18	-3.36	8.78	5.07
Car-to-car	-9.08	-1.45	-2.47	4.39	-47.41	-2.05	3.67	4.27
Truck-to-Obstructed car	-51.07	-1.01	-5.33	5.57	-12.17	-3.40	6.42	4.24
Car-to-Obstructed car	-61.51	-1.62	-3.61	5.11	-15.68	-3.34	6.81	4.72

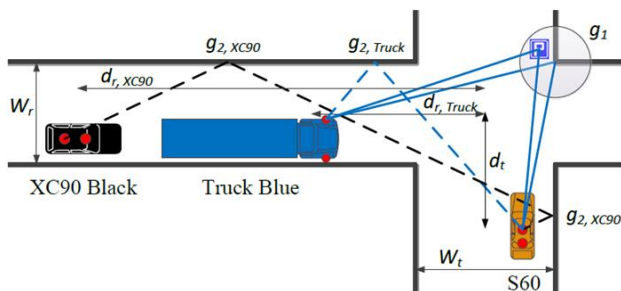


**Figure 2.20: Description of the channel gain model for a typical NLOS communication link between vehicles in an urban intersection.**

The solid blue lines in Figure 2.20 represent single interactions from the center area of the intersection which are only seen by Truck Blue and the S60. The XC90 Black is blocked by Truck Blue and has NLOS towards the intersection center, therefore it has no single interactions towards the S60. Dashed lines represent multiple interactions between the S60 and the Truck Blue and between the S60 and the XC90 Black, respectively.

The large-scale fading,  $\Psi_\sigma$ , is achieved by subtracting the distance dependent mean from the overall channel gain. Then, the spatial autocorrelation of the large-scale fading can be written as

$$r(\Delta d_i) = E\{\Psi_\sigma(d_i)\Psi_\sigma(d_i + \Delta d_i)\},$$

where  $d_i$  is the Manhattan-distance (distance following the street) between TX and RX. The autocorrelation of the shadowing process can be approximated by a well-known model proposed by Gudmundson, based on a negative exponential function,

$$r(\Delta d_i) = \sigma^2 e^{-|\Delta d_i|/d_c} = \sigma^2 \rho(\Delta d_i).$$

In Figure 2.21 the histograms of the decorrelation distance for the two intersections are shown.

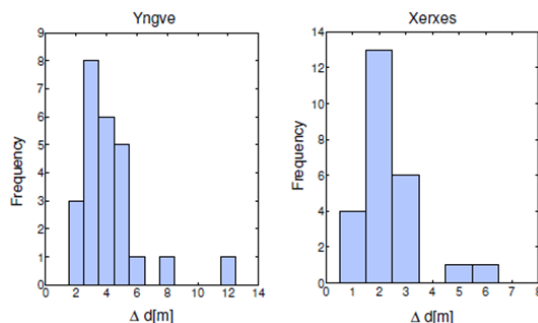


**Figure 2.21: Histograms of the de-correlation distances of all NLOS communication links in the intersections Yngve and Xerxes.**

By using the proposed channel gain model [NGA+18], the analysis shows that the cross-correlations between different links are small, even for communication links with antennas located at the same vehicle (values  $\rho$  in Figure 2.22). With the possibility to neglect the cross-correlation, will make the implementation of realistic models in VANET simulations much easier.

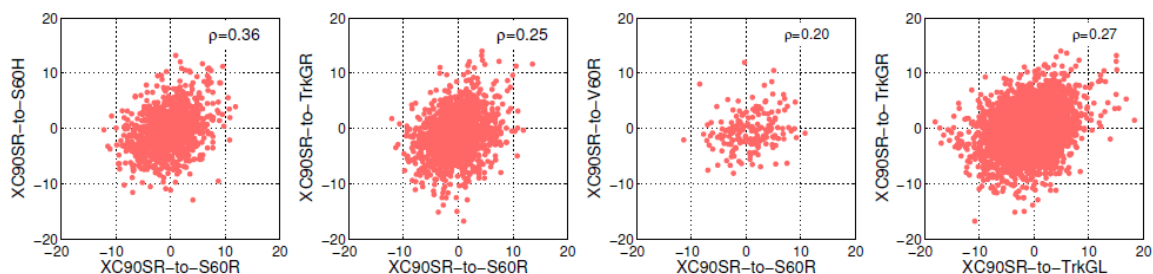


**Figure 2.22: Multilink shadowing correlation between different links in intersection Yngve.**



The x-axis for the first three subfigures represents the link between XC90 Silver Roof antenna to S60 Roof antenna, the y-axis represents the communication between XC90 Silver roof and one antenna on each vehicle in the other convoy. The last subfigure shows the cross-correlation of the links between XC90 Silver Roof and the two antennas on Truck Gold. Note, both the first from left and last scatter plots are cross-correlation when using different antennas on the same vehicle.

## 2.4 New Channel Measurements for Predictor Antenna for M-MIMO Adaptive Beamforming

This section summarizes the methodology that has been used to make new channel measurements that are detailed in [PWB+18]. The exploitation of these measurements for the assessment of the Predictor Antenna for M-MIMO Adaptive Beamforming is depicted in [5GC18-D31].

Adaptive Massive Multiple Input Multiple Output (M-MIMO) is a key feature of 5G [RPL+13], [JMZ+14]. Adaptive M-MIMO exploits a large number of antenna elements at the network side and performs downlink adaptive beamforming, either to reduce the radiated energy for a given target data rate (with maximum ratio transmission beamforming for instance) or to increase the spectral efficiency for a given transmit power (with for instance zero forcing beamforming).

However, M-MIMO performance is known to be very sensitive to channel aging [TH13], [PHH13]. Indeed, between the time when the network measures the channel  $h_p$ , and the time when the network transmits data to the vehicle through the channel  $h_m$ , there is a time delay  $\tau$ , so the vehicle has moved by a displacement  $\delta = v\tau$ , where  $v$  is the velocity of the vehicle. The network uses  $h_p$  as a prediction of  $h_m$ , and computes the downlink beamforming coefficients based on this prediction. Hence,  $\tau$  is a required “prediction horizon”. An estimate of  $h_m$  is an accurate prediction of  $h_p$  if the following three conditions (which are all equivalent to each other) are met:

$$\delta \ll \lambda,$$

$$\tau \ll \frac{c}{fv},$$

$$v \ll \frac{c}{f\tau},$$

where  $\lambda$  is the carrier wavelength,  $c$  is the speed of light and  $f$  is the carrier frequency. If these conditions are not met, then the channel is outdated. Figure 2.23 illustrates the case where  $\delta = \lambda$ .

Legend

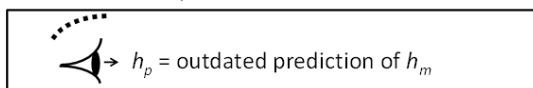
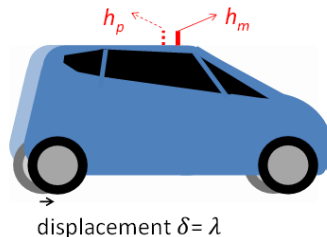
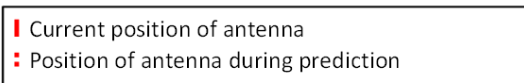


**Figure 2.23: Outdated channel prediction.**

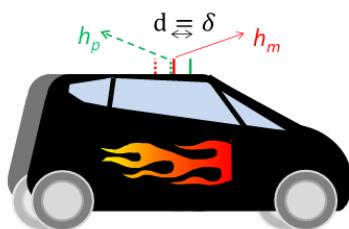
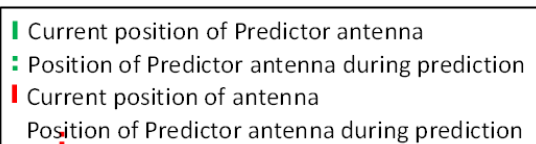
For M-MIMO, because of multi-path propagation and scattering around the vehicle, the effect of beamforming mis-pointing is large even with a small  $\delta$  [PSS15].

The most efficient known way to perform channel prediction for a single vehicle antenna consists of accumulating several successive measurements (several  $h_p$ 's) and using Kalman filtering and extrapolation to predict  $h_m$  [Aro11; EAS02; Ekm02; DH07]. Such a strategy has recently been applied to adaptive M-MIMO [KMB+07]. However, in most fading environments, it works only for limited horizons of at most half a wavelength, i.e. only for:

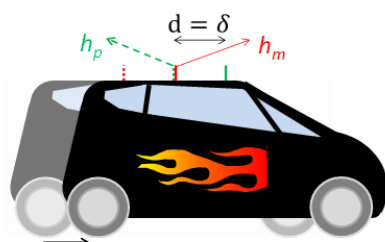
$$\begin{aligned} \delta &< 0.5\lambda, \\ \tau &< 0.5 \frac{c}{fv}, \\ v &< 0.5 \frac{c}{f\tau}. \end{aligned}$$

Recently, a different approach has been proposed that uses a “Predictor Antenna” [SGA+12; JAB+14; BSG17; BSG17; PSS15]. In this approach, illustrated in Figure 2.24, a “Predictor Antenna” is placed at the front of the “Main Antenna”, aligned with the direction of movement of the vehicle. In the case where the inter-antenna spacing  $d$  is larger or equal to  $\delta$ , as illustrated in Figure 2.24-a) and Figure 2.24-b), even though  $\delta$  is close to or higher than  $\lambda$ , the prediction can, in theory, be accurate. In general,  $d$  should be selected so that the longest prediction horizon in time that is required by the communication system should correspond to a movement of at most  $d$  in space, at the maximum vehicle velocity. This approach exploits the fact that the “Predictor Antenna” and the “Main Antenna” experience the same channel, when they occupy the same position in space, but simply at different moments in time. Note that this does not contradict the fact that, at a given moment in time, the two antennas of a vehicle see different channels (this has been observed in Section 2.3.3).

Legend



a) displacement  $\delta \sim 0.8\lambda$



b) displacement  $\delta \sim 3\lambda$

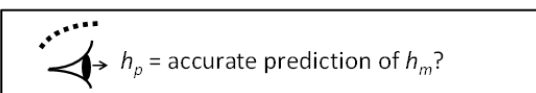


**Figure 2.24: Predictor Antenna that accommodates a prediction horizon that corresponds to a) a displacement  $\delta \sim 0.8\lambda$  and b) a displacement  $\delta \sim 3\lambda$ .**

The accuracy of this novel prediction method has been studied using experimental measurements from drive-tests in [SGA+12; JAB+14; BSG17; BSG17-2]. These results show that the predictor antenna provides a channel prediction that can obtain useful prediction accuracy for a prediction horizon (at least  $3\lambda$ ), that is an order of magnitude longer than when using Kalman/Wiener extrapolation (typically up to  $0.3\lambda$ ). The attainable Normalized Mean Square Errors (NMSE) of predicted complex valued OFDM channel coefficients was around -10 dB in these experiments and holds fairly constant for an increasing  $\delta$ . In [BSG17-2], a real-time prediction algorithm exploiting the Predictor Antenna that does not require  $\delta$  to be equal to  $d$  is proposed and it exhibits a good performance. However, all these studies were so far limited to Single Input Single Output (SISO) systems. Use of predictor antennas has been studied for M-MIMO, but so far only based on simulations in [PSS15; PSS+16].

For the first-time experimental measurements from drive-tests will be used to measure whether the predictor antennas can provide a gain when Maximum Ratio Transmission (MRT) or Zero Forcing for a prediction horizon of 3 wavelengths (as illustrated in Figure 2.24-b) for massive MIMO downlinks.

## Measurement Set-Up

The channel measurements were conducted on the Nokia Bell Labs campus in Stuttgart, Germany.

At the network side, a 64-element antenna array was mounted on the roof top of a large building at a height of 20m with a mechanical downtilt of 10 degrees. As shown in Figure 2.25, the array consisted of 4 rows with 16 (dual-polarized, but only one polarization direction was used) patch antennas each, with a horizontal antenna spacing of  $\lambda/2$ , and a vertical separation of  $\lambda$ . The array transmitted an Orthogonal Frequency Division Multiplex (OFDM) waveform of around 10 MHz bandwidth, at the carrier frequency of 2.180 GHz. The sub-carrier spacing was 15 kHz. In total, 600 sub-carriers are transmitted, and 64 Time/Frequency-orthogonal pilots are used for estimating channels from all the 64 antenna elements. The pilot signals were transmitted with a periodicity of 0.5 ms.



**Figure 2.25: Massive MIMO antenna of 64 antenna elements (4 lines and 16 columns of antenna elements) on the roof of a building of Nokia Bell Labs campus in Stuttgart.**

At the vehicle side, the measurement set-up consisted of a Pendulum GPS-12R Portable unit, a Rohde & Schwarz TSMW receiver and a Rohde & Schwarz IQR hard disk recorder. As receive antenna we used two monopole antennas that are illustrated in Figure 2.26-b), and positioned as in Figure 2.24-a) and Figure 2.24-b). These antennas were mounted on metallic plane installed upon the roof of the vehicle, as illustrated in Figure 2.26-a). Based on the GPS signal, the receiver was time/frequency synchronized to the transmit array and captured the received pilot signal along each route continuously over periods of 30 s to 40 s.

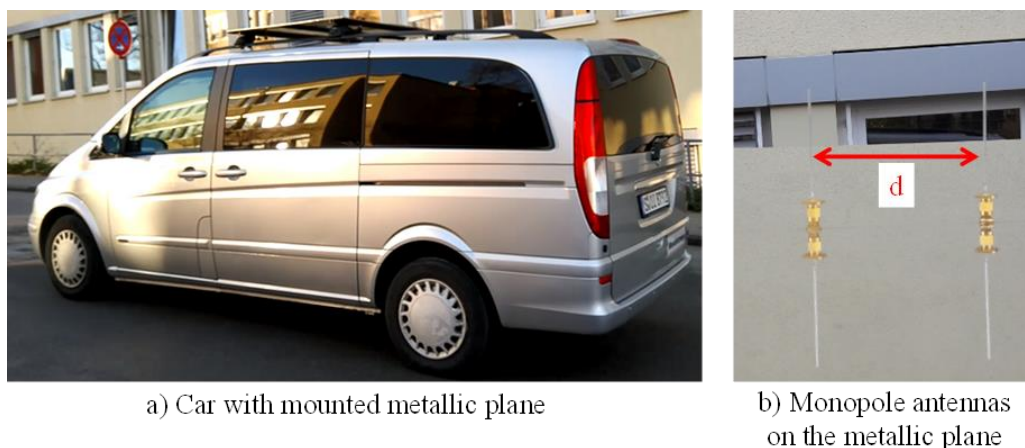


**Figure 2.26: Antennas on the roof of the vehicle.**

Drive-tests have been made over Route 2 illustrated in Figure 2.27. The position of the M-MIMO antenna is illustrated in Figure 2.27 and Figure 2.28. The velocity during the drive-tests was below 30 km/h. During the drive-tests, the channel between the 64 antenna elements of the M-MIMO and the two receive antennas of the vehicle has been measured for each of the 600 subcarriers spaced by 15 kHz, every 0.5 ms and stored, together with their time-stamps.

Finally, for each block of 180kHz, some sub-carriers were left empty. These are used to measure the receiver noise power, to deduce the receive Signal-to-Noise Ratio (SNR) and the noise-free receive signal power.

These channel measurements have been exploited to compute the beamforming gain with and without the Predictor Antenna in [5GC18-D31; PWB+18].

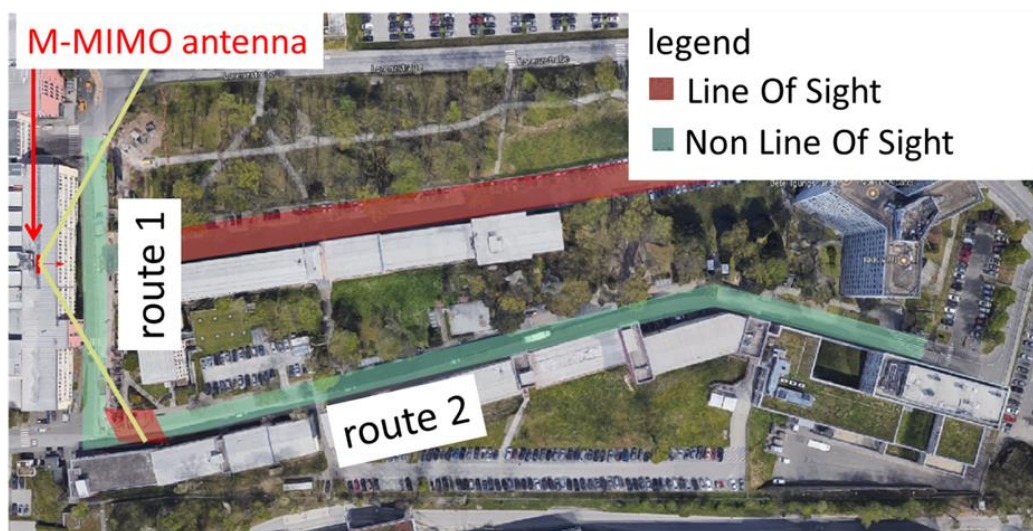


**Figure 2.27: M-MIMO antenna, Route 1 and Route 2.**

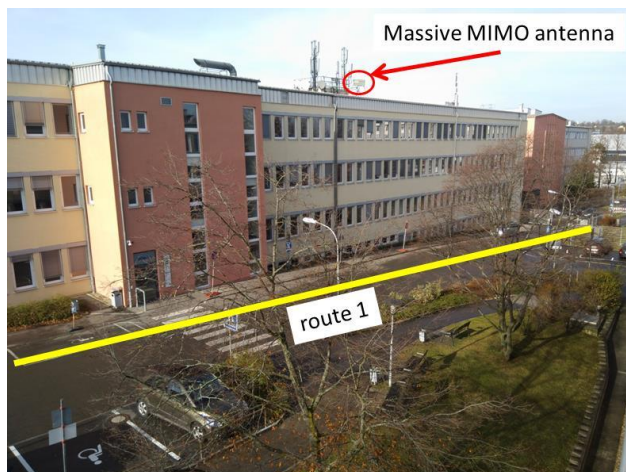


Figure 2.28: M-MIMO antenna, Route 1.

## 2.5 Status of Standardization and Contributions of 5GCAR

The intention of this section is to summarize the status of V2X channel modelling in 3GPP standardization and assess the proposed solutions in this deliverable with respect to 3GPP channel models.

3GPP, in RAN plenary meeting #76, agreed the Study Item (SI) “Study on evaluation methodology of new V2X use cases for LTE and NR” [3GPP17-171093]. This SI targeted to further improve the evaluation methodology of LTE V2X and finalize it for NR-based V2X. Consecutive email discussions (summarized in [3GPP17-1715092; 3GPP17-1717293; 3GPP17-1721545]) were conducted for the survey of specific issues on the eV2X evaluation methodology, and discussions went on in RAN1 meetings. The SI was completed by RAN plenary meeting #80, resulted into a technical report [3GPP18-37885] and concluded on the following elements:

- Identification of the regulatory requirements and design considerations of potential operation of direct communications between vehicles in spectrum allocated to ITS beyond 6 GHz
- Evaluation scenarios including performance metric, vehicle dropping, traffic model
- Sidelink channel model for spectrum above 6 GHz.

Regarding specifically the channel model, the SI’s focus was on the sidelink channel model for spectrum above 6 GHz but several agreements were made for below 6 GHz spectrum as well. As of 3GPP RAN1 #93, May 2018, the following agreements have been made regarding channel models for NR V2X [3GPP18-180909]:

- The carrier frequency for above 6 GHz is as follows:
  - 30 GHz





- Macro BS (i.e., Inter-Site Distance ISD = 500 m) to/from vehicle/pedestrian UE
- BS-type-RSU to/from vehicle/pedestrian UE
- 63 GHz
  - Between vehicle/pedestrian UE
  - UE-type-RSU to/from vehicle/pedestrian UE.
- At least for above 6 GHz, “vehicle blockage modelling” is introduced.
- For above 6 GHz, the fast fading parameters of “UMi-Street Canyon in [3GPP17-38901]” with some modification, e.g., setting statistics of AOD to be the same for V2V link, is a starting point for sidelink in urban environment when the channel is LOS or blocked by a building. Details are for further study for other cases, e.g., in highway environment, when channel is blocked by other vehicles.
- For above 6 GHz, “oxygen absorption” is modelled by introducing additional loss which is derived based on [3GPP17-38901].
- To reflect the effect of blockage in the channel parameters, if the channel between a Tx/Rx pair is turned out to be blocked by other vehicles, an additional loss to the path loss equation is used. Details, e.g., how to determine value of additional loss, whether the additional loss is a function of the number and size of blocking vehicles, are for further study.
- For above 6GHz, “dual mobility” should be modelled and details, e.g., how to handle impact of moving scatters, are for further study.
- At least for above 6 GHz, the V2V sidelink channel is modeled according to the following three states:
  - i) LOS
    - A V2V link is in LOS state if the two vehicles are in the same street and the LOS path is not blocked by vehicles.
  - ii) NLOS: LOS path blocked by buildings
    - A V2V link is in NLOS state if the two vehicles are in different streets.
  - iii) NLOSv: LOS path blocked by vehicles
    - A V2V link is in NLOSv state if the two vehicles are in the same street and the LOS path is blocked by vehicles.
- The following path loss equation for V2V links applies to both below and above 6 GHz

LOS/NLOS	Path Loss (PL) [dB]
LOS	For Highway case, $PL = 32.4 + 20\log_{10}(d) + 20\log_{10}(fc)$ (fc is in GHz and d is in meters)  For Urban case, $PL = 38.77 + 16.7\log_{10}(d) + 18.2\log_{10}(fc)$ (fc is in GHz and d is in meters)
NLOS	$PL = 36.85 + 30\log_{10}(d) + 18.9\log_{10}(fc)$ (fc is in GHz and d is in meters) where d is the Euclidean distance between TX and RX



- A link between two vehicles in the same street is either in LOS state or NLOSv state. The probability of LOS and NLOSv is given by the following table:

Highway	
LOS	If $d \leq 475$ m, $P(\text{LOS}) = \min\{1, a * d^2 + b * d + c\}$ where $a = 2.1013 * 10^{-6}$ , $b = -0.002$ and $c = 1.0193$ If $d > 475$ m, $P(\text{LOS}) = \max\{0, 0.54 - 0.001 * (d - 475)\}$
NLOSv	$P(\text{NLOSv}) = 1 - P(\text{LOS})$
Urban	
LOS	$P(\text{LOS}) = \min\{1, 1.05 * \exp(-0.0114 * d)\}$
NLOSv	$P(\text{NLOSv}) = 1 - P(\text{LOS})$

- Vehicle UE location is updated every 100 ms. State transition between LOS/NLOSv and NLOS is checked for each link at each location update during the system level simulation runtime.
- When a V2V link is in NLOSv, additional vehicle blockage loss is added as follows:
  - The blocker height is the vehicle height which is randomly selected out of the three vehicle types according to the portion of the vehicle types in the simulated scenario.
  - The additional blockage loss is  $\max\{0 \text{ dB}, \text{a log-normal random variable}\}$ .
  - Case 1: Minimum antenna height value of TX and RX  $>$  Blocker height
    - No additional blockage loss
  - Case 2: Maximum antenna height value of TX and RX  $<$  Blocker height
    - Mean: 12.5 dB, standard deviation: 4.5 dB
  - Case 3: Otherwise
    - Mean: 5 dB, standard deviation: 4 dB.
- Pathloss equation of V2V is reused for that of V2P, P2P, V2R, R2R.
- Pathloss in V2B, P2B, B2R link is given as follows
  - LOS propagation type is used for Vehicle-to-Base Station (V2B) and Base Station-to-Roadside Unit (B2R) links in Highway scenario.
  - LOS/NLOS propagation types are used for V2B, Pedestrian (-UE)-to-Base Station (P2B) and B2R links in Urban scenario and maintain spatial consistency following the procedure in sub-clause 7.6.3.3 of [3GPP17-38901]. Propagation type is derived based on the probability formula.
    - The effective environment height is 0.25 m.
- The following table summarizes path loss models of V2B, P2B, B2R for Highway and Urban scenarios:



	Below 6 GHz		Above 6 GHz	
	LOS	NLOS	LOS	NLOS
<b>V2B</b>	Urban:	Urban:	Urban:	Urban:
<b>B2P</b>	[3GPP17-38901] UMa	[3GPP17-38901] UMa	[3GPP17-38901] UMa	[3GPP17-38901] UMa
<b>B2R</b>	LOS	NLOS	LOS	NLOS
	Highway:	Highway:	Highway:	Highway:
	[3GPP17-38901] RMa	N/A	For further study	N/A
	LOS			

- For shadowing model
  - For V2V, V2P, P2P, V2R, R2R links, the shadowing model in [3GPP16-36885] is used. The LOS shadowing model in [3GPP16-36885] applies to NLOSv.
  - For B2V, B2P, B2R links, the shadowing model associated with the used pathloss model in [3GPP17-38901] is used.
- For fast fading model
  - The following table summarizes large scale parameters of fast fading for V2B, B2P, B2R:

	V2B/B2P/B2R	
	LOS	NLOS
<b>Freeway</b>	[3GPP17-38901] RMa LOS	N/A
<b>Urban</b>	[3GPP17-38901] UMa LOS	[3GPP17-38901] UMa NLOS

- For sidelink in Urban and Highway, the fast fading parameters of “UMi-Street Canyon” in [3GPP17-38901] was used as the starting point and was modified considering sidelink characteristics. The detailed list of parameters for each scenario is given in Table 6.2.3-1 of [3GPP18-37885].
- Rel-14 dual mobility is modified for sidelink such that a random Doppler shift is added to each reflected path and the detailed equations are provided in [3GPP18-37885].

**In summary, the following key agreements have been made in 3GPP RAN1**

- Model the V2V channel with three states to capture the impact of vehicle blockage. This is new compared to channel model for LTE V2X.
- Largely reuse channel models used for cellular communication (uplink and downlink) available in [3GPP17-38901] for V2B, B2P, B2R.
- The need to model dual mobility and the impact of moving scatterers in channel parameters.



By comparing the outcome of Sections 2.2 and 2.3 in this deliverable with the key agreements of V2X channel modelling in 3GPP it can be readily seen that 5GCAR solutions are very well aligned with the channel modelling in 3GPP. Especially, the need to model the impact of vehicle blockage has been confirmed by 3GPP and the three-state channel model presented in Section 2.2 has also been agreed in 3GPP. In fact, some partners in 5GCAR have been leading the discussions on V2X channel modelling in 3GPP and results in the present deliverable have appeared in 3GPP in the form of contributions of 5GCAR partners. It can also be noted that the results in this deliverable will further contribute to resolving the remaining open issues in 3GPP channel models.

Besides the abovementioned contributions of 5GCAR to 3GPP V2X channel modelling, 5GCAR have results that either go beyond the current status of 3GPP (namely modelling the effect of multi-link shadowing) or exemplary measurement methodology that can be used for future study of the promising technique of predictor antenna. These achievements are expected to be very useful for future standardization.



## 3 Positioning

One of the key objectives of 5GCAR is to introduce features in the New Radio air interface that enable highly accurate and ubiquitous real-time positioning of road users. We address the following use cases, which are specified in [5GC17-D21]:

- UC1: Lane merge (1-4 meters accuracy)
- UC2: See-through (10 meters accuracy)
- UC3: Network assisted Vulnerable Road User (VRU) protection (10-50 centimeters accuracy)
- UC4: High definition local map acquisition (5-50 centimeters accuracy)
- UC5: Remote driving for automated parking (5-50 centimeters accuracy).

This section is organized as follows: In Section 3.1 we briefly review the existing positioning techniques Global Navigation Satellite Systems (GNSS), cooperative positioning in IEEE 802.11p as well as radio-based positioning in LTE. The next Section 3.2 will introduce the following technology components being developed in 5GCAR and map them to the abovementioned use cases:

- TC3.1: Trajectory prediction with channel bias compensation and tracking
- TC3.2: Beam-based V2X Positioning
- TC3.3: Tracking of a vehicle's position and orientation with a single base station in the downlink
- TC3.4: Harnessing data communication for low-latency positioning
- TC3.5: Enhanced assistance messaging scheme for GNSS and OTDOA positioning
- TC3.6: Multi-array V2V relative positioning: Performance bounds.

These technology components build a framework for positioning in New Radio 5G including solutions tailored for frequency bands below and above 6 GHz. They cover both dense urban and highway scenarios. They can be applied as stand-alone solution, but also smoothly integrated with any on-board vehicle equipment like GNSS, video, radar, lidar, and other sensors.

Finally, in Section 3.3, we summarize the progress of the ongoing standardization of positioning techniques in 5G New Radio Rel-16.

### 3.1 Review of Existing Solutions

In the following we discuss prominent existing solutions and explain why they are not sufficient to meet the stringent performance requirements of the considered V2X use cases.

#### 3.1.1 Positioning with GNSS

Global Navigation Satellite System (GNSS) is a common terminology referring to satellite navigation systems with global coverage. Examples of GNSS include the Global Positioning



System (GPS) of the U.S., the GLONASS of Russia, the GALILEO of the European Union, and the BeiDou of China. Each satellite in a GNSS constellation knows its time and orbit position very accurately and the satellite broadcasts such information together with its ID and status. A GNSS receiver processes received signals from the satellites to derive its own time and location. Typically, a network of stations on the ground is used for controlling, synchronizing, monitoring, and uploading data to the satellites of a GNSS.

Thanks to its accurate information about time and position as well as its global coverage, GNSS is widely used for positioning purposes. Positioning using GNSS is based on a geometric principle called “trilateration.” It means you can determine your own position in a two-dimensional space if you know the distances from you to three known anchor points. The additional third anchor point is required because of the unknown clock offset between transmitters and receiver. Similarly, distances to four anchor points are needed to determine a position in a three-dimensional space. In the case of GNSS positioning, the satellites play the role of the anchor points and the distances are derived from the GNSS signals. Therefore, a GNSS receiver often needs Line-of-Sight (LOS) condition to at least four GNSS satellites to be able to determine its position accurately. The GNSS receiver is programmed so that its clock is advanced or delayed in such a way that the ranges to the satellites intersect. This process transfers the high accuracy in time and position from the GNSS satellites to the GNSS receiver.

There are many sources of errors in GNSS, most notably errors in satellite clocks, orbit errors, ionospheric and tropospheric delays, receiver noise, and errors due to the multipath effect of the signals. These errors degrade the accuracy of positioning using GNSS and therefore need to be corrected. Common methods for error correction include averaging over multiple measurements, modelling error sources, and using Differential correction GNSS (DGNSS). DGNSS means correcting a GNSS signal using a differential term, often obtained from a network of ground-based reference stations. A well-known technique of this type is the Real-Time Kinematics (RTK), which uses the differential term to resolve ambiguity in the number of carrier cycles between the satellite and the receiver, potentially achieving centimeter-level positioning accuracy.

GNSS is generally recognized as an important part in realizing ITS and automotive use cases. In particular, GNSS is regarded as an important sensor in advanced driving vehicles. Starting from Rel-14, GNSS has been adopted by 3GPP as one of the main synchronization sources for V2X communications. Additionally, 3GPP Rel-15 provides signaling protocols to support GNSS RTK in cellular networks. With GNSS RTK the positioning accuracy in LTE and NR networks is expected to be down to submeter level, from meters level in today’s assisted GNSS, strengthening the role of GNSS in ITS and automotive use cases. Nonetheless, further enhancements are needed for using LTE GNSS positioning for V2X. For example, the LTE Positioning Protocol (LPP) [3GPP17-36355] controls the GNSS-based positioning procedure and include the exchange of messages between the Location server and the UE for the latter to acquire assistance information. A main drawback of LTE GNSS positioning is the requirement from the UE to transmit an Assistance request message. This causes extra positioning delay and energy consumption at the UE. The situation is even worse when the UE is not in



connected state (e.g. when the UE inactivity timer runs out or in handover, which are typical for vehicle UEs) as several messages must be exchanged between the BS and the UE device to establish the LTE connection. Besides, the assistance scheme has the drawbacks that a) it is always unicasted (sent to a unique UE device, which is not well-suited for highly-dense vehicular scenarios) while the ephemeris could be broadcasted to all the UEs within a cell, and b) it is sent for each positioning session even if the assistance has not changed (e.g. because ephemeris can be valid for several hours).

### **3.1.2 Positioning in IEEE 802.11p Vehicular Ad-Hoc Networks (VANET)**

In addition to cellular broadband communication, vehicles can communicate directly through 802.11p Dedicated Short Range Communication (DSRC) in the US and correspondingly ITS-G5 in Europe (where ITS stands for Intelligent Transportation Systems), broadcasting environment and state information with cooperative awareness messages and distributed environmental notification messages [Fes15]. Broadcast messages can be utilized to perform inter-vehicle ranging through Received Signal Strength (RSS) measurements. In combination with onboard sensors, such as GPS or inertial navigation, range measurements and transmitter locations can then be fused in a cooperative localization approach. Such approaches can improve the accuracy and availability over GPS-only localization, and are particularly relevant for distributed implementation, as 802.11p operate without centralized infrastructure. Conversely, centralized infrastructure, e.g., in the form of road-side units can enable more sophisticated processing, e.g., based on fingerprinting [CSS09]. The achievable performance depends critically on the quality of the range measurements, which in turn is limited due to RSS estimation errors [DCF+10]. Early studies [PV07] show that an extended Kalman filter can lead to accuracies below 5 m, outperforming localization based on local sensors, in particular in GPS-challenged conditions and when combined with digital maps. Several impairments can, however, affect achievable performance, most importantly limitations of the DSRC communication, including channel load due to high traffic density, communication delays, and limited transmission range [YBA+10]. Recent studies have highlighted the impact of propagation effects, in particular shadowing, on the ranging performance: [CAX+17] found that performance similar to GPS is achievable, even when GPS is limited, though sub-meter accuracies cannot be attained due to shadowing, while [HDH+16] demonstrated the effect of spatial correlation of shadowing, which adversely affects localization performance. In the recent survey [Mul17], it is mentioned that RSS ranging generally has accuracies around 5-20 meters, far worse than any local sensor.

This has led to investigations of cooperative positioning in other forms: [OMS+12] proposes to use DSRC communication to share GPS corrections and perform map matching, while [SNG+17] relies on 802.11p communication to share perception information from on-board sensors such as radar or stereo camera. As RSS-based measurements have been found to only lead to marginal performance improvements over local sensors, alternative types of measurements from DSRC are currently receiving increased attention, including range-rate from Doppler [LCW16] or Fine-Time Measurements (FTM), proposed in the IEEE 802.11mc task group. The latter approach was experimentally validated [NEJ+17], indicating ranging errors of



less than one meter, provided sufficiently large bandwidth is available (80 MHz). In contrast to RSS measurements, both Doppler and time measurements are sensitive to synchronization errors. These findings are also echoed in the survey [Mul17] on ranging and cooperative techniques for vehicular positioning, highlighting that the role of DSRC in vehicular localization will likely be limited to carry information from other sensors, rather than providing stand-alone measurements.

### 3.1.3 Positioning with Cellular Radio Access Technologies

In this section we briefly summarize the functionalities for the support of Observed Time Difference of Arrival (OTDOA) and Uplink Observed Time Difference of Arrival (UTDOA) based localization as currently defined in 3GPP and the Open Mobile Alliance (OMA).

OTDOA is a downlink localization method supported since Rel-9. The UE measures the time-of-arrival of signals received from  $M$  BSs. This measurement is usually done with a correlation receiver. The time-of-arrival of received signals from  $M-1$  BSs in relation to one particular reference BS are evaluated. Consequently, for two-dimensional positioning (latitude/longitude) at least  $M=3$  BSs are required. Geometrically, each time difference determines a hyperbola, and the point, where these curves intersect is the location of the UE. This algorithm is called multilateration. The UE reports the OTDOA measurements to the network, and the localization of the UE is done there.

The time-of-arrival measurements are based on Gold sequences, so called Positioning Reference Signals (PRS) [3GPP17-36211]. These are designed for the special purpose of positioning. To increase the number of measurable BSs, the PRS from a near BS can be muted in order to increase the SINR of the PRS from a more distant BS. In LTE six different PRS patterns, i.e. mutually orthogonal time-frequency resources are defined. Further parameters of the PRS transmission are the occupied bandwidth that can be smaller than the system bandwidth, and its periodicity (minimum is 160ms). In 5G New Radio the PRS design and related parameters may be different from LTE in order to enable methods as described in this deliverable, and, finally, to achieve performance requirements of new use cases addressed in 5GCAR. This topic is addressed in Section 3.4.

Since Rel-11, LTE also supports UTDOA based localization. Here BSs measure the time-of-arrival of the Sounding Reference Signal (SRS) sent out from the UE and forward these measurements to a server where the multilateration is carried out as described above.

The complete procedure is controlled by the LTE Positioning Protocol (LPP) [3GPP17-36355] which is executed between a Location Server in the network and the target UE. Two principle architecture variants are available, the Control Plane (CP) and the User Plane (UP) solution. While the CP solution requires an individual standardization for each radio access technology, the UP counterpart is much more flexible in the sense that the required information is simply included in a data packet which is independent from the utilized radio access technology. Only the required signaling is specific for the air interface and may be defined in 5G New Radio in a different way than in LTE. Independent from the LPP variant, the localization procedure usually consists of three phases, namely capability transfer, assistance data transfer, and location





information transfer. The first includes information such as supported bandwidth for time-of-arrival measurements and support of UE-based mode. In the second phase, the server provides information such as PRS configuration for a list of BSs to be measured as well as their position if needed. Finally, in the third phase the actual measurements and/or location estimates are exchanged.

The main drawbacks of OTDOA-based localization include insufficient synchronization between BSs, bad geometrical relation between BSs and target UE, insufficient number of measurable BSs and the radio environment with multipath propagation and Non-Line-of-Sight (NLOS) in dense urban areas [Qua14]. Also, OTDOA positioning works only in a UE-assisted way; the UE device only reports TOA measurements, but it cannot compute its own position as this would require knowledge of position of the BSs. The drawbacks of such a scheme are that assistance is mandatory for OTDOA positioning, UE device is totally unable to compute its position which prevents some use cases (for instance, OTDOA positioning cannot be used to replace GNSS on a watch for runners) and UE device must use energy to transmit the report. In addition, the assistance scheme shares the two drawbacks mentioned for GNSS-based positioning. In LTE, assistance message is always unicasted and is sent for each positioning session.

### 3.2 5GCAR Technology Components

In this section, we describe different technology components being elaborated in 5GCAR to overcome the abovementioned limitations. The methods in Section 3.2.1 can be applied independently from a certain scenario and frequency band. The positioning algorithm is based on time-of-arrival measurements at multiple base stations. In contrast, the remaining proposals assume the availability of antenna arrays to exploit spatial information, i.e. the angles of departure and angles of arrival of directive beams. These methods address primarily the dense urban scenario and are tailored for frequencies above 6 GHz. While the algorithm presented in subsection 3.2.2 still assumes the transmission of more than one beam, the solutions in subsections 3.2.3 (downlink transmission) and 3.2.4 (uplink transmission) operate with a single base station and antenna arrays both at the base station and terminal. Finally, in section 3.2.5, we propose extensions of the LPP. The main characteristics are summarized in Table 3.1.

**Table 3.1: Characterization of 5GCAR technology components for positioning.**

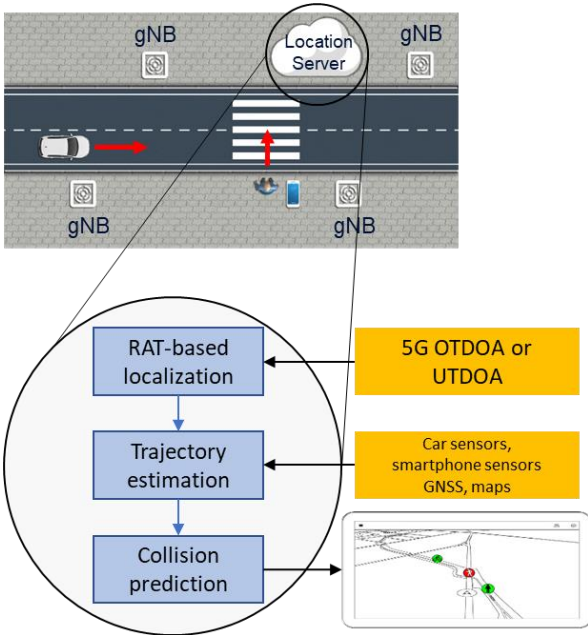
Technology component	Addressed scenarios and use cases	Frequency bands	Requirements	Main characteristics
Trajectory prediction with channel bias compensation and tracking	All scenarios, focus on UC3	all	Synchronized base stations; extended positioning protocol	Blind learning of channel bias distribution; tracking with Unscented Kalman Filter (UKF) and Particle Filter (PF)
Beam-based V2X	Dense urban,	Above	No time synchronization	UE-centric positioning, exploit beam-based



positioning	UC1, UC4, UC5	6 GHz	required. 2D antenna array at the base station providing 3D angular measurements. Linear array at the vehicle UE side.	angular information; downlink (+sidelink) measurement, particle filter
Tracking of a vehicle's position and orientation with a single base station in the downlink	Dense urban, UC1, UC4, UC5	Above 6 GHz	No time synchronization, mild multipath diversity. Large signal bandwidth and large array of antennas at the base station.	Uses virtual anchors to model NLOS paths. Stores a priori info on virtual anchors and vehicle's position and orientation. Uses data association + particle filter. OFDM.
Harnessing data communication for low-latency positioning	Dense urban	Above 6 GHz	No time synchronization required. 2D antenna array at the base station providing 3D angular measurements. Linear array at the vehicle UE side. Joint processing of data and pilot transmissions	Network-centric positioning, exploit uplink data transmission with high reliability to infer channel parameters, thus location. Reduce positioning and orientation estimation latency to sub-frame duration.
Enhanced assistance messaging scheme for GNSS and OTDOA positioning	All	Below 6 GHz	Extended positioning protocol; encryption scheme for BS position broadcasting in OTDOA case	Per-cell broadcasting of GNSS/OTDOA assistance messages and positions of neighboring BSs
Multi-array V2V relative positioning	Dense urban, UC1, UC4	all	Multiple antenna arrays on vehicles, OFDMA of Tx arrays, no Tx-Rx clock synchronization	UE-centric positioning. Exploitation of the dominant angle information from multiple arrays to achieve high positioning accuracy and alleviate the need for synchronization

We describe the positioning techniques in more detail in the following subsections and provide key results where possible.

### 3.2.1 Trajectory Prediction with Channel Bias Compensation and Tracking

<p style="text-align: center;"><b>System Model</b></p> 	<p style="text-align: center;"><b>Main Idea</b></p> <ul style="list-style-type: none"> <li>• Compensation of the impact of NLOS and unresolvable multipath propagation in RAT-based localization through estimation of channel bias distribution parameters</li> <li>• Improvement of initial localization accuracy through sensor fusion and trajectory estimation with adaptive Particle Filters and soft map-matching</li> <li>• Prediction of future road user trajectories with physical- and manoeuvre-based models, as well as prediction of collisions</li> <li>• Release of warning messages according to an optimized collision probability threshold.</li> </ul>
<p style="text-align: center;"><b>Test Cases</b></p> <ul style="list-style-type: none"> <li>• Simulation with parameters according to Annex A.</li> </ul>	<p style="text-align: center;"><b>Main Benefits</b></p> <ul style="list-style-type: none"> <li>• Enhanced safety for Vulnerable Road Users (VRU) through reliable real-time localization and collision prediction</li> <li>• Mobile radio network serves as virtual eye for the vehicle driver, complementing existing on-board equipment.</li> </ul>

#### Description of Technical Component

We address use case UC3: Network assisted vulnerable road user protection [5GC17-D21]. The goal is to detect the presence of pedestrians, wheelchair users, or cyclists, in the following referred to as Vulnerable Road Users (VRU), and to avoid accidents by reliably detecting a potentially critical situation and by releasing respective warning messages to both vehicle driver and VRU. In addition to already existing systems mostly based on video cameras, radar, and sensors directly at the vehicle, we complement this road safety use case with novel features of 5G networks. The new functionality is part of the Mobile Edge Computing (MEC), more precisely



it is included in a network entity called Location Server (LS). The benefits of data processing in the MEC are lower latency and reduced complexity.

The proposed algorithms will be implemented and integrated in a joint 5GCAR demonstrator [5GC17-D51]. In the following we describe the building blocks in more detail.

### **RAT-based localization**

Our localization scheme is based on UTDOA but can be applied for OTDOA as well. Both VRU and vehicle transmit a Positioning Reference Signal (PRS), and a set of base stations determine the time of arrival relative to a reference base station. As the location of the base stations is known, it is easily possible to determine the current position of the user with the measured UTDOA values.

However, major error sources in such a localization algorithm are Non-Light-Of-Sight (NLOS) propagation of the PRS between user and base station and unresolvable multi-path [PLH16]. Consequently, the measured UTDOA does not solely reflect the direct line between transmitter and receiver, but the complete NLOS propagation path. We define this additional unknown component as channel bias. It falsifies the position estimate of the user drastically. Without compensation of the impact of the channel bias, the expected accuracy of the UTDOA localization does by far not satisfy the stringent use case performance requirement of below 1 meter given in [5GC17-D21].

Recently a Blind Learning Algorithm for the channel bias Distribution Estimation (BLADE) has been proposed [PLH16] aiming at compensating the impact of NLOS propagation. Basic idea is to consider the Probability Density Function (PDF) of the channel bias in the cost function of the Maximum-A-Posteriori (MAP) estimator for the UE position. The PDF can be modeled as a Gaussian mixture distribution, and the respective mean values, standard deviations, as well as the weight of each Gaussian component are determined and continuously updated by an iterative leave-one-out algorithm. BLADE is applied in our RAT-based localization solution.

RAT-based localization requires tight synchronization between the base stations in the order of a few nanoseconds. Otherwise the accuracy drops significantly. While we ignore this fact in WP3, it is addressed in the scope of the demonstrator implementation in WP5 [5GC17-D51].

### **Trajectory estimation**

The second building block in our processing chain is trajectory estimation. We track the UE position and optionally other state variables like speed and turn rate over time. The estimation of the current position of the UE, i.e. its current state, is based on two models:

State transition model: It describes how the current state depends on the previous state and includes the so-called process noise. The latter is an innovation term that considers model mismatches and motion changes, e.g., acceleration in a Constant Velocity (CV) model.

Measurement model: It describes how the current measurement, e.g., the network-based localization as described in the previous paragraph, depends on the current state and includes the measurement noise.



It is known that for linear models the Kalman filter is the best solution with respect to the mean squared error of the state estimation. While the CV state transition model is linear, more sophisticated models, e.g., Constant Turn Rate and Velocity (CTRV) [SRW08], become non-linear, and different estimation methods must be applied:

The Unscented Kalman Filter (UKF) [JU97; KFI08] is a parametric estimation method that iterates over a finite set of points sampling the PDF of the state. Its main advantage is the low complexity. However, its accuracy decreases if the models are too complex and the PDF is multi-modal.

The Particle Filter (PF) [AMG+02] is a non-parametric estimation method that approximates the PDF by a swarm of so-called particles. Main advantage is the good performance even if the PDF is multi-modal. However, the computational complexity is significantly higher because many particles need to be tracked to have good performance, instead of a few parameters that are present in the UKF.

### Collision prediction

Finally, the third building block in the location server is collision prediction between each pair of road users by comparing their trajectories. Obviously, the algorithm must anticipate future states of the users without having the corresponding measurements. [LVL14] introduces three categories of motion models, *Physics-based*, *Maneuver-based* and *Interaction-based*. In 5GCAR we focus on a combination of the first two categories.

In this deliverable we disclose a first, simplified approach. We determine several potential future trajectories and assign a certain probability to each of them. We determine one potential future trajectory by letting the motion model evolve. In case of the CTRV, turn rate and velocity of the current state is used without any modification to calculate all future states. Other potential future trajectories can be generated by keeping the turn rate constant, but to modify the velocity for the calculation of the future states. This means we imply a slight acceleration or deceleration of the vehicle. Vice versa, we can keep the velocity constant and modify the turn rate. Hence, we generate a table with probabilities that the road user will be at a certain position (or area) at a certain point in time. Obviously, the probability for a collision is the sum of joint probabilities that two road users will be at the same time in the same areas.

In the toy example shown in Figure 3.1 we assigned 50% probability to the inertial (unmodified) trajectory. All other trajectories (turn more to the right, turn more to the left, acceleration, and deceleration) have probabilities 12.5%. The final collision probability is the sum of all joint probabilities assigned to areas, where the boxes around the vehicles overlap. In this example it is  $0.5^2 + 0.5 * 0.125 + 3 * 0.125^2 = 35.9\%$ . This value is valid for one single point in time in the future, also referred to as prediction window. The prediction window is typically in the range of a few seconds. A warning message to the road users will be released if the collision probability for at least one prediction window exceeds a certain threshold. This is subject to further concept development and evaluation that we will present in the final deliverable. Aim is to select combinations of prediction windows and thresholds such that the false alarm rate is minimized while we are still able to detect most of the critical situations.

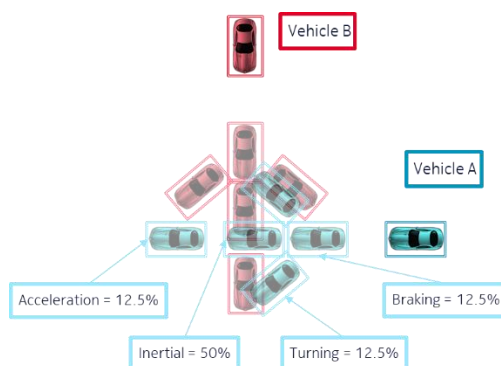


Figure 3.1: Simplified model for collision prediction.

### Key result

Most important result is the achievable positioning accuracy. In Figure 3.2 we compare the position error CDF of the UKF and the PF (10.000 particles) with pure LTE OTDOA- and GNSS-based localization without tracking. We apply the CTRV model and assume for the sake of simplicity fixed standard deviations of OTDOA measurements (6m) and GNSS measurements (5m) on a given drive route. The measurement updates are 200ms for OTDOA, and 1s for GNSS, respectively. We feed only the OTDOA measurements in the tracking algorithm.

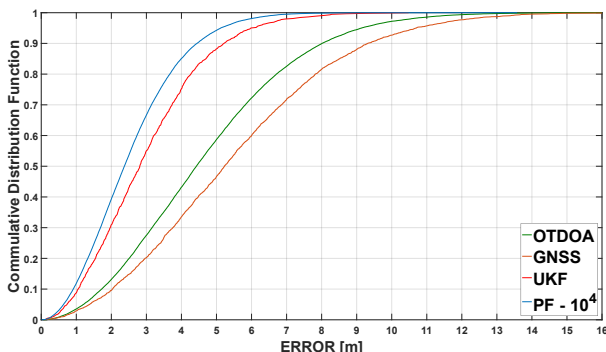


Figure 3.2: Error CDF of tracking solutions with UKF and PF compared with pure GNSS and OTDOA.

In the considered scenario, the solutions with tracking clearly outperform the reference cases (pure GNSS and LTE OTDOA) roughly by factor 2. The PF provides the smallest error with a mean value around 2.3m. However, this result as well as the computational complexity depends a lot on the number of particles.



### 3.2.2 Beam-Based V2X Positioning

<p style="text-align: center;"><b>System Model</b></p> <ul style="list-style-type: none"><li>• BSs/TRPs equipped with 2D antenna array at rooftop/roadside</li><li>• 2D AoD measurements obtained at V-UE</li><li>• LoS links.</li></ul>	<p style="text-align: center;"><b>Main Idea</b></p> <ul style="list-style-type: none"><li>• Apply network-assisted UE-centric approach</li><li>• Exploit angular information obtained using 3D beamforming</li><li>• Investigate NR-specific technology with respect to positioning accuracy.</li></ul>
<p style="text-align: center;"><b>Test Cases</b></p> <ul style="list-style-type: none"><li>• V-UE obtains angular measurements from one, two or three TRPs</li><li>• At least one TRP at rooftop level available.</li></ul>	<p style="text-align: center;"><b>Main Benefits</b></p> <ul style="list-style-type: none"><li>• Understanding the impact of the number of reference TRPs and the geometric setting of the selected reference TRPs on the positioning accuracy.</li></ul>

Given the new technologies adopted by 5G new radio, the enhanced positioning/location service targets to meet a full set of performance requirements, such as accuracy, latency and availability. Large bandwidth in the mmWave band, deployment of antenna panels at the base station as well as the mobile terminal, advanced computational facilities may all play a role in 5G NR based positioning. Unlike the current system where location service requests mainly originate from the network side, the next generation location service must deal with service requests from massive number of mobile terminals, most of which come with hard requirements on latency and accuracy.

In this section, we consider network-assisted UE-centric V2X positioning scenarios and exploit the angular information obtained using beamforming. This aims to investigate the potential of NR-specific technology with respect to positioning accuracy. Given less hardware and power constraints at V-UEs, more complex functionalities can be implemented on the UE side. A UE-centric approach allows the vehicle to estimate its absolute/relative position based on the locally available measurements. Compared to the network-based approach where the location server in the core network calculates the UE positions, the UE-centric approach avoids the communication over the location server, thus conserves network traffic overhead and reduces latency as well.

#### Description

In this scenario, we consider the deployment of uniform rectangular panel array on the base station side, the angular information in both the horizontal and the elevation plane can be obtained by a vehicular UE via downlink channel estimation.

For the LOS path from the anchor base station  $a$ , let  $\theta_a$  denote the estimated AOD in the horizontal plane and  $\phi_a$  denote the estimated AOD in the elevation plane. Given the knowledge of the anchor base station's 3D coordinates  $(x_a, y_a, z_a)$ , the UE's 3D position can be determined using simple linear regression. Since each anchor base station provides two measurements, namely  $\theta_a$  and  $\phi_a$ , at least two anchor base stations are required to estimate a UE's 3D coordinates. However, for a vehicular UE whose height  $z$  assumed to be known, the 2D position in the x-y plane can be obtained given a LOS path from a single base station.

For a positioning system whose dynamics can be described as a state space model, Bayesian filtering is a statistically optimal solution [AMG+02]. Given that the system is non-linear and non-Gaussian, we choose to apply particle filtering which approximates the posterior probability density function using Monte Carlo method [AMG+02].

### Key results

Performance evaluation has been carried out in the urban canyon scenario. One rooftop Transmit-Receive Point (TRP) of height 25 meter is located at the intersection of two streets, covering a street of width 30 meter. In addition, two light pole type TRPs of height 5 meters are located on the street side, serving as anchor nodes for positioning. A Vehicular UE (V-UE) of height 1.5 m is driving down the street at a speed of 30 km/h, as depicted in Figure 3.3. The V-UE obtains AOD measurements in the horizontal and the elevation plane using the downlink transmission signal. Such measurements are updated every 10ms. Such measurement interval may be adjusted accordingly to the V-UE velocity. In this experiment, the estimation error of the observed angular information from all TRPs is assumed to follow Gaussian distribution with zero mean and standard deviation of two degree.

Figure 3.3 compares the positioning error of Particle Filter (PF) based Bayesian filtering and that of Linear Regression (LR). Significant improvement can be observed for PF based scheme given the same angular information compared to the LR based one. Figure 3.3 also shows the positioning error when one/two/three TRPs are utilized as reference points. For PF based cases, only minor improvements can be observed since prior measurements are already taken into account. However, for LR based cases, increasing the number of reference points may improve estimation performance significantly. It is also seen that although the positioning accuracy improves in general as the number of reference anchor points increase, the geometric setting of the selected anchor points plays an important role. For instance if two TRPs are involved, TRP 3 is preferred than TRP2 for the given UE. This may lead to an anchor selection problem while implementing positioning method in practice.



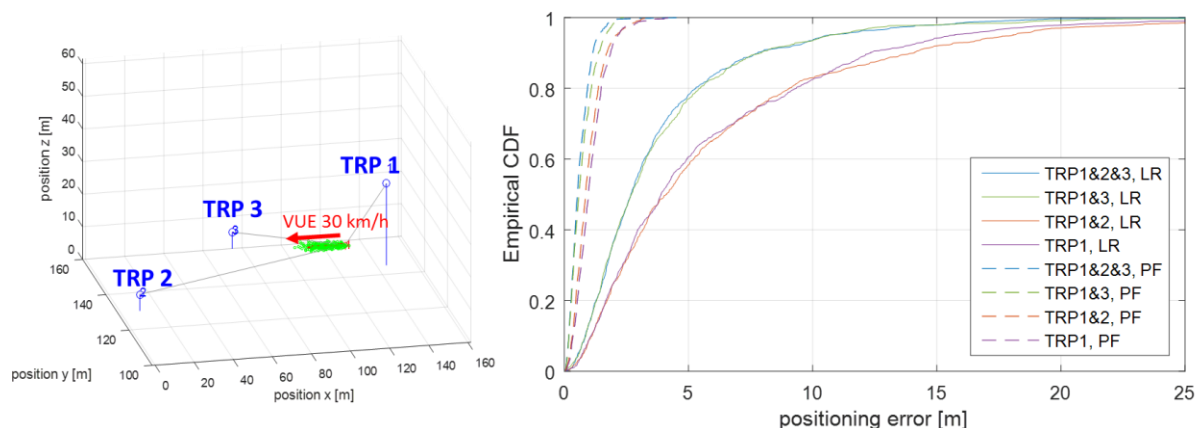


Figure 3.3: Evaluation scenario and CDF of positioning error.

### 3.2.3 Tracking of a Vehicle’s Position and Orientation with Single Base Station in the Downlink

System Model	Main Idea
<ul style="list-style-type: none"> <li>• Single vehicle - User Equipment (UE)</li> <li>• mmWave Base Station (BS)</li> <li>• The environment comprises of reflecting surfaces causing multipath</li> <li>• The locations of these surfaces, the UE’s 2D position, 1D heading, and 1D clock bias are unknown.</li> </ul>	<p>The UE receives downlink mmWave signals, which are used to determine the channel parameters of each multipath component, characterized by a complex gain, a 1D delay, a 2D angle of arrival, and a 2D angle of departure. These channel parameter estimates are then used to solve for the UE state (position, heading, clock bias), as well as to build up a map of the environment.</p>
Test Cases	Main Benefits
<p>Scenario with</p> <ul style="list-style-type: none"> <li>• 4 vertical walls (i.e., 4 virtual anchors)</li> <li>• Single BS and single UE.</li> </ul> <p>Prior information:</p> <ul style="list-style-type: none"> <li>• UE location’s standard deviation of 3.2 meters (horizontal plane)</li> <li>• 3 Vertical Anchors (VA) location standard deviation of 10 meters (also in the horizontal plane)</li> <li>• 1 VA with no prior information.</li> </ul>	<ul style="list-style-type: none"> <li>• Determination of the UE position and heading with a single BS without a priori synchronization from a downlink transmission</li> <li>• Generation of a map of the environment, useful for other UEs to determine their position and heading</li> <li>• Determination of UE position is possible even in absence of LOS.</li> </ul>

## Description of Technical Component

A technique utilizing only downlink mmWave signals from a single BS are used at the UE to jointly estimate the vehicle's position and orientation, its clock bias and the channel parameters (locations and orientations of the reflectors). The reflectors are parameterized as Virtual Anchors (VA). As described in Figure 3.4, the proposed technique (circled in orange) consists of three stages:

1. Channel estimation: A search-free beam-space tensor-ESPRIT algorithm is developed for estimating the directions of departure and arrival, as well as the time of flight and channel gains of the individual paths. The proposed approach is based on higher-order singular value decomposition and it is a generalization of the beam-space ESPRIT method. Furthermore, the parameters associated to each path are automatically associated.
2. Data association: Since the paths are not yet tied to the VAs, a data association step must follow. We consider a simple technique based on the global nearest neighbor assignment which provides hard decisions regarding the associations of measurements to VAs.
3. Positioning and mapping: We aim to compute the marginal posteriors of the UE position and orientations, the VAs' positions, and the clock bias. It is achieved by executing belief propagation on a factor graph representation of all the parameters. When dynamic objects appear (moving cars, people, etc.), they will be added to the map, and then removed after they exit. They can be regarded as clutter for the proposed algorithm. Of course, performance may be affected.

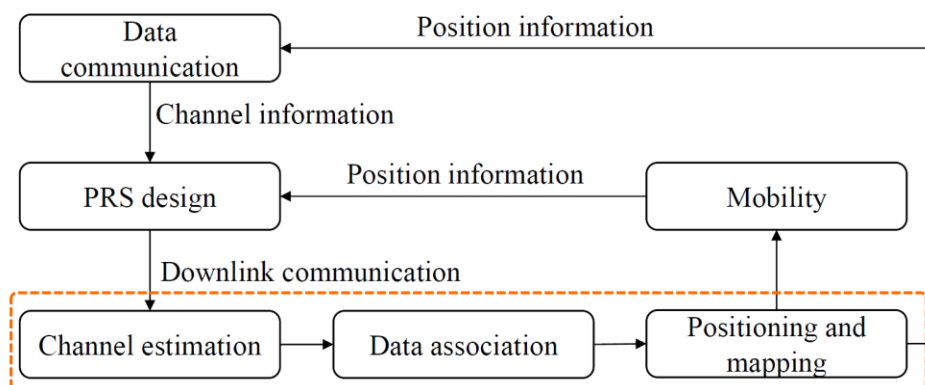


**Figure 3.4: The stages of the proposed 5G mmWave downlink positioning technique. The vehicle estimates channel parameters from a dedicated PRS (including precoding and combining), which it associates to prior map information and then uses to refine the vehicle position, heading, and clock bias.**

## Key result

A Fisher information analysis was performed, and two main conclusions were obtained:

- The multipath channel and the vehicle's clock bias can be estimated, albeit with some performance penalty compared to a perfectly synchronized scenario/
- In the absence of multipath components, localization of an unsynchronized UE using a single BS is impossible.

We observed a number of other interesting facts. In all cases, having more paths is beneficial assuming they are resolvable. In practice, if the number of paths grows too large, paths will not be resolvable, and performance will degrade. Thankfully mmWave channels have fewer paths with non-negligible energy compared to their microwave counterpart. The best performance is achieved when the both LOS and NLOS paths are available, and when the clock bias and VA positions are known (referred to as “map”), while the worst performance is achieved when only NLOS paths are available, and neither the clock bias nor the VA positions are known. Provided enough paths are available, the system state is always identifiable in spite of the fact that the UE has not a synchronized clock. With an unknown clock bias, one NLOS path is needed when LOS is present. When LOS is not present, at least three NLOS paths are needed, or only two in case map information is available (i.e., the position of the VAs). These results are corroborated by Figure 3.5, which clearly confirms that the clock bias can be estimated even with one-way transmission as long as the scenario provides enough diversity in terms of NLOS paths.

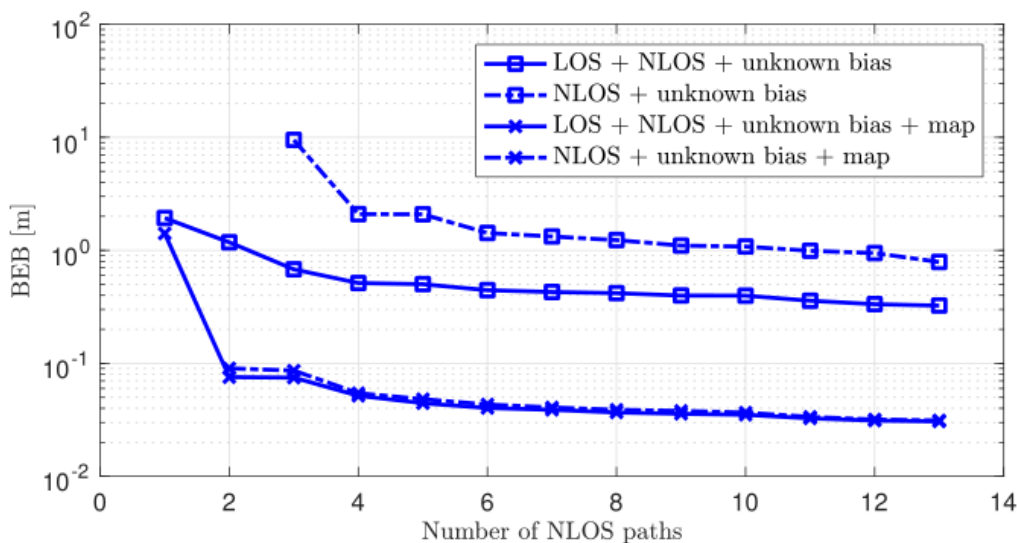


**Figure 3.5: Bias Error Bound (BEB) as a function of the number of NLOS paths for 4 combinations: with and without a LOS path, with and without knowledge of the map (VA positions).**



### 3.2.4 Harnessing Data Communication for Low-Latency Positioning

<p style="text-align: center;"><b>System Model</b></p> <ul style="list-style-type: none"> <li>• It is assumed an up-link mmW transmission model where channel is LOS-dominant. Both at the transmitter and receiver side, beamforming is applied to provide sufficient SNR for data transmission.</li> <li>• At the receiver (gNB), the location-orientation of the transmitter is estimated based on pilot and data symbols.</li> <li>• The communication is based on OFDM. Pilot symbols are known, whereas data reference symbols are provided by the communication chain. An uncertainty to the data symbols is computed based on the SNR.</li> </ul>	<p style="text-align: center;"><b>Main Idea</b></p> <p>The main idea of the UL position-rotation estimation is to jointly use the data and pilot symbols for a quasi-continuous estimation of the location and orientation of the device. To implement this idea, a graphical model connecting pilot-based positioning and data-aided positioning is developed.</p> <p>The challenge is to exploit the synergy between</p> <ol style="list-style-type: none"> <li>a) Data and pilot symbols for position estimation</li> <li>b) Location information to channel parameter estimation and prediction.</li> </ol>
<p style="text-align: center;"><b>Test Cases</b></p> <p>Scenario</p> <ul style="list-style-type: none"> <li>• 1 Base-station</li> <li>• 1 UE with unknown-location and orientation</li> <li>• 2D positioning</li> <li>• LOS</li> <li>• Free-space path-loss.</li> </ul> <p>OFDM</p> <ul style="list-style-type: none"> <li>• 1024 FFT</li> <li>• SCS 60 kHz</li> <li>• Carrier frequency, 28GHz</li> <li>• Used subcarrier: 128</li> <li>• Pilot-allocation: combo-4</li> <li>• Data: 128 subcarriers.</li> </ul>	<p style="text-align: center;"><b>Main Benefits</b></p> <ul style="list-style-type: none"> <li>• Determination of the UE position and heading with a single BS</li> <li>• Quasi-continuous estimation of the location and orientation</li> <li>• Estimate channel information as Rx gain, Tx gain and delay to use in location-aware channel prediction model.</li> </ul>

UE single antenna, gNB beamforming <ul style="list-style-type: none"> <li>• Hybrid digital-analog architecture</li> <li>• ULA antenna model.</li> </ul>	
--	--

### Description of Technical Component

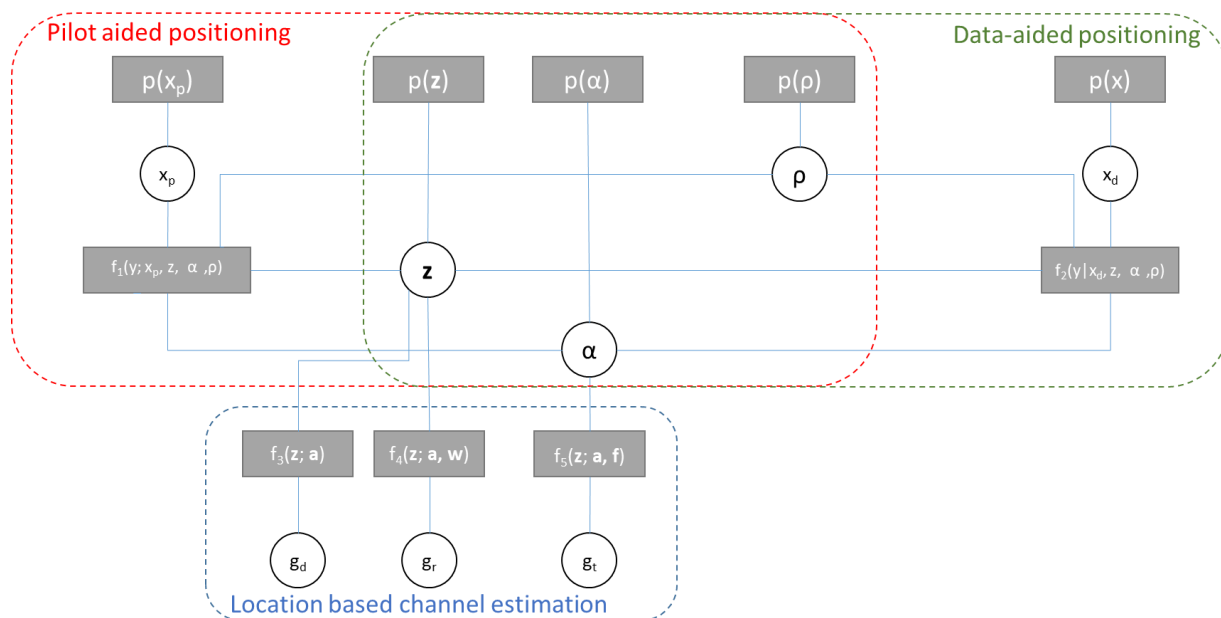


**Figure 3.6: Graphical model for pilot-data aided position-rotation estimation.**

The technical component is a Bayesian inference algorithm that uses the uplink pilot and data symbols to estimate the location and orientation of the UE in LOS channel condition. One of key aspect is the location-based parameterization of the channel, which provides the advantage of inferring directly the position and rotation from the received signal.

With focus on the positioning task, the graph of interest is that enclosed in the red and green boxes, which can be treated separately by implementing a two-step inference approach:

- 1) pilot based positioning using full-beam scanning procedure: uplink pilot reference symbols are received at the gNB by multiple beams, scanning the whole area of interests. The gNB processes the received signal using pilot-based sub-graph and provides an estimate of the UE location and orientation.
- 2) data-based positioning using location-based beamforming: uplink data are received using a beam pointing to UE estimate direction. The I-Q samples of the data streams are then estimated and used as reference symbol symbols. The gNB re-processes

the received data signal using data-based sub-graph and provides an estimate of the UE location and orientation. In this subgraph, the pilot-based position information is used as prior.



### Key Results

In this technical component, an enhancement of pilot-based positioning is proposed. More specifically, we leverage data transmission to refine location information and achieve over 50 % of accuracy improvement along with faster location update.

In figure 3.7 the average 2D position error as a function of the SNR is illustrated. It can be noticed that a significant gain can be achieved when the pilot-based positioning is relatively accurate. In other words, when a pilot-based positioning can provide sufficiently reliable position information. On the other hand, if beamforming is assisted by a genie providing the exact UE direction, the performance gain is significant also in the low SNR regime.

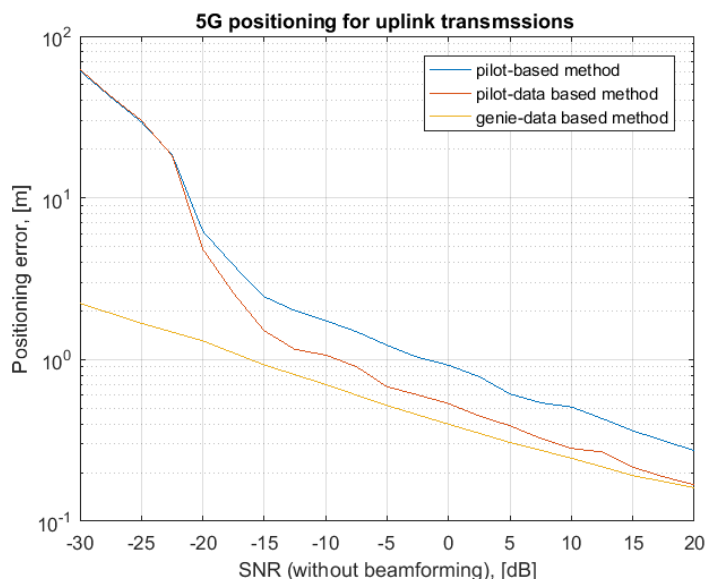


Figure 3.7: Comparison of positioning error between pilot and data-aided methods



### 3.2.5 Enhanced Assistance Messaging Scheme for GNSS and OTDOA Positioning

System Model	Main Idea
<p><u>Conventional positioning session:</u></p> <ul style="list-style-type: none"><li>• The location server requests the UE to provide its measurement capabilities, i.e., the positioning technologies it supports.</li><li>• UE answers the server request by providing its capabilities.</li><li>• Location server provides assistance information to the UE which can be e.g. OTDOA assistance</li><li>• Location server then requests the location information.</li><li>• UE answers the server requests and provide either the measurements and/or the position.</li></ul>	<p>Introduce new mechanism in legacy Positioning Protocol (LPP) to transmit assistance messages in order to improve GNSS and OTDOA positioning. The main idea is to broadcast messages per cell.</p> <ul style="list-style-type: none"><li>• 1<sup>st</sup> option: New System Information Block (SIB) messages updated and reacquired by the UE whenever there is change on the vehicular network topology</li><li>• 2<sup>nd</sup> option: Introduce unsolicited messages at the NAS level.</li></ul>
<p><u>Proposed positioning session:</u></p> <ul style="list-style-type: none"><li>• Broadcast assistance messages per cell.</li></ul>	<p><b>Main Benefits</b></p> <ul style="list-style-type: none"><li>• Reduce positioning delay and power consumption at UE device by reducing number of transmitted messages</li><li>• Increased system resource efficiency from per cell sharing of assistance information</li><li>• Allow new usages and use cases by allowing UE-based positioning and reducing positioning delay.</li></ul>

#### Description of Technical Component

In this contribution, considering the LTE positioning mechanisms as baseline, we introduce new mechanisms to transmit assistance messages in order to improve GNSS and OTDOA positioning in cellular radio technologies. The main idea is to broadcast messages per cell. The broadcasting scheme can be implemented in two ways. In first option, new System Information Block (SIB) messages, which can be updated and reacquired by the UE whenever there is change on the vehicular network topology, can be introduced to carry such assistance information. Alternatively, unsolicited assistance reception may be introduced at the control plane level or at the user plane level. For GNSS positioning, those broadcast messages will



include some GNSS assistance. For OTDOA positioning, the messages will include some OTDOA assistance as well as the positions of the BSs surrounding the cell.

The envisaged changes are expected to provide the following benefits:

- Help in significantly reducing the power consumption of the device with both GNSS and OTDOA positioning by reducing significantly the number of transmitted (and received) messages
- Help the operator to save bandwidth by sharing some positioning information among the UEs of a cell rather than sending it in a unicast manner
- Allow some new usages and use cases for both GNSS and OTDOA positioning.

### **Description of conventional mechanism**

The protocols currently used for positioning in 3GPP (LTE) include the LPP and the SUPL and NAS protocol for the transport layer. LPP is a protocol that works by positioning session: each time a position/positioning measurement is required, a new LPP session starts. This session will happen either at the user plane level (above IP) using the SUPL protocol as a transport layer, or at the control plane level using the NAS as a transport layer. In both cases, the device has to be in connected mode so that the LPP exchanges can take place.

In general, a positioning session works most of the time as follows (see Figure 3.8):

- The location server requests the UE to provide its measurement capabilities, i.e., the positioning technologies it supports.
- UE answers the server request by providing its capabilities.
- Then the actual positioning phase starts.
- Location server provides assistance information to the UE which can be:
  - OTDOA assistance
  - GNSS assistance for UE-based session (e.g., ephemeris, almanacs, ...)
  - GNSS assistance for UE-assisted session (satellites to measure with ranges for satellite phase and Doppler search).
- Location server then requests the location information.
- UE answers the server requests and provide either the measurements and/or the position.
- Then the session is ended.



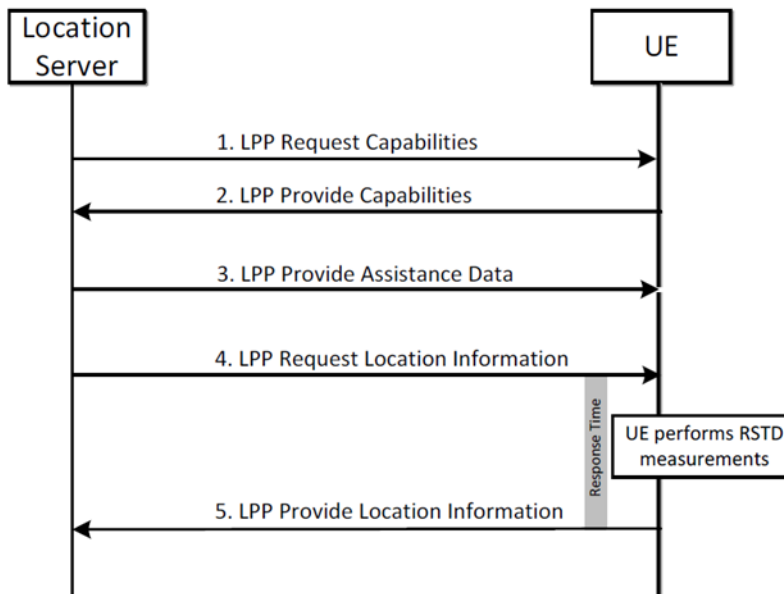


**Figure 3.8: Positioning session in LTE.**

On top of the aforementioned messages, LPP also contains some mechanisms to support duplicate detection, message acknowledgements, retransmissions, error handling and abort procedures. This can increase the number of exchanged messages in both DL and UL directions.

**Drawbacks of conventional mechanism**

GNSS positioning

Typical GNSS positioning session in LTE can be summarized in Figure 3.9 below for UE-based and UE-assisted, respectively.

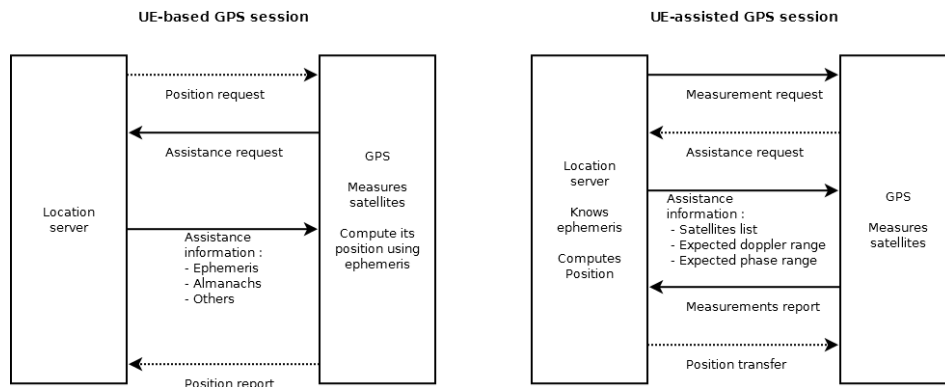


**Figure 3.9: Typical GNSS positioning session in LTE.**

Note that not all the exchanges depicted in the figure will always happen; some may be omitted in some cases and those optional exchanges are depicted using dashed arrows. For example, the server may decide to send assistance before the position request in which case assistance

will not requested by the device. Furthermore, when the UE computes its position, it may decide to do it without position request from the server and UE may also omit to report its position to the server. Finally, at the end of a UE-assisted session, the network may or may not transmit the computed position to the UE.

The drawbacks in the case of UE-based positioning are the following: a) Assistance request requires the UE to transmit the assistance request message resulting to delay and energy consumption. An example where this assistance request is mandatory is when the GNSS-enabled UE wants to compute its position on its own without server request; b) in case the UE is not connected, it will first need to establish network connectivity before being able to transmit the assistance request which will cause further delay and energy consumption as several messages have to be exchanged between the base station and the UE to establish the connection. In case of UE-assisted positioning, the drawbacks are slightly different. Assistance request may cause energy loss if it is not transmitted spontaneously by the network. However, as the network requires the measurement request, it can add the assistance information to avoid the request, but still, the UE has to transmit the measurement report as it is unable to compute itself its position. In fact, one up to several UL messages will be transmitted by the GNSS-enabled UE resulting into delays (as well as battery life impact). Besides, in both cases, the assistance information is always unicasted (sent to a unique UE) while the ephemeris could be broadcasted to all the UEs within a cell, and it is sent for each positioning session even if the assistance has not changed (e.g. because ephemeris can be valid for several hours).

### OTDOA positioning

Typical OTDOA positioning session in 3GPP can be summarized in Figure 3.10 below.

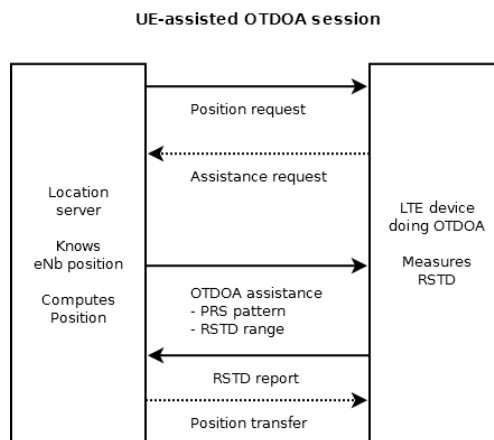


**Figure 3.10: Typical OTDOA positioning session in LTE.**

In LTE, OTDOA works only in a UE-assisted way and the UE only reports RSTD measurements but it cannot compute its own position as this would require knowledge of position of the base stations. The drawbacks of such a scheme are obvious: a) assistance is mandatory for OTDOA positioning; b) UE is totally unable to compute its position which prevents the support of certain use cases; c) UE must use energy to transmit the report. Besides, the assistance scheme has again the disadvantage that it is always unicasted (while the PRS and expected RSTD could be



broadcasted to all UEs in a cell) and that it is sent for each positioning session even if the assistance has not changed (which is useless as the assistance is not expected to change unless the UE has done a handover to a new cell).

### **Introduction of new SIBs**

System Information Block (SIB) message is a broadcasting scheme used in LTE and NR to allow a base station broadcast information to all UEs. In LTE for example, several SIBs exist and a UE is not required to decode all of them: only SIB1 (defines the other SIBs broadcasted by the base station) and SIB2 (defines, together with SIB1, the essential cell configuration to allow the UE establish connectivity) must be decoded, while other SIBs may or may not be decoded depending on the UE service usage (e.g. a UE not needed to receive TV simply ignores SIB13). On top of this, a tag is present in SIB1 to notify that the other SIBs have changed. This way, a UE has to reacquire SIBs only if they have changed (or if UE's serving cell has changed, either after a handover or after loss of service).

Considering the above, for enhancing positioning mechanism via efficient per-cell message broadcasting, we propose to introduce four new SIBs:

#### For GNSS positioning

- To allow a GNSS-enabled UE to receive ephemeris without wasting any energy for requesting assistance, *SIBpos1* can be introduced which will contain the GNSS assistance information for UE-based positioning (ephemeris, time, almanacs). Besides, as the ephemeris is broadcasted and hence shared between all the UEs in a cell, the operator can save bandwidth as the ephemeris no longer needs to be sent per positioning device and positioning session. The overhead reduction will depend on the number of UEs performing UE-based/assisted positioning as well as how often the UEs perform the UE-based/assisted positioning. Finally, this also allows a GNSS-enabled UE to receive the ephemeris without having established network connectivity; a UE in idle mode will be able to receive them which will help to reduce further its energy consumption.
- To enable the UEs reduce the satellites' acquisition time, *SIBpos2* can be introduced which will include the GNSS assistance information for UE-assisted positioning (expected phase and Doppler ranges). This can also result in energy saving as the acquisition phase is shortened. Note that both *SIBpos1* and *SIBpos2* content mostly depends on the time of the day as well as the rough position of the cell.

#### For OTDOA positioning

- To allow mostly broadcasting of the OTDOA assistance, hence share such information among all the devices in a cell, *SIBpos3* can be introduced. This will help the operator to save bandwidth as the OTDOA assistance will not need to be sent per positioning device. This also helps reducing the UE power consumption by avoiding useless receptions of the assistance when it is known to be unchanged. *SIBpos3* will contain the



OTDOA assistance information for the cell (e.g. list of base stations with associated PRS pattern and expected RSTD range), therefore, its contents will depend on the cell.

- To allow OTDOA receivers to compute their own position, *SIBpos4* can be introduced which will contain base station's position for a given area (typically the area surrounding the cell). This way, UE will not need to waste energy to transmit the RSTD measurements. Besides, a joint usage of *SIBpos3* and *SIBpos4* enables OTDOA positioning at the UE-side which is even possible without network connectivity; a UE has to just listen the network broadcasted signal with no need to be connected to it. Of course, an operator may be reluctant to broadcast its BS positions; therefore, a new mechanism to allow only authorized users to make use of the broadcasted messages is needed and we plan to look further into this issue.

### Unsolicited message at NAS level

Another way to introduce positioning message broadcasting is through unsolicited messages at the NAS level. In that option, the network may decide to send from time to time some unsolicited assistance using NAS as a transport layer. This scheme would be less efficient than the SIB broadcasting described previously as the transmission would be unicasted. However, this option still allows to avoid unnecessary assistance request/exchanges through the LPP. A mechanism to implement such approach would be to introduce a new NAS message type for the generic message container.

### Summary of key benefits

The following key benefits can be obtained with the proposed assistance messaging scheme for GNSS and OTDOA positioning:

- Allow some new usages and use cases
  - for OTDOA positioning: By allowing UE-based positioning (= UE-based GNSS-independent with much better than GNSS availability and delay)
  - for GNSS positioning: By reducing the positioning delay.
- Help in reducing positioning delay as well as the power consumption of the UE device with both GNSS and OTDOA positioning by reducing significantly the number of transmitted (and received) messages. For example, with the use of new SIB messages, assistance request from UE may not be needed during a UE-based GNSS session; or even no need for communication between UE and network will be needed during a UE-based OTDOA session. Moreover, the case where the UE is not in connected state is addressed.
- Help the operator to save bandwidth at system level since, by broadcasting messages per cell, the assistance information is shared among the UEs of a cell rather than being sent in a unicast manner.



### 3.2.6 Multi-Array V2V Relative Positioning: Performance Bounds

In this work we consider Tx and Rx vehicles equipped with multiple antenna arrays, referred to as panels in 5G New Radio (NR) standardization, which are distributed around the vehicle to support 5G NR side link (V2V) communication between vehicles. Our goal is to leverage these arrays and the side link to also perform V2V relative positioning using e.g. position reference signals.

<p style="text-align: center;"><b>System Model</b></p> <ul style="list-style-type: none"><li>• Vehicles equipped with conformal antenna arrays at the edges of their bumpers</li><li>• OFDMA access to shared channel</li><li>• Transmission through fixed beamforming vectors -&gt; No AOD estimation</li><li>• Asynchronous Tx-Rx clocks</li><li>• LOS links.</li></ul>	<p style="text-align: center;"><b>Main Idea</b></p> <ul style="list-style-type: none"><li>• Derivation of the performance bounds of V2V relative positioning</li><li>• Comparison with 5G NR V2X requirements</li><li>• Evaluation of the relative significance of channel measurements (AOA, TDOA).</li></ul>
<p style="text-align: center;"><b>Test Cases</b></p> <ul style="list-style-type: none"><li>• Overtaking: Rx vehicle overtaking the Tx vehicle</li><li>• Platooning: Rx vehicle behind the Tx vehicle.</li></ul>	<p style="text-align: center;"><b>Main Benefits</b></p> <ul style="list-style-type: none"><li>• Determination of the achievable V2V relative positioning accuracy and the range of distances for which 5G NR V2X requirements can be met</li><li>• Understanding the significance of angular measurements compared to that of delay measurements with potential applications to reference signal design.</li></ul>

#### Description of Technical Component

The following assumption are made:

- The clocks between the Tx and Rx vehicles are not synchronized or the time of transmission is not known. Thus, range information from Time of Arrival (TOA) measurements cannot be extracted and only Time-Difference of Arrival (TDOA) measurements are possible.
- We consider short reference signal transmission time and small relative velocity between vehicles, such that the setup is static over the observation interval. To this end, we avoid a beam-scanning procedure at the Tx and assume the reference signal is transmitted through a fixed (wide) beam. Consequently, Angles of Departure (AODs) cannot be measured; thus, they are not considered for position estimation.

- Being interested in relatively short distance between neighbor vehicles, which is mainly dominated by LOS paths, we only consider LOS propagation for simplicity and to obtain initial insight.
- The Tx arrays have orthogonal frequency division multiple access (OFDMA) to the shared medium

We derive geometrically intuitive expressions for the Fisher information on the relative position and orientation of the Tx vehicle, when AOA measurements with or without TDOA measurements are available. These expressions are then used to obtain the CRB for the lateral and longitudinal positioning error. The bounds are evaluated for vehicles equipped with 4 antenna arrays placed at the corners of their front and rear bumpers.

### Key results

Using the abovementioned Fisher information and CRB analysis, we studied two relevant V2V scenarios, namely overtaking and platooning (see Figure 3.11). We compare the bounds with the positioning accuracy requirements defined in [3GPP17-TS22186], where it is stated that the lateral and longitudinal position errors (see Figure 3.11b) should be less than 0.1m and 0.5m, respectively. The Tx and Rx vehicles, with length  $l_v = 4.5\text{m}$  and width  $w_v = 1.8\text{m}$ . The arrays are designed as appropriate quarters of a uniform circular array with  $\lambda_c/2$ -spaced elements, where  $\lambda_c$  is the carrier wavelength. The fixed beamforming vector for each Tx array is chosen so that the signals are transmitted omnidirectionally in the  $270^\circ$ -sector that is not blocked by the vehicle.

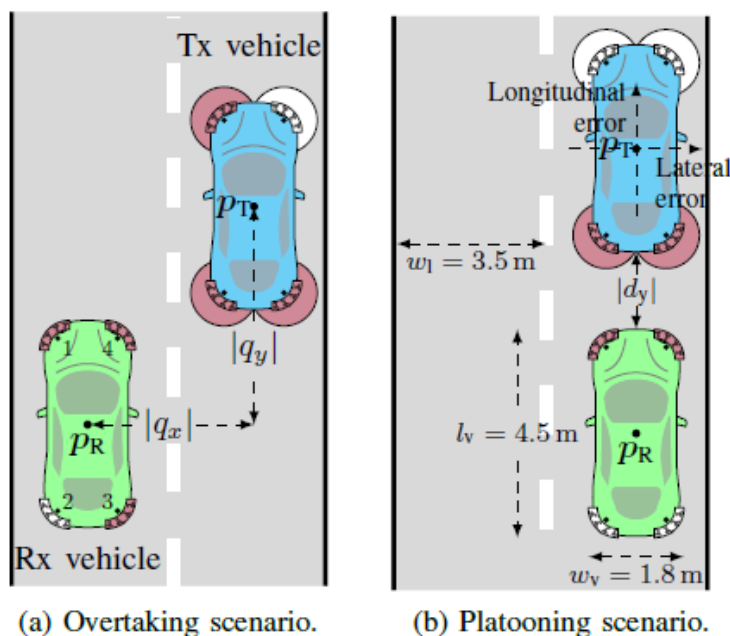


Figure 3.11: Overtaking and platooning scenarios. Arrays with at least one LOS link are shown darker.

Hence, all potential LOS links are excited, without the need of a beam-scanning process. Similarly, each of the Rx arrays can receive signals in an angular range of  $270^\circ$ . Thus, the links between some Tx-Rx array pairs might be blocked. In Figure 3.11 the arrays that have at least one LOS link are shown darker. The width of the lane is assumed to be  $w_l = 3.5\text{m}$ . The channel gain of each link is computed assuming free space propagation for the respective wavelength. We transmit one OFDM symbol with 2048 subcarriers and put pilot symbols on the subcarriers with indices  $P = \{-600, \dots, -1, 1, 600\}$ , leaving the rest empty. The used subcarriers are uniformly distributed to the Tx arrays in an interleaved manner. Also, the power is uniformly allocated among Tx arrays and subcarriers. For the rest of the system parameters we consider two configurations:

- (i) carrier frequency  $f_c = 3.5\text{ GHz}$ , subcarrier spacing  $\Delta f = 60\text{ kHz}$  and number of receive antennas per array  $N_{R,r} = 4, \forall r$ ;
- (ii)  $f_c = 28\text{ GHz}$ ,  $\Delta f = 240\text{ kHz}$  and  $N_{R,r} = 25, \forall r$ .

The transmit power and the per-antenna noise variance are set so that, when the vehicles are next to each other in neighboring lanes ( $q_x = -3.5\text{m}$ ;  $q_y = 0\text{m}$ ), the receive SNR after Rx beamforming for the Tx-Rx array pair with the shortest distance is 36 dB for the 3.5 GHz configuration and 30 dB for the 28 GHz configuration. The number of antenna elements for the two configurations has been chosen so that the receiving arrays have (approximately) the same size, assuming the inter-element spacing is  $\lambda_c/2$ .

The overtaking scenario is shown in Figure 3.11a. The lateral offset of the Rx vehicle's center w.r.t. to the Tx vehicle's center is constant and equal to  $q_x = -3.5\text{m}$  (lane width) and a range of longitudinal offsets  $q_y$  from  $-30\text{m}$  to  $30\text{m}$  is considered. For all considered relative positions in this scenario, each vehicle has three arrays with at least one LOS link to the other vehicle, except for  $q_y = 0\text{m}$  (where the vehicles are next to each other); then, each vehicle has two arrays with at least one LOS link. In Figure 3.12 we plot the lateral and the longitudinal positioning errors  $PEB_{\text{lat}}$  and  $PEB_{\text{lon}}$  as functions of the longitudinal offset  $q_y$ , when both AOA and TDOA or only AOA measurements are used, for the two aforementioned configurations.

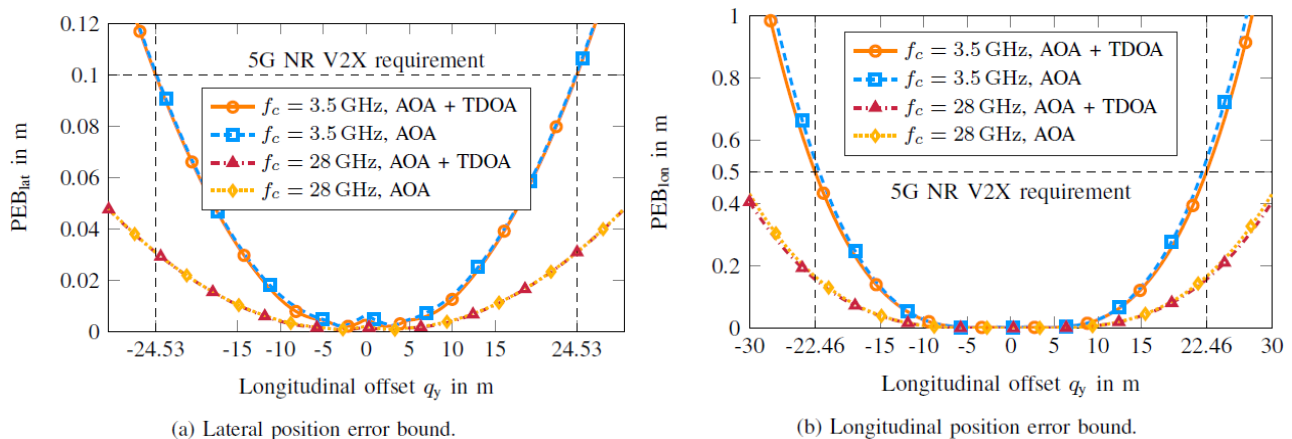


**Figure 3.12: Lateral and longitudinal position error bound for the overtaking scenario.**

For both configurations, we observe that TDOA measurements do not provide much additional positioning information compared to that provided by the AOA measurements. Despite the lower receive SNR, the 28 GHz configuration has better positioning accuracy than the 3.5 GHz configuration, with the higher angular resolution offered by the higher number of antennas being the key factor for its superiority. We stress that the bandwidth does not impact the angle information. While with the 28 GHz configuration the 5G V2X positioning requirements are always met for the depicted vehicle distances, the 3.5 GHz configuration achieves the lateral positioning accuracy requirement for longitudinal offsets  $|q_y| < 24.53\text{m}$  and the longitudinal requirement for  $|q_y| < 22.46\text{m}$ , when both AOA and TDOA measurements are used. For the case when solely AOA measurements are used, the corresponding values are only slightly lower.

In the platooning scenario the vehicles are vertically aligned, i.e.  $q_x = 0\text{m}$ . Consequently, as seen in Figure 3.11b, only the two rear panels of the Tx vehicle and the two front panels of the Rx vehicle have an active communication link. We consider only negative longitudinal offsets  $-30\text{m} < q_y \leq -4.5\text{m}$  and in Figure 3.13 we plot  $\text{PEB}_{\text{lat}}$  and  $\text{PEB}_{\text{lon}}$  as functions of  $|q_y|$  (lower horizontal axis) and of  $d_y = |q_y| - 4.5\text{m}$  (upper horizontal axis), which is the distance between the rear part of the Tx vehicle and the front part of the Rx vehicle (see Figure 3.11b).

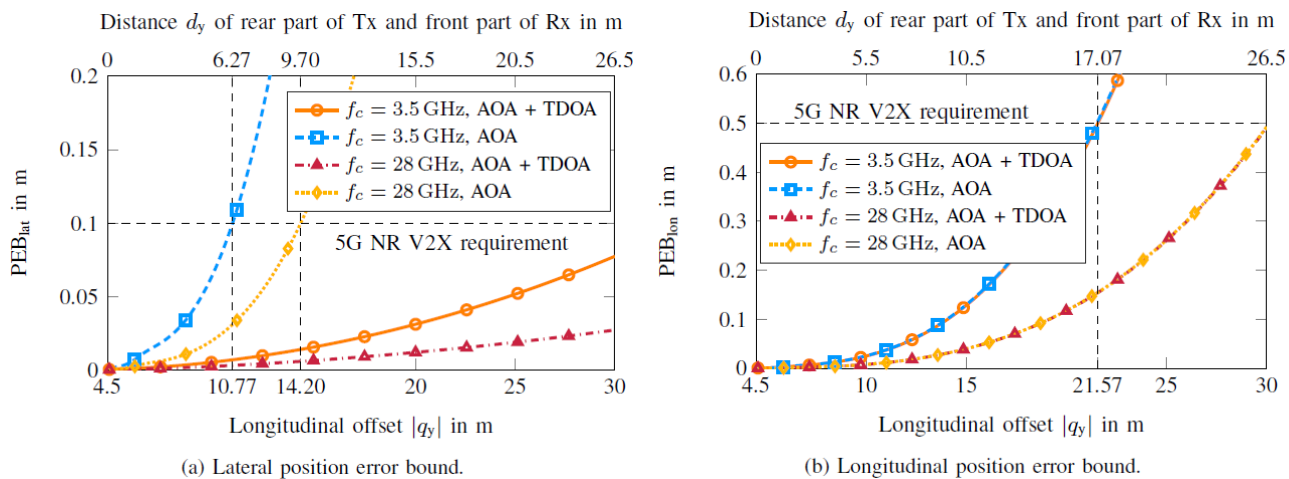


**Figure 3.13: Lateral and longitudinal position error bound for the platooning scenario.**

The 28 GHz configuration provides again better lateral and longitudinal positioning accuracy. As we can see Figure 3.13b, similar to the overtaking scenario, the use of TDOA measurements in addition to the AOA measurements has a very small impact on the longitudinal positioning accuracy, with the 3GPP longitudinal requirement being satisfied for  $d_y < 17.07\text{m}$  for the 3.5 GHz configuration and for all considered distances for the 28 GHz configuration. On the other hand, we see that the TDOA measurements strongly influence the lateral position error bound. When AOA and TDOA are used, the lateral requirement is satisfied for all considered distances for both configurations. However, when only AOA measurements are used, the lateral



requirement can only be met for  $d_y < 6.27\text{m}$  for the 3.5 GHz configuration and for  $d_y < 9.70\text{m}$  for the 28 GHz configuration. Numerical results, not included here due to space constraints, show that i) when the orientation  $\alpha_T$  of the Tx vehicle is known, the TDOA measurements do not significantly improve the lateral positioning accuracy; ii) when  $\alpha_T$  is unknown the TDOA measurements substantially increase the Fisher information on  $\alpha_T$ . These two observations explain the reason why TDOA measurements are important for this scenario.

The main outcomes can be summarized as follows [KCS+18]:

- The 28 GHz configuration can provide better positioning accuracy pertaining mainly to its higher angular resolution, as a result of the larger number of antennas that can be packed in the same physical area.
- In the overtaking scenario, angular measurements are sufficient and the 5G NR V2X requirements can be easily met for a wide range of distances.
- TDOA measurements can drastically improve the lateral positioning accuracy in the platooning scenario, as they provide valuable Fisher information on the unknown orientation of the Tx vehicle. With known Tx vehicle orientation, AOA measurements are sufficient for accurate position estimation.

These results can serve as a guideline for positioning reference signal design. In addition, the analytic expression can be used for the optimization of the position of the arrays and their respective elements in order to meet specific lateral and longitudinal error requirements.

### 3.3 Status of Standardization

In this section we will link the positioning solutions described in the previous section with the ongoing standardization in 3GPP. The aim is to list required extensions in the standard which are required for a full exploitation of the performance potential of our solutions. Apart from that we will also propose modifications of the LPP to overcome the disadvantages mentioned in section 3.1.3.

The description of the general New Radio (NR) Work Item (WI) [3GPP17-171780] stated support of work on positioning to comply with regulatory requirements. To this end, efforts were made to start a RAN1-led Study Item (SI) on NR positioning for Rel-16 at beginning of 2018 (see [3GPP17-172746; 3GPP17-172553]) but nothing was approved at that time mainly due to current 3GPP big focus on finalizing the specification of non-standalone NR. At the same time, Rel-16 proposals on NR V2X were made in parallel (see [3GPP17-172738; 3GPP17-172765]). At RAN#78, it was decided for Rel-16 proposals (including NR positioning and NR V2X) to be consolidated between companies via email discussion [3GPP17-172795]. Summaries of discussions were provided at RAN#79 [3GPP18-180319; 3GPP18-181063].

It was initially expected that study on V2X positioning will be included in both 3GPP proposed SIs, V2X and Positioning, with different focuses. With the Positioning SI focusing on general architecture, protocols, and technologies (RAT-dependent, RAT-independent, V2X-assisted) of V2X positioning, and the V2X SI focusing on the PC5 protocol to support V2V and network-



assisted UE positioning. In fact, during the V2X SI consolidation procedure an objective about V2X positioning was proposed in order to evaluate the feasibility & mechanisms to improve vehicle positioning accuracy including solutions such as ranging. In the end, however, it was decided to remove this objective since part could be covered by NR positioning SI and also since NR sidelink has not been defined yet.

Consolidated SI on NR positioning was finally prepared for RAN#80 (June-2018) and TSG-RAN approved the proposed SI: “Study on NR positioning support” [3GPP18-182155] with the following objectives:

- Select the requirements, and study corresponding evaluation scenarios/methodologies to enable positioning in regulatory and commercial use cases
  - Identify requirements such as accuracy, latency, capacity, coverage, and etc.
    - For evaluation purpose, radio layer level latency is considered rather than end-to-end latency.
  - Define a representative number of evaluation scenarios for indoor and outdoor
    - One use case representing indoor (e.g. Indoor Office as a baseline)
    - One use case representing outdoor (UMi-street canyon and Uma scenario as baseline)
    - One macro deployment from [3GPP15-37857] for FR1
    - Note: Any specific deployment scenarios are also studied including evaluation scenarios for FR2.
  - Define evaluation methodologies considering the above evaluation scenarios including:
    - System parameters including operating bands for both FR1 and FR2 at least for RAT-dependent (NR-based) positioning and for hybrid of RAT-dependent and RAT-independent positioning
    - User dropping procedures
    - Performance metrics to evaluate vertical/horizontal positioning and the above identified requirements
    - The evaluation scenarios/methodologies developed for above regulatory aspects can be a baseline for other positioning evaluations at least by taking [3GPP15-37857] into account.
- Study and evaluate potential solutions of positioning technologies based on the above identified requirements, evaluation scenarios/methodologies
  - The solutions should include at least NR-based RAT dependent positioning to operate in both FR1 and FR2 whereas other positioning technologies are not precluded.
  - Minimum bandwidth target (e.g. 5MHz) of NR with scalability is supported towards general extension for any applications.

It is noted within the SI description that “*sidelink (including V2V) and Sidelink + Radiolink (including V2X) based positioning study are not part of this SI scope whereas general radio link based positioning will also take high speed UEs into account*”.



In addition to the aforementioned standardization directions, there was intent shown within 3GPP to investigate positioning options with sufficient positioning accuracies for demanding IoT use cases [3GPP17-172666]. For example, in line with 5GCAR interests, video surveillance when AI is used to assist image processing and make decisions is described as a potential use case of mMTC in [3GPP17-172485]. Furthermore, in earlier Rel-14/15 work, 3GPP was looking to simplify the positioning support, especially for the case of low power UE device (one of the objectives in even further enhanced MTC (efeMTC) or NB-IOT enhanced) and a similar upcoming requirement for LTE-A and/or NR may rise.

Last but not least, highly accurate and ubiquitous real-time positioning may also be the focus of some work in LTE-A. For example, Rel-15 WI: UE Positioning Accuracy Enhancements for LTE [3GPP17-181298] investigated solutions for GNSS positioning enhancements, broadcasting of assistance data, and IMU positioning support.

According to the above, a list of aspects currently considered by 3GPP contributing parties regarding positioning for future V2X use cases can be summarized:

- NR provides potential for obtaining higher positioning accuracy but the requirements of positioning accuracy and latency to target certain use-cases introduce more strict requirements.
- The accurate GNSS positioning support introduced in Rel. 15 is accurate where available. It is desirable to investigate hybrid positioning solutions to ensure seamless support for accurate positioning. Mechanisms to improve vehicle positioning accuracy by complementing other existing positioning technologies could include solutions utilizing
  - sidelink-based range measurements, and/or
  - IMUs as a means of updating position estimates.
- One of the limitations of V2V is the need of GNSS. So, it would be great to have in LTE-A and/or NR autonomous positioning technique that could come from V2X (under coverage).
- Continuous use of positioning service will consume high amounts of power and power consumption in many cases would be useful to be minimized.
- Demanding data rate communication between massive number of UE devices and/or network is required to enable accurate positioning for a potential use case of mMTC where video surveillance when AI is used to assist image processing and make decisions.

The work made into the 5GCAR project can allow to bring a harmonized view on the objectives of such future SI/WI. Generally, 5GCAR will contribute to the definition of the SI/WI about positioning through its 3GPP members by participating in the discussions. A more ambitious plan is to steer 3GPP interest on improvement areas related to 5GCAR solution space in order to later on promote our specific solutions on potentially approved NR positioning SI/WI.

In Table 3.2, we try to match 5GCAR solutions to the aforementioned 3GPP considered positioning aspects as a means to indicate possible candidates for standardization.



**Table 3.2: Recommendations for standardization.**

<b>5GCAR solution</b>	<b>3GPP considered aspect(s)</b>	<b>Comments</b>
Improve positioning accuracy	Provide option to illuminate different directions during PRS	Can allow UE to estimate angles and delays of multipath components
Optimize scheduling between PRS and communication	PRS parameters	Positioning can benefit from channel estimates and channel estimation can benefit from position information
Improve accuracy of ToA measurements	Allow PRS transmission on the complete system bandwidth	A large PRS bandwidth allows for a better resolution of propagation paths
Increase number of transmitters / receivers of PRS	Allow PRS transmission in sidelink resources	V2X-specific network elements like RSUs can support the positioning of road users
Broadcast assistance messages per cell	Autonomous positioning technique, reduced power consumption, reduced positioning delay	Positioning can benefit from faster and reduced assistance message exchange between BS and UEs
Provide V2V distance measurements based on radio positioning using multiple panels.	V2V relative positioning requirements have been defined. V2V relative positioning will be considered for 3GPP NR Rel-17.	Proposed TC can meet the requirements set by 3GPP.



## 4 Conclusions

In this deliverable we discussed two important topics related to V2X: channel modelling and positioning. Section 2 deals with channel modelling and related measurements. At first the considered scenarios urban and highway as well as the different V2X link types have been introduced. Next, the state-of-the-art channel models for V2X communications have been described including their most relevant components: LOS blockage analysis, path loss and shadow fading modelling, and fast fading modelling. Section 2.2 describes the gaps in terms of the key missing components required for complete solution for V2X channel modelling. Based on these gaps Sections 2.3 and 2.4 presents: i) new V2V measurements and characterization of channels above 6 GHz; ii) multi-link shadowing model based on measurements below 6 GHz; and iii) channel measurements for massive MIMO adaptive beamforming.

In fact, some partners in 5GCAR have been leading the discussions on V2X channel modelling in 3GPP, and results in the present deliverable have appeared in 3GPP in the form of contributions of 5GCAR partners. It can also be noted that the results in this deliverable will further contribute to resolving the remaining open issues in 3GPP channel models. We claim that 5GCAR solutions are very well aligned with the channel modelling in 3GPP. Especially, the need to model the impact of vehicle blockage has been confirmed by 3GPP and the three-state channel model presented in Section 2.2 has also been agreed in 3GPP.

Besides the abovementioned contributions of 5GCAR to 3GPP V2X channel modelling, 5GCAR has results that either go beyond the current status of 3GPP (namely modelling the effect of multi-link shadowing) or exemplary measurement methodology that can be used for future study of the novel concept of predictor antennas. These achievements are expected to be very useful for future standardization (Rel-17 and beyond).

Concerning positioning, in Section 3 we have first presented existing non-radio and radio-based techniques as well as their limitations. The conclusion of this analysis is that the required accuracy for the considered 5GCAR use cases cannot be guaranteed everywhere and every time. Consequently, different technology components being elaborated in 5GCAR to overcome these limitations have been described in the following. We have mapped the technology components to the primarily addressed scenario (urban or highway) and use cases.

The methods in subsection 3.2.1 (trajectory prediction with channel bias compensation and tracking) can be applied independently from a certain scenario and frequency band. The positioning algorithm is based on time-of-arrival measurements at multiple base stations. It has been shown that the reference case LTE OTDOA can achieve mean position errors of below 10 m. Hence, combination with sophisticated tracking algorithms like the Particle Filter is required, and the accuracy can be improved roughly by factor 2 with respect to the reference case. We have also disclosed a first concept for collision prediction, which is subject to ongoing enhancements

The remaining proposals assume the availability of antenna arrays to exploit spatial information, i.e. the angles of departure and angles of arrival of directive beams. These methods address the



dense urban scenario and are tailored for frequencies above 6 GHz. The algorithm presented in Section 3.2.2 (Beam-based V2X positioning) still assumes the transmission of more than one beam. It is a network-assisted UE-centric approach which exploits angular information obtained using 3D-beamforming. We investigate NR-specific technologies aiming to maximize positioning accuracy. The presented results show that the solution with Particle Filter outperforms linear regression. We observed that although the positioning accuracy improves in general as the number of reference anchor points increase, the geometric setting of the selected anchor points plays an important role. Depending on the number of transmission points and their geometrical relation, a mean position accuracy of below one meter can be achieved.

The solutions in Sections 3.2.3 (downlink transmission) and 3.2.4 (uplink transmission) operate with a single base station and antenna arrays both at the base station and terminal. Consequently, the position accuracy becomes better if the number of propagation paths increases. Basic idea of the downlink scheme is that the UE receives downlink mmWave signals, which are used to determine the channel parameters of each multipath component, characterized by a complex gain, a 1D delay, a 2D angle of arrival, and a 2D angle of departure. These channel parameter estimates are then used to solve for the UE state (position, heading, clock bias), as well as to build up a map of the environment. The best performance is achieved when the both LOS and NLOS paths are available, and when the clock bias and virtual anchor positions are known. The obtained bias error bounds imply that the desired sub-meter accuracy can be achieved in many of the investigated cases.

A particularity of the uplink approach in Section 3.2.4 is to jointly use the data and pilot symbols for a quasi-continuous estimation of the location and orientation of the device. To implement this idea, a graphical model connecting pilot-based positioning and data-aided positioning has been developed. It was found that data-aided method can be a valid alternative to improve and track location-information in a quasi-continuous way without compromising complexity and overhead.

In Section 3.2.6 we presented performance bounds for multi-array V2V relative positioning (sidelink transmission at 3.5 GHz and 28 GHz) for two important use cases: overtaking and platooning. Main achievement was to understand the significance of angular measurements compared to that of delay measurements with potential applications to reference signal design. The 28 GHz configuration can provide better positioning accuracy pertaining mainly to its higher angular resolution, as a result of the larger number of antennas that can be packed in the same physical area. We found out that angular measurements are sufficient for the overtaking scenario, and that TDOA measurements can drastically improve the lateral positioning accuracy in a platooning scenario.

Finally, in Section 3.2.5 (Enhanced assistance messaging scheme for GPS and OTDOA positioning), we propose extensions to the legacy LTE Positioning Protocol (LPP) in order to improve GNSS and OTDOA positioning. The main idea is to broadcast messages per cell. Two different options have been compared, namely introduction of new SIBs, and unsolicited message at NAS level. The main benefits of the proposed protocol enhancements are reductions of the positioning delay, the UE power consumption as well as the required radio resources.



## 5 References

- [3GPP14-36843] 3GPP TR 36.843, "Study on LTE Device to Device Proximity Services; Radio Aspects (Rel-12)", 2014.
- [3GPP15-37857] 3GPP TR 37.857, "Study on indoor positioning enhancements for UTRA and LTE (Rel-13)", 2015.
- [3GPP16-167219] R1-167219, "Modelling the Evolution of Line-of-Sight Blockage for V2V Channels", 3GPP TSG-RAN1 Meeting #86, Gothenburg, Aug. 2016.
- [3GPP16-36885] 3GPP TR 36.885, "Study on LTE-based V2X Services (Rel-14)", 2016.
- [3GPP17-171093] RP-171093, "Study on evaluation methodology of new V2X use cases for LTE and NR", June 2017.
- [3GPP17-1713225] R1-1713225, "Summary of email discussion [89-28] eV2X evaluation methodology", 3GPP TSG-RAN1 Meeting #90, Prague, Aug. 2017.
- [3GPP17-1715092] R1-1715092, "Summary of email discussion [89-28] eV2X evaluation methodology", Aug. 2017.
- [3GPP17-1717293] R1-1717293, "Summary of email discussion [90-30] on eV2X evaluation methodology", Oct. 2017.
- [3GPP17-171780] RP-171780, "Revised WID on New Radio Access Technology", 3GPP TSG RAN Meeting #77, September 2017.
- [3GPP17-1720604] R1-1720604, "Comparison of V2V channels at 60 GHz under LOS and non-LOS due to vehicle blockage", 3GPP TSG-RAN1 Meeting #91, Reno, Nov. 2017.
- [3GPP17-1721545] R1-1721545, "Summary of email discussion [90b-NR-02] on eV2X evaluation methodology", Nov. 2017.
- [3GPP17-172485] RP-172485, "Discussion on NR MMTTC", Huawei, 3GPP TSG RAN Meeting #78, December 2017.
- [3GPP17-172553] RP-172553, "Motivation for New SI on high accuracy/Low Latency NR positioning", Ericsson, 3GPP TSG RAN Meeting #78, December 2017.
- [3GPP17-172666] RP-172666, "New SID on NR-IoT", Ericsson, 3GPP TSG RAN Meeting #78, December 2017.
- [3GPP17-172738] RP-172738, "New SI proposal: Study on 3GPP V2X phase 3 based on NR", 3GPP TSG RAN Meeting #78, December 2017.
- [3GPP17-172746] RP-172746, "New SID: Study on NR positioning support," 3GPP TSG RAN Meeting #78, December 2017.
- [3GPP17-172765] RP-172765, "New WID on study on V2X phase 3 based on NR", 3GPP TSG RAN Meeting #78, December 2017.
- [3GPP17-172795] RP-172795, "Handling new SI/WI proposals in RAN", 3GPP TSG RAN Meeting #78, December 2017.



- [3GPP17-36211] 3GPP TS 36.211, "Physical channels and modulation", Rel-14, 2017.
- [3GPP17-36355] 3GPP TS 36.355, "LTE Positioning Protocol (LPP)", Rel-14, 2017.
- [3GPP17-38802] 3GPP TR 38.802, "Study on New Radio access technology: Physical layer aspects (Rel-14)", 2017.
- [3GPP17-38901] 3GPP TR 38.901, "Study on channel model for frequencies from 0.5 to 100 GHz (Rel-14)", 2017.
- [3GPP18-1802720] R1-1802720, "V2X path loss and shadowing", 3GPP TSG-RAN1 Meeting #92", Athens, Feb. 2018.
- [3GPP18-1802721] R1-1802721, "V2X fast fading model", 3GPP TSG-RAN1 Meeting #92, Athens, Feb. 2018.
- [3GPP18-180319] RP-180319, "Email discussion summary for Rel-16 SI proposal on NR positioning", Intel Corporation, RAN#79, March 2018.
- [3GPP18-1803671] R1-1803671, "V2X sidelink channel model", 3GPP TSG-RAN1 Meeting #92bis, Sanya, China, April 2018.
- [3GPP18-180909] RP-180909, "Status Report to TSG for "Study on evaluation methodology of new V2X use cases for LTE and NR", LG Electronics, RAN#80, June 2018.
- [3GPP18-181063] RP-181063, "Phase II of [NR\_V2X] Study Item email discussion", Vodafone, RAN#79, March 2018.
- [3GPP18-181298] RP-181298, "WID Update: UE Positioning Accuracy Enhancements for LTE", 3GPP TSG RAN Meeting #80, June 2018.
- [3GPP18-182155] RP-182155, "3GPP Study Item Description "Study on NR Positioning Support", RAN#81, Intel Corporation, Ericsson, September 2018.
- [3GPP18-37885] TR 37.885, "Study on evaluation methodology of new Vehicle-to-Everything V2X use cases for LTE and NR", LG Electronics, RAN1#93, May 2018.
- [5GC17-D21] 5GCAR D2.1, "5GCAR Scenarios, Use Cases, Requirements and KPIs", August 2017.
- [5GC18-D31] 5GCAR D3.1, "Intermediate 5G V2X Radio", May 2018.
- [ABV+16] B. Aygun, M. Boban, J.P. Vilela, & A.M. Wyglinski, "Geometry-Based Propagation Modelling and Simulation of Vehicle-to-Infrastructure Links", in Vehicular Technology Conference (VTC Spring), 2016 IEEE 83rd (pp. 1-5). IEEE, May 2016.
- [AI07] G. Acosta-Marum and M. A. Ingram, "Six time- and frequency- selective empirical channel models for vehicular wireless LANs", in IEEE Vehicular Technology Magazine, vol. 2, nr. 4, p. 4-11, December 2007.
- [AMG+02] Arulampalam, M. S., Maskell, S., Gordon, N., Clapp, T., "A Tutorial on Particle Filters for Online Nonlinear/Non-Gaussian Bayesian Tracking", IEEE Transaction on Signal Processing, vol. 50, no. (February 2002).
- [Aro11] D. Aronsson, "Channel Estimation and Prediction for MIMO OFDM Systems - Key Design and Performance Aspects of Kalman-based Algorithms", Ph.D. Thesis,





- Signals and Systems, Uppsala University, March 2011.  
[www.signal.uu.se/Publications/pdf/a112.pdf](http://www.signal.uu.se/Publications/pdf/a112.pdf).
- [ASK+15] T Abbas, K Sjöberg, J Karedal, F Tufvesson, "Measurement based shadow fading model for vehicle-to-vehicle network simulations", International Journal of Antennas and Propagation, 2015.
- [BBT14] M. Boban, J. Barros, and O. Tonguz, "Geometry-based vehicle-to-vehicle channel modelling for large-scale simulation", in IEEE Transactions on Vehicular Technology, vol. 63. no. 9, pp. 4146-4164, November 2014.
- [BGX16] M. Boban, X. Gong, and W. Xu, "Modelling the evolution of line-of-sight blockage for V2V channels", in Proceedings of the 2016 IEEE 84th Vehicular Technology Conference (VTC2016-Fall), Montréal, Canada, September 2016, pp. 1-6.
- [BSG17] J. Björnell, M. Sternad and M. Grieger, "Using predictor antennas for the prediction of small-scale fading provides an order-of-magnitude improvement of prediction horizons", 2017 IEEE International Conference on Communications Workshops (ICC Workshops), Paris, June 2017, pp. 54-60.
- [BSG17-2] J. Björnell, M. Sternad and M. Grieger, "Predictor Antennas in Action", 2017 IEEE PIMRC, Montreal, October 2017.
- [BVF+11] M. Boban, T. T. V. Vinhoza, M. Ferreira, J. Barros, and O. K. Tonguz, "Impact of vehicles as obstacles in vehicular ad hoc networks", in IEEE Journal on Selected Areas in Communications, vol. 29, no. 1, pp. 15-28, January 2011.
- [BVT13] M. Boban, W. Viriyasitavat, and O.K. Tonguz, "Modelling vehicle-to-vehicle line of sight channels and its impact on application-layer performance", in Proceeding of the 10th ACM international workshop on Vehicular inter-networking, systems, and applications (VANET 13), Taipei, Taiwan, June 2013, pp. 91-94.
- [CAX+17] Cruz, S. B., Abrudan, T. E., Xiao, Z., Trigoni, N., Barros, J., "Neighbor-Aided Localization in Vehicular Networks", IEEE Transactions on Intelligent Transportation Systems, 2017.
- [CBK+17] Y. Choi, D. Bai, S. Kim and J. Lee, "Towards the Performance Limit of Data-Aided Channel Estimation for 5G", 2017 IEEE Wireless Communications and Networking Conference (WCNC), San Francisco, CA, 2017, pp. 1-6.
- [CSS09] Caceres, M., Sottile, F., Spirito, M. A., "WLAN-based real time vehicle locating system", in Vehicular Technology Conference, 2009. VTC Spring 2009. IEEE 69th (pp. 1-5). IEEE, 2009.
- [DCF+10] Dulmage, J., Cioffi, R., Fitz, M. P., & Cabric, D., "Characterization of distance error with received signal strength ranging", in Wireless Communications and Networking Conference (WCNC), 2010.
- [DDS+10] N. Decarli, D. Dardari, S. Gezici and A. D'Amico, "LOS/NLOS detection for UWB signals: A comparative study using experimental data", IEEE 5th International Symposium on Wireless Pervasive Computing 2010, Modena, 2010, pp. 169-173.
- [DH07] A. Duel-Hallen, "Fading channel prediction for mobile radio adaptive transmission systems", Proc. of the IEEE, vol. 95, no. 12, pp. 2299-2313, Dec. 2007.



- [EAS02] T. Ekman, A. Ahlén and M. Sternad, "Unbiased power prediction on Rayleigh fading channels", IEEE Vehicular Technology Conference VTC2002-Fall, Vancouver, Canada, Sept. 2002.
- [Ekm02] T. Ekman, "Prediction of Mobile Radio Channels: Modelling and Design", Ph.D. Thesis, Signals and Systems, Uppsala Univ., 2002. Available: [www.signal.uu.se/Publications/pdf/a023.pdf](http://www.signal.uu.se/Publications/pdf/a023.pdf).
- [ETSI09-102638] ETSI TR 102 638 V1.1.1, "Intelligent Transport Systems (ITS); Vehicular Communications; Basic Set of Applications; Definitions", 2009.
- [Fes15] Festag, A., "Standards for vehicular communication-from IEEE 802.11 p to 5G", Elektrotechnik und Informationstechnik 132.7 (2015): 409-416.
- [HDH+16] Hoang, G. M., Denis, B., Härri, J., Slock, D. T., "Breaking the gridlock of spatial correlations in GPS-aided IEEE 802.11 p-based cooperative positioning", IEEE Transactions on Vehicular Technology, 65(12), 9554-9569.
- [HNL+07] C. Herzet, N. Noels, V. Lottici, H. Wymeersch, M. Luise, M. Moeneclaey, L. Vandendorpe, "Code-Aided Turbo Synchronization", in Proceedings of the IEEE, vol. 95, no. 6, pp. 1255-1271, June 2007.
- [ITU13] ITU-R, Recommendation P.526, "Propagation by diffraction", International Telecommunication Union Radiocommunication Sector, Geneva, November 2013.
- [JAB+14] N. Jamaly, R. Apelfröjd, A. Belen Martinez, M. Grieger, T. Svensson, M. Sternad and G. Fettweis, "Analysis and measurement of multiple antenna systems for fading channel prediction in moving relays", European Conference on Antennas and Propagation, (EuCAP 2014), April 6-11, 2014, Hauge, The Netherlands.
- [JJD+17] M. Ju, L. Xu, L. Jin and D. Defeng Huang, "Data aided channel estimation for massive MIMO with pilot contamination", 2017 IEEE International Conference on Communications (ICC), Paris, 2017, pp. 1-6.
- [JMZ+14] V. Jungnickel, K. Manolakis, W. Zirwas, B. Panzner, V. Braun, M. Lossow, M. Sternad, R. Apelfröjd and T. Svensson, "The role of small cells, coordinated multipoint, and massive MIMO in 5G", IEEE Comm. Magazine, vol.52, no.5, pp.44-51, May 2014.
- [JU97] Julier, S. J., Uhlmann, J. K., "A new extension of the Kalman filter to nonlinear systems", The 11th International Symposium on Aerospace/ Defence Sensing, Simulation and Controls, Orlando, Florida, USA, 1997.
- [KBH06] M. A. Khalighi, J. J. Boutros and J. F. Helard, "Data-aided channel estimation for turbo-PIC MIMO detectors", in IEEE Communications Letters, vol. 10, no. 5, pp. 350-352, May 2006.
- [KCP11] J. Karedal, N. Czink, A. Paier, F. Tufvesson, and A. Molisch, "Path loss modelling for vehicle-to-vehicle communications", in IEEE Transactions on Vehicular Technology, vol. 60, no. 1, pp. 323-328, January 2011.
- [KCS+18] A. Kakkavas, M. H. Castañeda Garcia, R. A. Stirling-Gallacher, and J. A. Nossek, "Multi-array 5G V2V relative positioning: Performance bounds", in Proc. IEEE



- Global Commun. Conf. (GLOBECOM), Abu Dhabi, United Arab Emirates, Dec. 2018, to be published.
- [KFI08] Kandepu, R., Foss, B., Imsland, L., “Applying the Unscented Kalman Filter for Nonlinear State Estimation”, *Journal of Process Control*, 2008.
- [KMB+07] S. Kashyap, C. Mollén, E. Björnson and E. G. Larsson, “Performance analysis of (TDD) massive MIMO with Kalman channel prediction”, *2017 IEEE International Conference on Acoustics, Speech and Signal Processing (ICASSP)*, New Orleans, LA, 2017, pp. 3554-3558.
- [Kuh55] H.W. Kuhn, “The Hungarian method for the assignment problem”, *Naval Research Logistics (NRL) 2.1-2 (1955)*: 83-97.
- [LCW16] Liu, J., Cai, B. G., Wang, J., “Cooperative Localization of Connected Vehicles: Integrating GNSS With DSRC Using a Robust Cubature Kalman Filter”, *IEEE Transactions on Intelligent Transportation Systems*, 2016.
- [LMR+15] Leitinger, E., Meissner, P., Rüdissler, C., Dumphart, G., Witrisal, K., “Evaluation of Position-Related Information in Multipath Components for Indoor Positioning”, *IEEE Journal on Selected Areas in Communications*, 33(11), 2313 – 2328.
- [LVL14] Stéphanie Lefèvre, Dizan Vasquez, Christian Laugier, “A survey on motion prediction and risk assessment for intelligent vehicles”, *ROBOMECH Journal*, Springer, 2014, 1 (1), pp.1. <10.1186/s40648014-0001-z>. <hal-01053736>.
- [MET15-D14] ICT-317669 METIS, Deliverable 1.4, “METIS Channel Models”, July 2015.
- [Mul17] de Ponte Müller, F., “Survey on ranging sensors and cooperative techniques for relative positioning of vehicles”, *Sensors*, 17(2), 271.
- [NEJ+17] Niesen, U., Ekambaram, V. N., Jose, J., Wu, X., “Inter-vehicle range estimation from periodic broadcasts”, *IEEE Transactions on Vehicular Technology*, 2017.
- [Nil17] M. Nilsson, et al. “A Measurement Based Multilink Shadowing Model for V2V Network Simulations of Highway Scenarios”, *IEEE Transactions on Vehicular Technology*, 2017.
- [NGA+18] M. G. Nilsson, C. Gustafson, T. Abbas, and F. Tufvesson, “On Multilink Shadowing Effects in Measured Urban V2V Channels”, in *COST CA15104 Technical Meeting*, TD(18)06043, Nicosia, Cyprus, Jan. 2018.
- [OMS+12] Obst, M., Mattern, N., Schubert, R., Wanielik, G., “Car-to-Car communication for accurate vehicle localization—the CoVeL approach”, in *Systems, Signals and Devices (SSD)*, 2012 9th International Multi-Conference on (pp. 1-6), 2012.
- [PHH13] D.-T. Phan-Huy and M. Héléard, “Large MISO beamforming for high speed vehicles using separate receive & training antennas”, *IEEE Int. Symposium on Wireless Vehicular Communication*, June 2013.
- [PLH16] Perez-Cruz, F., Lin, C.-K., Huang, H., “BLADE: A universal, blind learning algorithm for ToA localization in NLOS channels”, *2016 IEEE Globecom Workshops*.



- [PSS15] D-T Phan-Huy, M. Sternad and T. Svensson, "Making 5G adaptive antennas work for very fast moving vehicles", IEEE Intelligent Transportation Systems Magazine, Summer, 2015, pp. 71-84.
- [PSS+16] D.-T. Phan-Huy, M. Sternad, T. Svensson, W. Zirwas, B. Villeforceix, F. Karim and S.-E. El-Ayoubi, "5G on board: How many antennas do we need on connected cars?", IEEE Globecom 2016 Workshop on 5G RAN Design, Washington DC, Dec. 2016.
- [PV07] Parker, R., Valaee, S., "Vehicular node localization using received-signal-strength indicator", IEEE Transactions on Vehicular Technology, 56(6), 3371-3380.
- [PWB+18] D.-T. Phan-Huy, S. Wesemann, J. Bjorsell, M. Sternad, "Adaptive Massive MIMO for fast moving connected vehicles: It will work with the Predictor Antennas", Workshop On Smart Antennas, March 2018, Bochum, Germany.
- [Qua14] Qualcomm Technologies, Inc., "Observed Time Difference of Arrival (OTDOA) Positioning in 3GPP LTE", 2014.
- [RPL+13] F. Rusek, D. Persson, B.K. Lau, E.G. Larsson, T.L. Marzetta, O. Edfors and F. Tufvasson, "Scaling up MIMO: Opportunities and challenges with very large arrays", IEEE Signal Processing Magazine, vol. 30, no. 1, Jan. 2013.
- [SGA+12] M. Sternad, M. Grieger, R. Apelfröjd, T. Svensson, D. Aronsson and A. Belen Martinez, "Using "predictor antennas" for long-range prediction of fast fading moving relays", IEEE Wireless Communications and Networking Conference (WCNC), Paris, April 2012.
- [SGD+18] A. Shahmansoori, G. E. Garcia, G. Destino, G. Seco-Granados and H. Wymeersch, "Position and Orientation Estimation Through Millimeter-Wave MIMO in 5G Systems", in IEEE Transactions on Wireless Communications, vol. 17, no. 3, pp. 1822-1835, March 2018.
- [SNG+17] Soatti, G., Nicoli, M., Garcia, N., Denis, B., Raulefs, R., Wymeersch, H., "Implicit Cooperative Positioning in Vehicular Networks", arXiv preprint arXiv:1709.01282, 2017.
- [SRW08] Schubert, R., Richter, E., Wanielik, G., "Comparison and Evaluation of Advanced Motion Models for Vehicle Tracking", 11th International Conference on Information Fusion, Cologne, Germany, July 2008.
- [TH13] K. T. Truong and R. W. Heath Jr., "Effects of channel aging in massive MIMO systems", J. Commun. and Networks, vol. 15, no. 4, pp. 338–351, Aug. 2013.
- [WSS+06] H. Wymeersch, F. Simoens, H. Steendam, M. Moeneclaey, "Code-aided channel tracking for OFDM", 4th International Symposium on Turbo Codes & Related Topics, 6th International ITG-Conference on Source and Channel Coding, Munich, Germany, 2006, pp. 1-6.
- [YBA+10] Yao, J., Balaei, A. T., Alam, N., Efatmaneshnik, M., Dempster, A. G., Hassan, M., "Characterizing cooperative positioning in VANET", in IEEE Wireless Communications and Networking (pp. 28-31).

# A Simulation Assumptions

This annex contains simulation assumptions to be used in performance evaluation of technical components proposed in WP3, divided into two parts:

- The first part contains simulation assumptions for system-level simulations, including the deployment scenarios, user deployment and mobility, antenna models, traffic models, channel models, and performance metrics.
- The second part contains a suggested list of parameters to be included in link-level evaluation results. Other parameters can be deduced from the system-level simulation assumptions, where appropriate.

The simulation assumptions in this annex may not be complete to cover all evaluations and are not restrictive. It rather provides a list of configuration options and environments, from which each partner can select an appropriate configuration for their evaluation. Partners are encouraged to provide detailed simulation assumptions used in the respective evaluation. Note some scenarios and parameters in this annex refer to the evaluation assumptions established in [3GPP-36885] and to an ongoing study item in 3GPP [3GPP-171093], where some partners of 5GCAR are active contributors.

## A.1 System-Level Simulation Assumptions

### A.1.1 Deployment Scenarios for Base Stations

Table A.1: Deployment scenarios for base stations.

Deployment scenario	Highway	Urban
BS antenna height	35m for ISD 1732m, 25m for ISD 500m	25m, above rooftop
Number of BS antennas elements (TX/RX)	Up to 256	Up to 256
Number of BS antenna ports	Up to 16	Up to 16
BS antenna gain	8dBi	17dBi
Maximum BS transmit power	49dBm per band (in 20 MHz)	49 dBm per band (in 20 MHz)



<b>BS noise figure</b>	5dB (below 6GHz) 7dB (above 6GHz)	5dB
<b>BS Carrier center frequency for evaluation</b>	800MHz, 2GHz, 3.5GHz, 4GHz 5.9GHz 28GHz, 63-64GHz (mmWave)	2GHz, 3.5GHz, 4GHz 5.9GHz 28GHz, 63-64GHz (mmWave)
<b>BS Carrier bandwidth for evaluation</b>	20MHz + 20MHz per carrier (below 6GHz) In case with CA, maximum number of carrier: up to 8 10MHz at 5.9GHz 200MHz per carrier (above 6GHz) In case with CA, maximum number of carrier: up to 5	20MHz + 20MHz per carrier (below 6GHz) In case with CA, maximum number of carrier: up to 8 10MHz at 5.9GHz 200MHz per carrier (above 6GHz) In case with CA, maximum number of carrier: up to 5
<b>BS Inter-site distance</b>	500m and 1732m	200m and 500m
<b>Backhaul/fronthaul (BS-BS, BS-RSU, RSU-RSU)</b>	For wireless self-backhaul/fronthaul, same technology as for radio access is used.  For non-ideal backhaul, values of [0.5, 1, 5 and 30] ms and [0.05, 0.5 and 10] Gbps can be used for one-way latency and throughput, respectively.	

## A.1.2 Deployment Scenarios for Road Sign Units

Table A.2: Deployment scenarios for RSUs.

Deployment scenario	Highway	Urban
<b>RSU antenna height</b>	5m - 10m (Applies for both BS-type and UE-type)	
<b>Inter-site distance</b>	100m - 500m	
<b>Number of RSU antennas elements (TX/RX)</b>	For BS-type-RSU: Up to 8 TX/RX	
<b>Number of RSU antenna ports</b>	Up to 8	
<b>Backhaul/fronthaul (BS-BS, BS-RSU, RSU-RSU)</b>	For wireless self-backhaul/fronthaul, same technology as for radio access is used.  For non-ideal backhaul, values of [0.5, 1, 5 and 30] ms and [0.05, 0.5 and 10] Gbps can be used for one-way latency and throughput, respectively.	



RSU type	BS- type	Vehicle / UE-type
RSU antenna gain	8dBi	3dBi
Maximum RSU transmit power	24dBm/33dBm (in 20MHz)	23dBm (in 20MHz)
RSU noise figure	5dB (below 6GHz) 7dB (above 6GHz)	9dB (below 6GHz) 13dB (above 6GHz)
RSU Carrier center frequency for evaluation	800MHz (only highway), 2GHz, 3.5GHz, 28GHz, 63-64GHz (mmWave)	2GHz, 3.5GHz, 28GHz, 63-64GHz (mmWave) 5.9GHz (RSU UE-type)
RSU carrier bandwidth for evaluation	10 – 20 MHz (below 6 GHz) Up to 100 MHz at 3.5GHz	

### A.1.3 Deployment Scenarios for UEs

Table A.3: Deployment scenarios for UEs.

Parameters	Pedestrian UE	Vehicle UE
Vehicle antenna height	1.0–1.8m	0.5–1.6m
Number of Vehicle antennas elements (TX/RX)	1/1, 2/2 (C-V2X), 4/4 (LTE Cat 16), 8/8	
Number of Vehicle antenna ports	4/4	
Vehicle antenna gain	0 dBi	V2I/V2N: 3dBi for non-mmWave; 14dBi (for 64GHz) V2V: 3dBi for non-mmWave; up to 21dBi (for 64GHz) Roof antenna 0dBi
Maximum UE transmit power	23 dBm	23dBm (33dBm can also be considered)
Vehicle noise figure	Below 6GHz: 9dB Above 6GHz: 13dB (baseline performance), 10dB (optional)	
Carrier center frequency for	5.9GHz, 3.5GHz,	

<b>evaluation (Direct/Sidelink Communication)</b>	28GHz, 62GHz (mmWave), 76-81GHz (currently for radar application)
<b>Distribution of antennas</b>	Co-located
<b>Polarization</b>	Co-polarized (vertical) as starting point
<b>Antenna array type</b>	Uniform Linear Array (ULA) and rectangular

## A.1.4 User Deployment and Mobility

### Urban Scenario

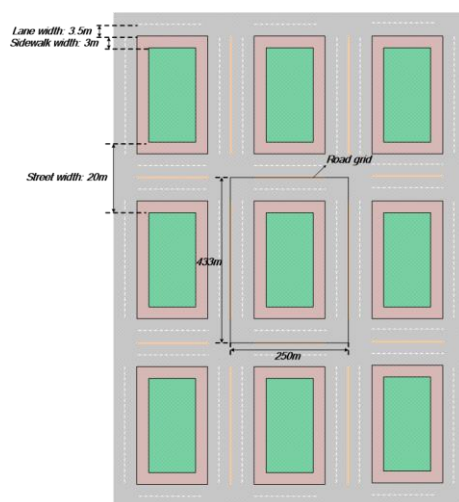


**Figure A.1: Road Configuration for Urban Traffic from [3GPP16-36885].**

Users in the urban scenario are deployed by the following procedure:

- Every road between the buildings contains two lanes per each direction (3.5m width).
- Vehicles are dropped on roads according to a spatial Poisson process with an average inter-vehicle distance of 2.5s times vehicle speed, in the middle of each lane.
- The total road length within the 433x250 area formed by 1 building, its surrounding sidewalk and rings of lanes, is equal to 2684m.
- In the urban synthetic deployment scenario, vehicles move along the streets with up to 60km/h.
- At the intersections, vehicles have 50% probability to go straight and 25% probability of turning left or right. Vehicle position is updated every 100ms on the simulation.
- In the urban realistic scenario, cars, buses, and pedestrians are dropped and move within the Madrid Grid according to vehicle mobility models and trace.



## Highway Scenario

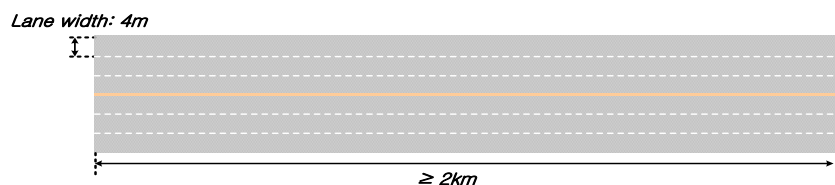


**Figure A.2: Road configuration for highway traffic efficiency and safety evaluation from [3GPP16-36885].**

- The depicted highway presents 3 lanes in each direction, with a lane width of 4m.
- It is required to have a highway length of at least 2km.
- Vehicles are dropped in the roads according to a spatial Poisson process with an average inter-vehicle distance of 2.5s times vehicle speed.
- In the highway (synthetic) scenario, vehicles move along the lanes of the highway at up to 250km/h. Vehicle position is updated every 100ms of the simulation.

Note:

- For platooning use case, the inter-vehicle distance can be shorter, e.g., 0.3s.
- Simulation of Urban Mobility (SUMO) traces could be generated & used. But this is an optional tool.

### A.1.5 Data Traffic Models

**Table A.4: Traffic models.**

Type of traffic	Description
<b>Periodic traffic model</b>	Deterministic model, i.e., no randomness in the message generation interval and message size.  On top of that, consider adding jitter (small variations) in packet arrival time and unexpected missed packet arrivals. The jitter can be modelled by assuming either uniform or truncated Gaussian distributions. Missed packets can be modelled with probability 'p'.
<b>Event-triggered traffic model</b>	The modelling can be done using randomized packet arrival, e.g., according to Poisson process.
<b>eMBB-like traffic model</b>	Necessary for eV2X use-cases like 3D video composition, local dynamic map sharing, tethering via vehicle, collective perception of environment with bursty eMBB-like traffic with a certain data rate.  MBB-like traffic can be modelled using FTP traffic model 2 with updated values on file sizes, reading time and burst length, etc.
<b>Full-buffer traffic model</b>	Always-on traffic.

Note: By varying different parameters in the traffic models, e.g., periodicity, packet size, data rate, various use cases can be covered.



### A.1.6 In-Band Emission Model

- Below 6GHz: Reuse the model in [3GPP14-36843] Table A.2.1.5-1 with [W,X,Y,Z]=[3,6,3,3].
- Above 6GHz: To be defined.

### A.1.7 Performance Metrics

Table A.5: Performance metrics for evaluations.

Metric	Description
Reliability	<p>Packet Reception Ratio (PRR):</p> <p>For one Tx packet, the PRR is calculated by <math>X/Y</math>, where Y is the number of UEs/vehicles that are located in the range (a, b) from the Tx, and X is the number of UEs/vehicles with successful reception among Y. CDF of PRR and PRR are used in evaluation.</p> <p>PRR is relevant to safety applications and should be the primary metric for reliability evaluations.</p> <p>PRR should be calculated taking into account the latency budget. This can then be represented as CDF of 'average PRR over latency' as well as "PRR over distance for a certain latency budget".</p>
Latency	<p>Received inter-packet spacing:</p> <p>A metric which can capture the aspect of persistent collisions</p> <p>Details can be found in Section 4.1.2 in [5GCAR17-D21]</p>
Throughput/spectrum efficiency	<p>SINR/ distribution</p> <p>Symbol error distribution, MSE</p> <p>Throughput distribution</p> <p>Spectral efficiency (bits/s/Hz)</p>
Positioning accuracy	<p>Absolute and/or relative accuracy.</p>



## A.2 Link-level Simulation Assumptions

Table A.6: Suggested list of parameters for link-level simulations.

Receiver algorithm
Time and frequency accuracy
Reference signal structure
PHY packet size
Channel codes (for control and data channels)
Modulation and code rates (for control and data channels)
Signal waveform (for control and data channels)
Subcarrier Spacing
CP length
Frequency synchronization error
Time synchronization error
Channel estimation (e.g. DMRS pattern and symbol location)
Number of retransmission and combining (if applied)
Number of antennas (at UE and BS)
Transmission diversity scheme (if applied)
UE receiver algorithm
AGC settling time and guard period
EVM (at TX and RX)